

สถานะพื้นของ  $e_g$  อิเล็กตรอนในแบบจำลองฮับบาร์ดแบบไรสปริน



นายพงษ์พันธุ์ พันธุ์เพชร

สถาบันวิทยบริการ

จุฬาลงกรณ์มหาวิทยาลัย

วิทยานิพนธ์ฉบับนี้เป็นส่วนหนึ่งของการศึกษาตามหลักสูตรปริญญาวิทยาศาสตรมหาบัณฑิต

สาขาวิชาฟิสิกส์ ภาควิชาฟิสิกส์

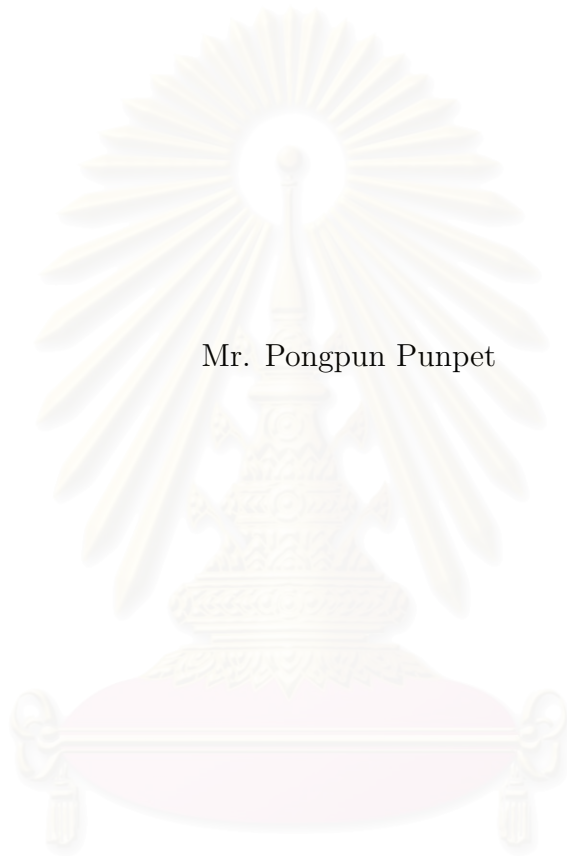
คณะวิทยาศาสตร์ จุฬาลงกรณ์มหาวิทยาลัย

ปีการศึกษา 2548

ISBN 974-53-2704-2

ลิขสิทธิ์ของจุฬาลงกรณ์มหาวิทยาลัย

GROUND STATE OF  $e_g$  ELECTRON IN THE SPINLESS HUBBARD MODEL



Mr. Pongpun Punpet

A Thesis Submitted in Partial Fulfillment of the Requirements  
for the Degree of Master of Science Program in Physics

Department of Physics

Faculty of Science

Chulalongkorn University

Academic year 2005

ISBN 974-53-2704-2



พงษ์พันธุ์ พันธุ์เพชร : สถานะพื้นของ  $e_g$  อิเล็กตรอนในแบบจำลองฮับบาร์ดแบบไร้สปิน.

(GROUND STATE OF  $e_g$  ELECTRON IN THE SPINLESS HUBBARD MODEL)

อ. ที่ปรึกษา : อ. ดร. จักรชัย ศรีนิติวรวงศ์, 84 หน้า. ISBN 974-53-2704-2.

ได้ศึกษาสมบัติของสถานะพื้นของแบบจำลองอย่างง่ายสำหรับสารประกอบ โลหะทรานซิชัน ออกไซด์ในสถานะแม่เหล็กเฟอร์โร แบบจำลองนี้ใช้อธิบายการเคลื่อนที่ของอิเล็กตรอนใน  $e_g$  ออบิทัล ในที่นี้จะใช้แบบจำลองฮับบาร์ดแบบไร้สปินที่ประกอบด้วยของศาอิสระแบบออบิทัลเท่านั้น โดยจะ ประกอบไปด้วยสองออบิทัลในเงื่อนไขที่อิเล็กตรอนมีอันตรกิริยาแบบคูมอมบ์กันอย่างแรงหากอยู่ใน ตำแหน่งแลตทิส (lattice) เดียวกัน การคำนวณสถานะพื้นของแบบจำลองนี้ จะกระทำในหนึ่งมิติใน อัตราส่วนของอิเล็กตรอนหนึ่งตัวต่อหนึ่งตำแหน่งของแลตทิส จะทำการแปลงแบบจำลองแบบฮับบาร์ดนี้ โดยการแปลงแบบบัญญัติ หลังจากการแปลงจะมีการตัดสถานะ ของการอยู่เป็นคู่ของอิเล็กตรอนออกจะทำให้ขนาดของปริภูมิฮิลเบิร์ตลดลง สำหรับแอมพลิจูดของการกระโดดของอิเล็กตรอนของแฮมิลโทเนียนยัง ผลที่คำนวณได้จะกำหนดตามระบบของสารเมงกาไนต์ ซึ่งประกอบขึ้นในสามแกน x, y และ z เนื่องจากการคำนวณสถานะพื้นจะกระทำในหนึ่งมิติ ดังนั้นผลของการคำนวณจึงถูกแบ่งออกเป็นสามกรณีตามทิศ การกระโดดของอิเล็กตรอนในแกน x, y และ z การคำนวณสถานะพื้นของแฮมิลโทเนียนยังผลใช้วิธี กลุ่ม การทำให้เป็นปกติอีกครั้งของเมตริกซ์ความหนาแน่น ( Density Matrix Renormalization Group) แบบอนันต์ ซึ่งวิธีการนี้จะทำให้ได้คำตอบดังกล่าวเข้าใกล้สถานะพื้นที่ขีดจำกัดอุณหพลศาสตร์ เมื่อจำนวน ของตำแหน่งของอิเล็กตรอนที่พิจารณามีมาก จากผลการคำนวณ พบว่าพลังงานที่สถานะพื้นในแต่ละแกน การกระโดดของอิเล็กตรอนมีค่าเท่ากัน นอกจากนั้นสหสัมพันธ์ของออบิทัลระหว่างตำแหน่งที่ใกล้ที่สุด ของอิเล็กตรอนที่สถานะพื้นในทุกแกนการกระโดดเป็นแบบแอนติเฟอร์โร

สถาบันวิทยบริการ

จุฬาลงกรณ์มหาวิทยาลัย

ภาควิชา ฟิสิกส์ ..... ลายมือชื่อนิสิต..... พงษ์พันธุ์ พันธุ์เพชร

สาขาวิชา ฟิสิกส์..... ลายมือชื่ออาจารย์ที่ปรึกษา.....

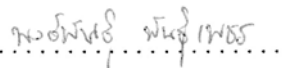
ปีการศึกษา 2548.....

## 4572396023 :MAJOR PHYSICS

KEY WORDS: DENSITY MATRIX RENORMALIZATION GROUP / HUBBARD MODEL / CANONICAL TRANSFORMATION

PONGPUN PUNPET : GROUND STATE OF  $e_g$  ELECTRON IN THE SPINLESS HUBBARD MODEL. THESIS ADVISOR : CHATCHAI SRINITIWARAWONG, PH.D., 84 pp. ISBN 974-53-2704-2.

The ground-state properties of a simple model for transition metal oxide compounds in ferromagnetic phase have been studied. This model only contains the orbital degree of freedom. The two-orbital spinless Hubbard model in the limit of strong on-site coulomb interaction ( $U$ ) has been used to describe the motion of electron in  $e_g$  orbital. In the large- $U$  and half-filling limits, the effective Hamiltonian has been derived from the Hubbard model by the canonical transformation. After the transformation, the doubly occupied states have been projected out and the size of the Hilbert space has been reduced. For this effective Hamiltonian, the hopping amplitudes have been defined according to the manganite system which consists of three axes: x-, y- and z-axis. Since the ground-state properties of the effective Hamiltonian have been calculated only in one-dimension, then the results of this work have been separated in three cases; the electrons hopping in x, y and z axes respectively. The ground-state wavefunction of this effective Hamiltonian has been calculated by infinite density matrix renormalization group algorithm. This algorithm leads to the ground state at the thermodynamic limit when the number of sites is large. It has been found that the ground-state energies are equivalent in all hopping axes. Furthermore, the nearest neighbor orbital correlations at the ground state for all axes are antiferro-orbital.

Department Physics ..... Student's signature 

Field of study Physics ..... Advisor's signature 

Academic year 2005.....

# ACKNOWLEDGEMENTS

First I would like to express my wholehearted love to my father, mother and sister for their love and support. I would also like to thank my advisor Dr. Chatchai Srinitiwara Wong for introducing me to this subject and for being very helpful during all states of my work in this thesis. Besides, I want to mention my sincere thankfulness to Assoc. Prof. Wichit Sritrakool, Assist. Prof. Chaisingh Poo-Rakkiat and Dr. Tonphong Kaewkongka for many good suggestions in this thesis. In addition, I would like to thank all academics staff at the Physics Department for their helps. During this work on I have learned a lot of physics and many other skills as programming and solving the large project.

I would also like to thank Ms. Jarunee Nimmananukroh for morale and care that she gives me all the times. Finally, I want to thank all my friends who associate and share a common fate with me.



สถาบันวิทยบริการ  
จุฬาลงกรณ์มหาวิทยาลัย

# TABLE OF CONTENTS

Abstract (Thai) .....	iv
Abstract (English).....	v
Acknowledgements .....	vi
Table of Contents.....	vii
List of Figures.....	xi
List of Tables.....	xii
List of Symbols.....	xvi
Chapter	
I Introduction.....	1
II Double Degenerate Hubbard Model with Strong Correlation..	4
2.1 Orbital Bases .....	4
2.2 Orbital Hamiltonian .....	7
2.2.1 Two-orbital Hubbard model .....	7
2.2.2 Local basis and projection operators .....	8
2.2.3 Pseudo-spin operators .....	9
2.2.4 Hopping process .....	9
2.2.5 Canonical transformation .....	17

<b>III Density Matrix Renormalization Group</b> .....	<b>24</b>
3.1 Concept of DMRG . . . . .	24
3.2 Example: The Heisenberg Model . . . . .	33
3.3 Measurement . . . . .	41
3.3.1 Ground state energy . . . . .	41
3.3.2 Correlations . . . . .	43
<b>IV Ground State Properties of the Spinless Two-Orbital Hubbard Model in One Dimension</b> .....	<b>46</b>
4.1 Definition of Hopping Amplitude . . . . .	46
4.2 DMRG for Spinless Orbital Hubbard Model . . . . .	48
4.3 Comparing of Orbital and Spin Model . . . . .	51
4.4 Ground State Energy . . . . .	53
4.5 Order Parameters . . . . .	53
4.6 Orbital Correlation . . . . .	56
<b>V Summary and Conclusion</b> .....	<b>66</b>
<b>References</b> .....	<b>69</b>
<b>Appendices</b> . . . . .	<b>73</b>
<b>Appendix A : Hubbard Operators</b> .....	<b>73</b>
<b>Appendix B : Derivation</b> .....	<b>75</b>
B.1 Choosing of $S'$ . . . . .	75
B.2 Substitute $S'$ in $i[S', H_U]$ . . . . .	76
B.3 Execution with $\frac{i^2}{2}[S, [S, H_U]]$ . . . . .	76



<b>Appendix C: Flow Chart of DMRG</b> .....	<b>78</b>
<b>Appendix D: Hamiltonian in the First Loop</b> .....	<b>79</b>
D.1 Left Enlarged Block Hamiltonian . . . . .	79
D.1.1 The Electron Hopping Along x-Axis . . . . .	79
D.1.2 The Electron Hopping Along y-Axis . . . . .	80
D.1.3 The Electron Hopping Along z-Axis . . . . .	80
D.2 Superblock Block Hamiltonian . . . . .	81
D.2.1 The Electron Hopping Along x-Axis . . . . .	81
D.2.2 The Electron Hopping Along y-Axis . . . . .	82
D.2.3 The Electron Hopping Along z-Axis . . . . .	83
<b>Vitae</b> .....	<b>84</b>


  
 สถาบันวิทยบริการ  
 จุฬาลงกรณ์มหาวิทยาลัย

# LIST OF FIGURES

2.1	The Perovskite structure. . . . .	6
2.2	The shape $t_{2g}$ and $e_g$ orbitals. . . . .	6
3.1	The left enlarged block . . . . .	26
3.2	The superblock . . . . .	28
3.3	Constructing the new system block . . . . .	32
3.4	Constructing the new left enlarged block . . . . .	32
3.5	Constructing the new superblock . . . . .	33
3.6	A DMRG calculation from The average ground energy per site for antiferromagnetic spin 1/2 Heisenberg chain keeping various number of kept states. . . . .	42
3.7	Different position of the two operators on the left enlarged block. . . . .	44
4.1	Comparison of ground state of Spin model and Orbital model using DMRG by keeping 16 states. . . . .	52
4.2	Ground-state energy per site of the one-dimension spinless orbital Hubbard model are plotted in three axis, namely x-, y- and z-axis with 16 kept states and 2002 sites of infinite DMRG algorithm. The optimum of a number of iteration are considered from the time of calculation and the convergence of ground-state energy. . . . .	54
4.3	The extrapolation is used to finding the ground-state energy as $N \rightarrow \infty$ . . . . .	55
4.4	A plot of $\langle \hat{\tau}_i^z(\theta_i) \hat{\tau}_j^z(\theta_j) \rangle$ on x-axis in $\theta_i$ and $\theta_j$ space. . . . .	59

- 4.5 A plot of  $\langle \hat{\tau}_i^z(\theta_i) \hat{\tau}_j^z(\theta_j) \rangle$  on y-axis in  $\theta_i$  and  $\theta_j$  space. . . . . 60
- 4.6 A plot of  $\langle \hat{\tau}_i^z(\theta_i) \hat{\tau}_j^z(\theta_j) \rangle$  on z-axis in  $\theta_i$  and  $\theta_j$  space. . . . . 61
- 4.7 Shape of electron density of states  $\pm(\frac{1}{2}|a\rangle + \frac{\sqrt{3}}{2}|b\rangle) = \pm(\frac{1}{2}(x^2 - y^2) + \frac{\sqrt{3}}{2}(3z^2 - r^2))$  and  $-\frac{\sqrt{3}}{2}|a\rangle + \frac{1}{2}|b\rangle = -\frac{\sqrt{3}}{2}(x^2 - y^2) + \frac{1}{2}(3z^2 - r^2)$ . . . 63
- 4.8 Shape of electron density of states  $\pm(\frac{\sqrt{3}}{2}|a\rangle + \frac{1}{2}|b\rangle) = \pm(\frac{\sqrt{3}}{2}(x^2 - y^2) + \frac{1}{2}(3z^2 - r^2))$  and  $-\frac{1}{2}|a\rangle + \frac{\sqrt{3}}{2}|b\rangle = -\frac{1}{2}(x^2 - y^2) + \frac{\sqrt{3}}{2}(3z^2 - r^2)$ . 64
- 4.9 Shape of electron density of states  $\pm|a\rangle = \pm(x^2 - y^2)$  and  $|b\rangle = 3z^2 - r^2$ . . . . . 65



สถาบันวิทยบริการ  
จุฬาลงกรณ์มหาวิทยาลัย

# LIST OF TABLES

- 3.1 Difference of the average ground-state energy per site for antiferromagnetic spin 1/2 Heisenberg chain between a DMRG calculation and the exact result keeping different number of kept states. . . . . 43
- 4.1 DMRG calculation of the orbital correlation for ground state at one dimension setting the number of sites to be 2002 and considering peaks from Figure 4.4, 4.5 and 4.6,  $\theta_i$  and  $\theta_j$  are chosen from the maximum of the expectation value of the pseudo-spin correlation operator. . . . . 62



สถาบันวิทยบริการ  
จุฬาลงกรณ์มหาวิทยาลัย

# LIST OF SYMBOLS

$H_{\text{hop}}$	hopping Hamiltonian
$H_U$	coulomb Hamiltonian
$U$	coulomb potential
$\hat{n}_{ia(b)}$	number operator of an $a(b)$ -orbital electron at site $i$
$c_{ia(b)}^\dagger$	creation operator for an $a(b)$ -orbital electron at site $i$
$c_{ia(b)}$	annihilation operator for an $a(b)$ -orbital electron at site $i$
$\hat{P}_{i0(d)}$	projector operator of empty occupied (doubly occupied) state at site $i$
$\hat{P}_{ia(b)}$	projector operator of singly occupied state in orbital $a(b)$ at site $i$
$\hat{\tau}_i^+$	raising of pseudo-spin operator at site $i$
$\hat{\tau}_i^-$	lowering of pseudo-spin operator at site $i$
$\hat{\tau}_i^z$	pseudo-spin operator in $z$ -direction at site $i$
$t$	hopping amplitude
$t_{aa}$	hopping amplitude of an electron from $a$ -orbital at site $i$ to $a$ -orbital at site $j$
$t_{ab}$	hopping amplitude of an electron from $a$ -orbital at site $i$ to $b$ -orbital at site $j$
$t_{ba}$	hopping amplitude of an electron from $b$ -orbital at site $i$ to $a$ -orbital at site $j$
$t_{bb}$	hopping amplitude of an electron from $b$ -orbital at site $i$ to $b$ -orbital at site $j$
$H_t^+$	Hamiltonian of creating doubly occupied state
$H_{t_{aa}}^+$	Hamiltonian of creating doubly occupied state when an electron

	hops from $a$ -orbital at site $i$ to $a$ -orbital at site $j$
$H_{tab}^+$	Hamiltonian of creating doubly occupied state when an electron hops from $a$ -orbital at site $i$ to $b$ -orbital at site $j$
$H_{tba}^+$	Hamiltonian of creating doubly occupied state when an electron hops from $b$ -orbital at site $i$ to $a$ -orbital at site $j$
$H_{tbb}^+$	Hamiltonian of creating doubly occupied state when an electron hops from $b$ -orbital at site $i$ to $b$ -orbital at site $j$
$H_t^-$	Hamiltonian of annihilating doubly occupied state
$H_{taa}^-$	Hamiltonian of annihilating doubly occupied state when an electron hops from $a$ -orbital at site $i$ to $a$ -orbital at site $j$
$H_{tab}^-$	Hamiltonian of annihilating doubly occupied state when an electron hops from $a$ -orbital at site $i$ to $b$ -orbital at site $j$
$H_{tba}^-$	Hamiltonian of annihilating doubly occupied state when an electron hops from $b$ -orbital at site $i$ to $a$ -orbital at site $j$
$H_{tbb}^-$	Hamiltonian of annihilating doubly occupied state when an electron hops from $b$ -orbital at site $i$ to $b$ -orbital at site $j$
$H_t^0$	Hamiltonian of no change doubly occupied state
$H_{taa}^0$	Hamiltonian of no change doubly occupied state when an electron hops from $a$ -orbital at site $i$ to $a$ -orbital at site $j$
$H_{tab}^0$	Hamiltonian of no change doubly occupied state when an electron hops from $a$ -orbital at site $i$ to $b$ -orbital at site $j$
$H_{tba}^0$	Hamiltonian of no change doubly occupied state when an electron hops from $b$ -orbital at site $i$ to $a$ -orbital at site $j$
$H_{tbb}^0$	Hamiltonian of no change doubly occupied state when an electron hops from $b$ -orbital at site $i$ to $b$ -orbital at site $j$
$H_{\text{eff}}$	effective Hamiltonian

$S$	generator operator
$S'$	generator operator for the first order of hopping amplitude ( $t$ )
$S''$	generator operator for the second order of hopping amplitude ( $t^2$ )
$X_i^{0 \leftarrow a(b)}$	Hubbard operator when state at site $i$ change from $a(b)$ -orbital state to be empty state
$X_i^{a(b) \leftarrow 0}$	Hubbard operator when state at site $i$ change from empty state to be $a(b)$ -orbital state
$X_i^{d \leftarrow a(b)}$	Hubbard operator when state at site $i$ change from $a(b)$ -orbital state to be doubly occupied state
$X_i^{a(b) \leftarrow d}$	Hubbard operator when state at site $i$ change from doubly occupied state to be $a(b)$ -orbital state
$\bullet^d$	added site where $d$ is the number of states
$B_l^M$	system block where $l$ is the number of lattice site and $M$ is the number of state
$H_{S(M \times M)}$	Hamiltonian of system block of $M \times M$ dimension
$A_{S(M \times M)}$	operator on system block of $M \times M$ dimension
$A_{\bullet(d \times d)}$	operator on added site of $d \times d$ dimension
$H_{E(Md \times Md)}^L$	Hamiltonian of the left enlarged block of $Md \times Md$ dimension
$A_{E(Md \times Md)}^L$	operator on the left enlarged block of $Md \times Md$ dimension
$H_{E(Md \times Md)}^R$	Hamiltonian of the right enlarged block of $Md \times Md$ dimension
$A_{E(Md \times Md)}^R$	operator on the right enlarged block of $Md \times Md$ dimension
$\delta_{d \times d}$	unit matrix of $d \times d$ dimension
$\delta_{M \times M}$	unit matrix of $M \times M$ dimension
$\delta_{Md \times Md}$	unit matrix of $Md \times Md$ dimension
$\delta_b$	unit matrix which corresponds to the system block

$\delta_d$	unit matrix which corresponds to the added site
$\delta_E^L$	unit matrix which corresponds to the left enlarge block
$\delta_E^R$	unit matrix which corresponds to the right enlarge block
$H_{((Md)^2 \times (Md)^2)}^{\text{super}}$	Hamiltonian of superblock of $(Md)^2 \times (Md)^2$ dimension
$\rho$	density matrix
$O_{m \times Md}$	truncate matrix of $m \times Md$ dimension
$\hat{\tau}_{\bullet}^z$	$\hat{\tau}^z$ operator for the added site
$\hat{\tau}_S^z$	$\hat{\tau}^z$ operator for the system block
$(\hat{\tau}_{\bullet}^z)_E^L$	$\hat{\tau}^z$ operator for the added site in the left enlarged block
$(\hat{\tau}_{\bullet}^z)_E^R$	$\hat{\tau}^z$ operator for the added site in the right enlarged block
$\hat{\tau}_{\bullet}^+$	$\hat{\tau}^+$ operator for the added site
$\hat{\tau}_S^+$	$\hat{\tau}^+$ operator for the system block
$(\hat{\tau}_{\bullet}^+)_E^L$	$\hat{\tau}^+$ operator for the added site in the left enlarged block
$(\hat{\tau}_{\bullet}^+)_E^R$	$\hat{\tau}^+$ corresponding to the added site in the right enlarged block
$\hat{\tau}_{\bullet}^-$	$\hat{\tau}^-$ operator for the added site
$\hat{\tau}_S^-$	$\hat{\tau}^-$ operator for the system block
$(\hat{\tau}_{\bullet}^-)_E^L$	$\hat{\tau}^-$ operator for the added site in the left enlarged block
$(\hat{\tau}_{\bullet}^-)_E^R$	$\hat{\tau}^-$ operator for the added site in the right enlarged block
$\hat{\tau}^z(\theta)$	$\hat{\tau}^z$ operator for the new basis by rotating with $\theta$



# CHAPTER I

## INTRODUCTION

At present, the research on the transition metal oxide (TMO) compounds is one of very active fields since these compounds exhibit interesting phenomena such as colossal magnetoresistance, high temperature superconducting state and metal-insulator transition [1, 2]. These behaviors have been used to develop many high efficiency electronic devices. In the theoretical study of electronic behavior of TMO, we always consider a combination of charge, spin and orbital degree of freedoms via reasonable models. In strongly correlated  $3d$  transition metal oxides [3], it is found that the orbital degeneracy has a large effect on magnetic, structural and electrical properties. The degeneracy of the  $d$  electron level is associated with five orbitals in which two orbitals are  $d_{x^2-y^2}$  and  $d_{3z^2-r^2}$  orbitals. These orbitals have higher energy than other three orbitals,  $d_{xy}$ ,  $d_{yz}$  and  $d_{zx}$  orbitals. The  $d_{x^2-y^2}$  and  $d_{3z^2-r^2}$  orbitals are called  $e_g$  orbitals and  $d_{xy}$ ,  $d_{yz}$  and  $d_{zx}$  orbitals are called  $t_{2g}$  orbitals. One system that the orbital degrees of freedom is very important is the manganite compound  $\text{La}_{1-x}\text{Ca}_x\text{MnO}_3$  with perovskite structure. When  $x \sim 0.3$ , the orbital degrees of freedom is only considered because the magnetic phase is ferromagnetic. Then, the spin degrees of freedom has been neglected. In the theoretical studies of electronic behaviors of this system, many crucial models have been invented for describing these systems. The Hubbard model [4] is one of the popular models that has been used to study strong correlated electronic systems in many systems. When it includes the orbital degree of freedom, it has been called the orbital Hubbard model. Therefore, it has been used to study the

effect of orbital occupied by electrons in many conditions; in finite on-site coulomb potential  $U$  with full cubic symmetries by Yuan *et al.* [5], in the strong-coupling limit with full cubic symmetries by Horsch *et al.* [6] and in  $U \rightarrow \infty$  with finite size in 2D Hamiltonian by C. Srinithiwarawong and G. A. Gerhring [7]. These works considered the finite system size as a full cubic symmetries and 2D cluster and they studied the orbital ordering of the system in each case.

In this work we have calculated the ground-state properties of the two-orbital Hubbard model at large- $U$  limit and half-filling in one dimension. Assuming that the Hamiltonian is in the ferromagnetic phase and the orbital degrees of freedom ( $e_g$  orbitals) is described by a pseudo-spin operator. Before the calculation, the Hamiltonian has been transformed by canonical transformation approach [8] to reduce the complexity of the problem from the degenerated Hubbard model. Accordingly, we will get the effective Hamiltonian. The ground state of the effective Hamiltonian has been obtained by using the Density Matrix Renormalization Group method, invented by White [9] [10] in 1992, with infinite size algorithm and the ground state energy is extrapolated to the thermodynamic limit. Afterward, the obtained ground-state wave function is used to calculate the orbital correlation.

This thesis is organized as follows: The strong correlation of doubly degenerate Hubbard model is presented in Chapter II. In this chapter we will derive this model with orbital states at large- $U$  limit and half-filling in one dimension into the effective Hamiltonian in pseudo-spin representation which depends on the electronic moving axes (x-, y- and z-axis). The crucial method in this chapter is the canonical transformation. The Density Matrix Renormalization Group which is described in Chapter III is constructed and tested with Heisenberg spin chain model in which the exact ground state has been known. Moreover, we will define some operators to observe the electronic correlation in the ground state. The definition of hopping amplitudes in each directions used in this calculation, the comparison between spin and orbital models and the result of ground-state prop-

erties from these calculations are shown in Chapter IV. Finally, the summary and conclusion are contained in Chapter V.



สถาบันวิทยบริการ  
จุฬาลงกรณ์มหาวิทยาลัย

# CHAPTER II

## DOUBLE DEGENERATE HUBBARD MODEL WITH STRONG CORRELATION

In this chapter, we will discuss a derivation of two orbitals Hubbard Hamiltonian in the large- $U$  limit at half-filling. This model considers orbital degrees of freedom which represents the shape of the electron in solid. It is one of three attributes (spin, charge and orbital) being important ingredients for causing the variety of phenomena in the transition metal oxide such as high-temperature superconductivity and colossal magnetoresistance. The correlation and ordering of the electrons lead to the understanding of these behaviors. The manganite compound, which is one of the transition metal oxides, is an important example for studying the strong correlated electronic system. We start with explaining how the orbital states are defined. Next, the orbital Hubbard Hamiltonian is described and the effective Hamiltonian in the large- $U$  limit at half-filling is derived in which the pseudo-spin operators are used.

### 2.1 Orbital Bases

In this thesis, the manganite compound  $\text{La}_{1-x}\text{Ca}_x\text{MnO}_3$  [1], which is one of the transition metal oxides, is considered to be the model for strongly correlated elec-

tronics system. The effects of electron correlation are intensively studied.

When we examine the structure of  $\text{La}_{1-x}\text{Ca}_x\text{MnO}_3$ , it is found that the separation of energy bands is due to the manganese atoms that are surrounded by oxygen atoms. The perovskite structure is shown in Figure 2.1[11]. This effects the occupation of electrons in  $d$ -orbital. They are degenerated into two groups, namely the  $t_{2g}$  and the  $e_g$  orbitals shown in Figure 2.2 [13]. The  $t_{2g}$  have three suborbitals  $d_{xy}$ ,  $d_{yz}$  and  $d_{zx}$ . They have lower energy than the  $e_g$  orbital, which have two suborbitals being  $d_{3z^2-r^2}$  and  $d_{x^2-y^2}$ . The important property of this compound is the ferromagnetic alignment of spin of electrons when the Ca atom are suitably doped ( $x \sim 0.3$ ). Moreover, it is found that the  $t_{2g}$  orbital are fully filled with electrons while the  $e_g$  orbital has only one electron associated with it. Therefore we consider only the  $e_g$  orbital, which we will get the new degree of freedom calling the orbital degree of freedom. This degree of freedom is slightly different from the spin degree of freedom which is neglected because the system is in ferromagnetic phase. We will define the basis of  $e_g$  orbital state that behaves in a solid similar to that of the spin state. For convenience, we denote  $|d_{x^2-y^2}\rangle = |a\rangle$  and  $|d_{3z^2-r^2}\rangle = |b\rangle$  [3].

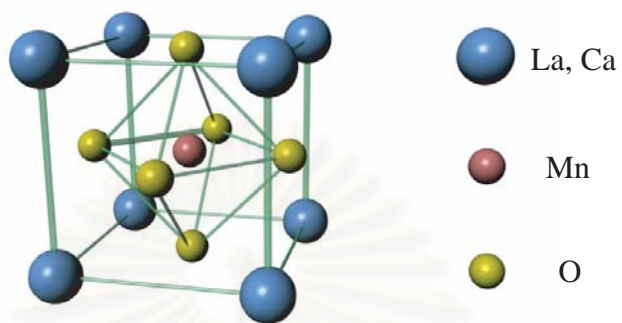
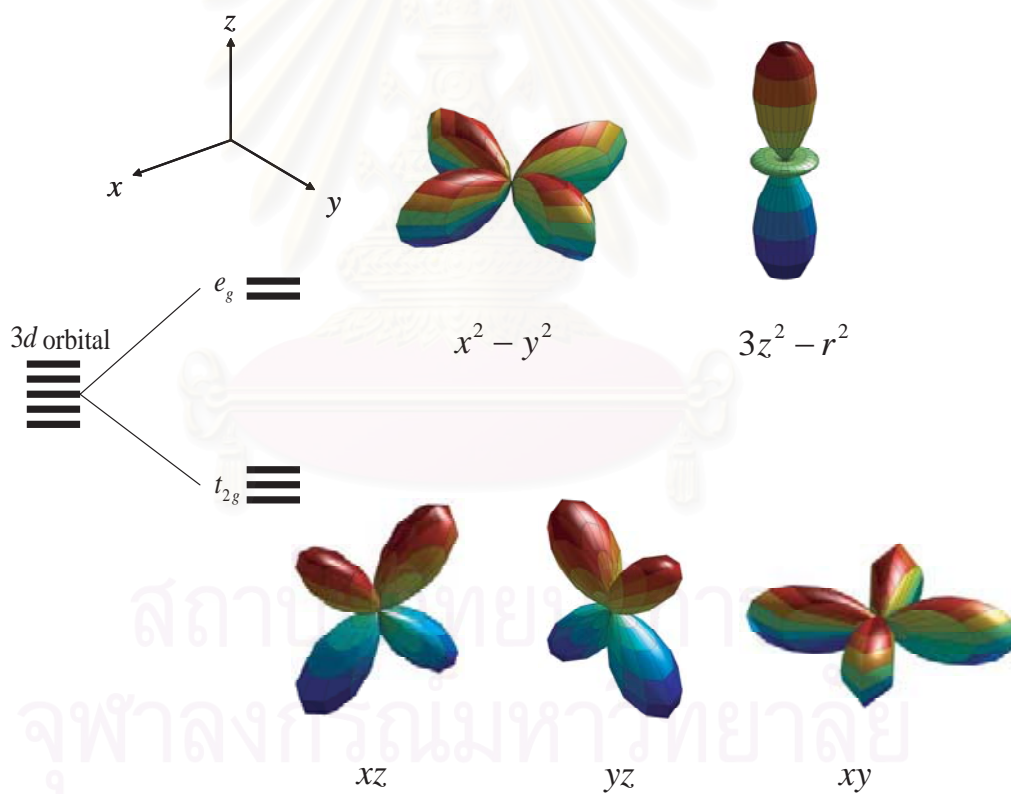


Figure 2.1: The Perovskite structure.

Figure 2.2: The shape  $t_{2g}$  and  $e_g$  orbitals.

## 2.2 Orbital Hamiltonian

As mentioned above, the  $e_g$  orbital states can be used to make the orbital Hamiltonian which will be explained in this section. First, all local bases that associate with the orbital exchange event and settings up the pseudo-spin in this system are elucidated. Second, we will create the hopping Hamiltonian terms to find the kinetic part. Next, the canonical transformation is used to evaluate the orbital Hamiltonian in large- $U$  limit and half-filling. Finally, we will derive the effective Hamiltonian in the form of pseudo-spins operators.

### 2.2.1 Two-orbital Hubbard model

In this thesis the ground state of the two-orbital Hubbard model [12, 14] for the case of one-dimensional chain is studied in the absence of spin degree of freedom. The Hamiltonian is written as

$$H = H_{\text{hop}} + H_U. \quad (2.1)$$

They are separated for the description of opposing tendencies: metallic and insulator phase. The  $H_U$  denotes the on-site interaction term, which can be written as

$$H_U = U \sum_i \hat{n}_{ia} \hat{n}_{ib}, \quad (2.2)$$

where  $\hat{n}_{ia(b)}$  is the number operator of an electron in  $a(b)$ -orbital at site  $i$ . This term explains the Coulomb repulsion among electrons sharing the same site, with  $U$  defines the Coulomb potential energy. The number operators are considered on the same site  $i$  at different orbitals. This term tends to resist the living of two electrons on the same site and leading to the insulator phase. In contrast, the  $H_{\text{hop}}$ , which denote the hopping of one electron to nearest neighbor site, brings about the metallic behaviors, which will be explained extensively in the next sections.

## 2.2.2 Local basis and projection operators

The states of electrons occupying on a particular site  $i$  are defined as four basis states in the followings:

$$|0\rangle_i \quad \text{empty state at site } i, (\text{No electron occupies at site } i) \quad (2.3)$$

$$|a\rangle_i = c_{ia}^\dagger |0\rangle_i \quad \text{electron occupies } a\text{-orbital at site } i, \quad (2.4)$$

$$|b\rangle_i = c_{ib}^\dagger |0\rangle_i \quad \text{electron occupies } b\text{-orbital at site } i, \quad (2.5)$$

$$|d\rangle_i = c_{ia}^\dagger c_{ib}^\dagger |0\rangle_i \quad \text{two electrons occupy both } a \text{ and } b\text{-orbital at site } i, \quad (2.6)$$

where  $c_{ia(b)}^\dagger$  is a creation operator which create an electron at site  $i$  with  $a(b)$  orbital. Note that  $c_{ib}^\dagger c_{ia}^\dagger$  also represents the doubly occupied state, however, according to (2.6) the relations  $c_{ia}^\dagger c_{ib}^\dagger |0\rangle_i = -c_{ib}^\dagger c_{ia}^\dagger |0\rangle_i$  and  $c_{ib}^\dagger c_{ia}^\dagger |0\rangle_i = -|d\rangle_i$  hold.

To describe the motion of electrons, the projector operators will be defined as

$$\hat{P}_{i0} = |0\rangle_{ii}\langle 0| = (1 - \hat{n}_{ia})(1 - \hat{n}_{ib}), \quad (2.7)$$

$$\hat{P}_{ia} = |a\rangle_{ii}\langle a| = \hat{n}_{ia}(1 - \hat{n}_{ib}), \quad (2.8)$$

$$\hat{P}_{ib} = |b\rangle_{ii}\langle b| = \hat{n}_{ib}(1 - \hat{n}_{ia}), \quad (2.9)$$

$$\hat{P}_{id} = |d\rangle_{ii}\langle d| = \hat{n}_{ia}\hat{n}_{ib}. \quad (2.10)$$

Where  $\hat{n}_{i\sigma}$  is the number operator at site  $i$  and orbital  $\sigma$  which defined as  $\hat{n}_{i\sigma} = c_{i\sigma}^\dagger c_{i\sigma}$ . Therefore the summation over all the local projector operators are equal to the unit operator

$$\hat{P}_{i0} + \hat{P}_{ia} + \hat{P}_{ib} + \hat{P}_{id} = \hat{1}. \quad (2.11)$$

All four basis states are chosen to be orthonormal on-site, that is

$$\langle 0|a\rangle = 0, \quad \langle 0|b\rangle = 0, \quad \langle 0|d\rangle = 0,$$

$$\langle a|a\rangle = 1, \quad \langle a|b\rangle = 0, \quad \langle a|d\rangle = 0,$$

$$\langle b|a\rangle = 0, \quad \langle b|b\rangle = 1, \quad \langle b|d\rangle = 0,$$

$$\langle d|a\rangle = 0, \quad \langle d|b\rangle = 0, \quad \langle d|d\rangle = 1.$$



### 2.2.3 Pseudo-spin operators

As the local states in Hamiltonian Eq. (2.1) involves the orbital of electrons, the operators that act on these states can be represented by a set pseudo-spin operators  $\vec{\tau}$  [3]. When orbital  $d_{x^2-y^2}$  is occupied,  $\hat{\tau}^z|d_{x^2-y^2}\rangle = \frac{1}{2}|d_{x^2-y^2}\rangle$  and when orbital  $d_{3z^2-r^2}$  is occupied,  $\hat{\tau}^z|d_{3z^2-r^2}\rangle = -\frac{1}{2}|d_{3z^2-r^2}\rangle$ . It is found that these operators have the commutation relation similar to that of the spin- $\frac{1}{2}$  operators, that is  $[\hat{\tau}^x, \hat{\tau}^y] = i\hat{\tau}^z$ . When  $|a\rangle = |d_{x^2-y^2}\rangle$  and  $|b\rangle = |d_{3z^2-r^2}\rangle$ , the raising and lowering of pseudo-spin operators being  $\hat{\tau}^+$  and  $\hat{\tau}^-$  are defined as

$$\begin{aligned}
 \hat{\tau}^+|a\rangle &= 0, \\
 \hat{\tau}^+|b\rangle &= |a\rangle, \\
 \hat{\tau}^-|a\rangle &= |b\rangle, \\
 \hat{\tau}^-|b\rangle &= 0, \\
 \hat{\tau}^z|a\rangle &= \frac{1}{2}|a\rangle, \\
 \hat{\tau}^z|b\rangle &= -\frac{1}{2}|b\rangle.
 \end{aligned} \tag{2.12}$$

These relations can be written in terms of the creation and annihilation operators as

$$\begin{aligned}
 \hat{\tau}^z &= \frac{1}{2}(c_{ia}^\dagger c_{ia} - c_{ib}^\dagger c_{ib}), \\
 \hat{\tau}^+ &= c_{ia}^\dagger c_{ib}, \\
 \hat{\tau}^- &= c_{ib}^\dagger c_{ia}, \\
 \hat{n}_i &= c_{ia}^\dagger c_{ia} + c_{ib}^\dagger c_{ib}.
 \end{aligned} \tag{2.13}$$

### 2.2.4 Hopping process

All possible hopping processes in two-orbital Hubbard model which correspond to the doubly occupied state are separated into three parts; creating, annihilating, and the processes that do not change the number of doubly occupied sites. In

order to simplify the study, the projection operators in Eqs. (2.7) - (2.10) are used.

The creation of doubly occupied site can be written in terms of a *projected hopping term*. When local bases in Eqs. (2.3) - (2.6) are used, all possible processes are shown in the diagrams below.

$$\begin{array}{ccc}
 \begin{array}{c} \overbrace{\hspace{2cm}}^{t_{aa}} \\ \boxed{\begin{array}{|c|c|} \hline \mathbf{a} & \mathbf{b} \\ \hline \end{array}} & \longrightarrow & \boxed{\begin{array}{|c|c|} \hline \mathbf{0} & \mathbf{d} \\ \hline \end{array}} \\
 \begin{array}{cc} \mathbf{i} & \mathbf{j} \end{array} & & \begin{array}{cc} \mathbf{i} & \mathbf{j} \end{array} \\
 \hat{P}_{i0}\hat{P}_{jd}c_{ja}^\dagger c_{ia}\hat{P}_{ia}\hat{P}_{jb} \Rightarrow \hat{P}_{jd}c_{ja}^\dagger c_{ia}\hat{P}_{ia} & & 
 \end{array} \quad (2.14)$$

$$\begin{array}{ccc}
 \begin{array}{c} \overbrace{\hspace{2cm}}^{t_{bb}} \\ \boxed{\begin{array}{|c|c|} \hline \mathbf{b} & \mathbf{a} \\ \hline \end{array}} & \longrightarrow & \boxed{\begin{array}{|c|c|} \hline \mathbf{0} & \mathbf{d} \\ \hline \end{array}} \\
 \begin{array}{cc} \mathbf{i} & \mathbf{j} \end{array} & & \begin{array}{cc} \mathbf{i} & \mathbf{j} \end{array} \\
 \hat{P}_{i0}\hat{P}_{jd}c_{jb}^\dagger c_{ib}\hat{P}_{ib}\hat{P}_{ja} \Rightarrow \hat{P}_{jd}c_{jb}^\dagger c_{ib}\hat{P}_{ib} & & 
 \end{array} \quad (2.15)$$

$$\begin{array}{ccc}
 \begin{array}{c} \overbrace{\hspace{2cm}}^{t_{ab}} \\ \boxed{\begin{array}{|c|c|} \hline \mathbf{a} & \mathbf{a} \\ \hline \end{array}} & \longrightarrow & \boxed{\begin{array}{|c|c|} \hline \mathbf{0} & \mathbf{d} \\ \hline \end{array}} \\
 \begin{array}{cc} \mathbf{i} & \mathbf{j} \end{array} & & \begin{array}{cc} \mathbf{i} & \mathbf{j} \end{array} \\
 \hat{P}_{i0}\hat{P}_{jd}c_{ja}^\dagger c_{ib}\hat{P}_{ia}\hat{P}_{ja} \Rightarrow \hat{P}_{jd}c_{jb}^\dagger c_{ia}\hat{P}_{ia} & & 
 \end{array} \quad (2.16)$$

$$\begin{array}{ccc}
 \begin{array}{c} \overbrace{\hspace{2cm}}^{t_{ba}} \\ \boxed{\begin{array}{|c|c|} \hline \mathbf{b} & \mathbf{b} \\ \hline \end{array}} & \longrightarrow & \boxed{\begin{array}{|c|c|} \hline \mathbf{0} & \mathbf{d} \\ \hline \end{array}} \\
 \begin{array}{cc} \mathbf{i} & \mathbf{j} \end{array} & & \begin{array}{cc} \mathbf{i} & \mathbf{j} \end{array} \\
 \hat{P}_{i0}\hat{P}_{jd}c_{ja}^\dagger c_{ib}\hat{P}_{ib}\hat{P}_{jb} \Rightarrow \hat{P}_{jd}c_{ja}^\dagger c_{ib}\hat{P}_{ib} & & 
 \end{array} \quad (2.17)$$

From observing an electronic transfer between sites, these processes can be classified into two types. The first case in Eq. (2.14) and Eq. (2.15), the hopping

electron does not change the orbital as it shifts from site  $i$  to  $j$ . Whereas the process has shown in Eq. (2.16) and Eq. (2.17), the hopping electron changes the orbital after moving from site  $i$  to  $j$ .

In Eqs. (2.14) - (2.17), the left hand side is a full projection operator form when we consider states at both sites (  $i$  and  $j$  ) before and after the hopping. However, only the states of exchanged electron before and after hopping are considered then *projected hopping terms* can be rewritten as short terms which are shown in the right hand side of Eqs. (2.14) - (2.17). For instance in Eq. (2.14), the *projected hopping terms* can be reduced to  $\hat{P}_{jd}c_{ja}^\dagger c_{ia}\hat{P}_{ia}$ . It means that the electron before hopping is in  $a$ -state at site  $i$  and after hopping it is in  $d$ -state at site  $j$ .

Using the definition of projection operators defined in Eqs. (2.7) - (2.10), one can modify the *projected hopping terms* to be the *number operator hopping terms* which will be

$$\hat{P}_{jd}c_{ja}^\dagger c_{ia}\hat{P}_{ia} = \hat{n}_{ja}\hat{n}_{jb}c_{ja}^\dagger c_{ia}\hat{n}_{ia}(1 - \hat{n}_{ib}) = \hat{n}_{jb}c_{ja}^\dagger c_{ia}(1 - \hat{n}_{ib}), \quad (2.18)$$

$$\hat{P}_{jd}c_{jb}^\dagger c_{ib}\hat{P}_{ib} = \hat{n}_{ja}\hat{n}_{jb}c_{jb}^\dagger c_{ib}\hat{n}_{ib}(1 - \hat{n}_{ia}) = \hat{n}_{ja}c_{jb}^\dagger c_{ib}(1 - \hat{n}_{ia}), \quad (2.19)$$

$$\hat{P}_{jd}c_{jb}^\dagger c_{ia}\hat{P}_{ia} = \hat{n}_{ja}\hat{n}_{jb}c_{jb}^\dagger c_{ia}\hat{n}_{ia}(1 - \hat{n}_{ib}) = \hat{n}_{ja}c_{jb}^\dagger c_{ia}(1 - \hat{n}_{ib}), \quad (2.20)$$

$$\hat{P}_{jd}c_{ja}^\dagger c_{ib}\hat{P}_{ib} = \hat{n}_{ja}\hat{n}_{jb}c_{ja}^\dagger c_{ib}\hat{n}_{ib}(1 - \hat{n}_{ia}) = \hat{n}_{jb}c_{ja}^\dagger c_{ib}(1 - \hat{n}_{ia}). \quad (2.21)$$

All the hopping terms creating a doubly occupied sites can be written as

$$H_{taa}^+ = -t_{aa} \sum_{\langle ij \rangle} \{ \hat{n}_{ib}c_{ia}^\dagger c_{ja}(1 - \hat{n}_{jb}) + H.c. \}, \quad (2.22)$$

$$H_{tbb}^+ = -t_{bb} \sum_{\langle ij \rangle} \{ \hat{n}_{ia}c_{ib}^\dagger c_{jb}(1 - \hat{n}_{ja}) + H.c. \}, \quad (2.23)$$

$$H_{tab}^+ = -t_{ab} \sum_{\langle ij \rangle} \{ \hat{n}_{ib}c_{ia}^\dagger c_{jb}(1 - \hat{n}_{ja}) + \hat{n}_{ja}c_{jb}^\dagger c_{ia}(1 - \hat{n}_{ib}) \}, \quad (2.24)$$

$$H_{tba}^+ = -t_{ba} \sum_{\langle ij \rangle} \{ \hat{n}_{ia}c_{ib}^\dagger c_{ja}(1 - \hat{n}_{jb}) + \hat{n}_{jb}c_{ja}^\dagger c_{ib}(1 - \hat{n}_{ia}) \}, \quad (2.25)$$

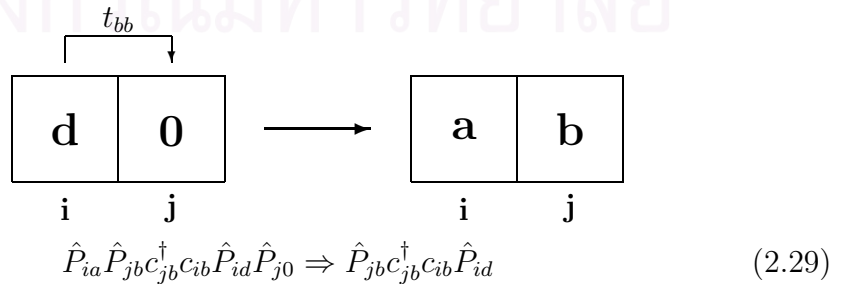
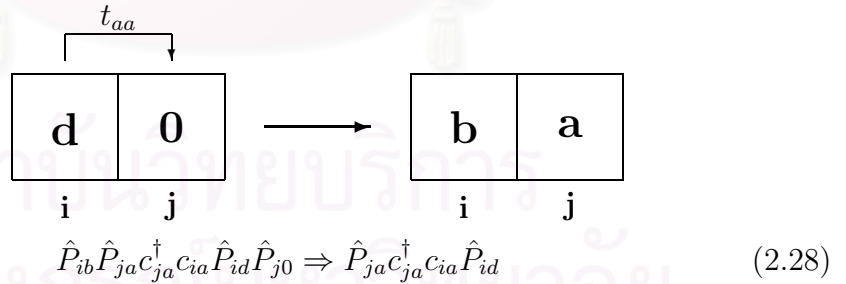
where  $t_{aa}$ ,  $t_{bb}$ ,  $t_{ab}$  and  $t_{ba}$  are the kinetic energy parameters according to the exchange of electrons among sites. Besides, the letters *H.c.* denote the Hermitian conjugate of the immediately preceding term. For instance,  $t_{aa}$  means that when the electron hops from orbital  $a$  at site  $i$  to the orbital  $a$  at site  $j$  it will use energy  $t_{aa}$  per one hopping. If site  $j$  has an electron orbital  $b$ , this site will be a doubly occupied site after the hopping. But if site  $j$  does not have an electron, it will have an electron at orbital  $a$  on site  $j$  after the hopping. It can be written in a general form as follows

$$H_{t_{\sigma,\sigma}}^+ = - \sum_{\langle ij \rangle} \sum_{\sigma} t_{\sigma,\sigma} \{ \hat{n}_{i,-\sigma} c_{i\sigma}^\dagger c_{j\sigma} (1 - \hat{n}_{j,-\sigma}) + H.c. \}, \quad (2.26)$$

$$H_{t_{\sigma,-\sigma}}^+ = - \sum_{\langle ij \rangle} \sum_{\sigma} t_{\sigma,-\sigma} \{ \hat{n}_{i-\sigma} c_{i\sigma}^\dagger c_{j,-\sigma} (1 - \hat{n}_{j\sigma}) + \hat{n}_{j\sigma} c_{j,-\sigma}^\dagger c_{i\sigma} (1 - \hat{n}_{i,-\sigma}) \}, \quad (2.27)$$

where  $\langle i, j \rangle$  means that the summation is taken only over the pair of nearest neighbor sites and  $\sigma$  means  $a(b)$ -orbital,  $-\sigma$  is  $b(a)$ -orbital. They sum over all orbital degrees of freedom which have the two states ( $a$  and  $b$  orbital).

Like the processes in 2.14 - 2.17, the processes of decreasing doubly occupied sites are as the followings:



$$\begin{array}{ccc}
\begin{array}{|c|c|} \hline & t_{ab} \\ \hline \mathbf{d} & \mathbf{0} \\ \hline \mathbf{i} & \mathbf{j} \\ \hline \end{array} & \longrightarrow & \begin{array}{|c|c|} \hline \mathbf{b} & \mathbf{b} \\ \hline \mathbf{i} & \mathbf{j} \\ \hline \end{array} \\
\hat{P}_{ib}\hat{P}_{jb}c_{ja}^\dagger c_{ib}\hat{P}_{id}\hat{P}_{j0} & \Rightarrow & \hat{P}_{jb}c_{jb}^\dagger c_{ia}\hat{P}_{id}
\end{array} \quad (2.30)$$

$$\begin{array}{ccc}
\begin{array}{|c|c|} \hline & t_{ba} \\ \hline \mathbf{d} & \mathbf{0} \\ \hline \mathbf{i} & \mathbf{j} \\ \hline \end{array} & \longrightarrow & \begin{array}{|c|c|} \hline \mathbf{a} & \mathbf{a} \\ \hline \mathbf{i} & \mathbf{j} \\ \hline \end{array} \\
\hat{P}_{ia}\hat{P}_{ja}c_{ja}^\dagger c_{ib}\hat{P}_{id}\hat{P}_{j0} & \Rightarrow & \hat{P}_{ja}c_{jb}^\dagger c_{ia}\hat{P}_{id}
\end{array} \quad (2.31)$$

When the change of electron orbital is considered before and after hopping, the process is divided into two types.

As in the case of creating doubly occupied site the processes in Eqs. (2.28)-(2.31) can be written in the number operator terms as

$$\hat{P}_{ja}c_{ja}^\dagger c_{ia}\hat{P}_{id} = \hat{n}_{ja}(1 - \hat{n}_{jb})c_{ja}^\dagger c_{ia}\hat{n}_{ia}\hat{n}_{ib} = (1 - \hat{n}_{jb})c_{ja}^\dagger c_{ia}\hat{n}_{ib}, \quad (2.32)$$

$$\hat{P}_{jb}c_{jb}^\dagger c_{ib}\hat{P}_{id} = \hat{n}_{jb}(1 - \hat{n}_{ja})c_{jb}^\dagger c_{ib}\hat{n}_{ia}\hat{n}_{ib} = (1 - \hat{n}_{ja})c_{jb}^\dagger c_{ib}\hat{n}_{ia}, \quad (2.33)$$

$$\hat{P}_{jb}c_{jb}^\dagger c_{ia}\hat{P}_{id} = \hat{n}_{jb}(1 - \hat{n}_{ja})c_{jb}^\dagger c_{ia}\hat{n}_{ia}\hat{n}_{ib} = (1 - \hat{n}_{ja})c_{jb}^\dagger c_{ia}\hat{n}_{ib}, \quad (2.34)$$

$$\hat{P}_{ja}c_{ja}^\dagger c_{ib}\hat{P}_{id} = \hat{n}_{ja}(1 - \hat{n}_{jb})c_{ja}^\dagger c_{ib}\hat{n}_{ia}\hat{n}_{ib} = (1 - \hat{n}_{jb})c_{ja}^\dagger c_{ib}\hat{n}_{ia}. \quad (2.35)$$

Consequently, the hopping terms become

$$H_{taa}^- = -t_{aa} \sum_{\langle ij \rangle} \{(1 - \hat{n}_{ib})c_{ia}^\dagger c_{ja}\hat{n}_{jb} + H.c.\}, \quad (2.36)$$

$$H_{tbb}^- = -t_{bb} \sum_{\langle ij \rangle} \{(1 - \hat{n}_{ia})c_{ib}^\dagger c_{jb}\hat{n}_{ja} + H.c.\}, \quad (2.37)$$

$$H_{tab}^- = -t_{ab} \sum_{\langle ij \rangle} \{(1 - \hat{n}_{ib})c_{ia}^\dagger c_{jb}\hat{n}_{ja} + (1 - \hat{n}_{ja})c_{jb}^\dagger c_{ia}\hat{n}_{ib}\}, \quad (2.38)$$

$$H_{tba}^- = -t_{ba} \sum_{\langle ij \rangle} \{(1 - \hat{n}_{ia})c_{ib}^\dagger c_{ja}\hat{n}_{jb} + (1 - \hat{n}_{jb})c_{ja}^\dagger c_{ib}\hat{n}_{ia}\}. \quad (2.39)$$

The general forms can be written as

$$H_{t_{\sigma,\sigma}}^- = - \sum_{\langle ij \rangle} \sum_{\sigma} t_{\sigma,\sigma} \{ (1 - \hat{n}_{i,-\sigma}) c_{i\sigma}^\dagger c_{j\sigma} \hat{n}_{j,-\sigma} + H.c. \}, \quad (2.40)$$

$$H_{t_{\sigma,-\sigma}}^- = - \sum_{\langle ij \rangle} \sum_{\sigma} t_{\sigma,-\sigma} \{ (1 - \hat{n}_{i-\sigma}) c_{i\sigma}^\dagger c_{j,-\sigma} \hat{n}_{j\sigma} + (1 - \hat{n}_{j\sigma}) c_{j,-\sigma}^\dagger c_{i\sigma} \hat{n}_{i,-\sigma} \}. \quad (2.41)$$

Another hopping processes which do not change the number of doubly occupied sites is shown below.

$$\begin{array}{ccc}
 \begin{array}{c} \overbrace{\hspace{2cm}}^{t_{aa}} \\ \boxed{\begin{array}{|c|c|} \hline \mathbf{d} & \mathbf{b} \\ \hline \mathbf{i} & \mathbf{j} \end{array}} & \longrightarrow & \boxed{\begin{array}{|c|c|} \hline \mathbf{b} & \mathbf{d} \\ \hline \mathbf{i} & \mathbf{j} \end{array}} \\
 \end{array} \\
 \hat{P}_{id} \hat{P}_{jb} c_{ja}^\dagger c_{ia} \hat{P}_{ib} \hat{P}_{jd} \Rightarrow \hat{P}_{jd} c_{ja}^\dagger c_{ia} \hat{P}_{id} \quad (2.42)
 \end{array}$$

$$\begin{array}{ccc}
 \begin{array}{c} \overbrace{\hspace{2cm}}^{t_{aa}} \\ \boxed{\begin{array}{|c|c|} \hline \mathbf{a} & \mathbf{0} \\ \hline \mathbf{i} & \mathbf{j} \end{array}} & \longrightarrow & \boxed{\begin{array}{|c|c|} \hline \mathbf{0} & \mathbf{a} \\ \hline \mathbf{i} & \mathbf{j} \end{array}} \\
 \end{array} \\
 \hat{P}_{ia} \hat{P}_{j0} c_{ja}^\dagger c_{ia} \hat{P}_{i0} \hat{P}_{ja} \Rightarrow \hat{P}_{ja} c_{ja}^\dagger c_{ia} \hat{P}_{ia} \quad (2.43)
 \end{array}$$

$$\begin{array}{ccc}
 \begin{array}{c} \overbrace{\hspace{2cm}}^{t_{bb}} \\ \boxed{\begin{array}{|c|c|} \hline \mathbf{d} & \mathbf{a} \\ \hline \mathbf{i} & \mathbf{j} \end{array}} & \longrightarrow & \boxed{\begin{array}{|c|c|} \hline \mathbf{a} & \mathbf{d} \\ \hline \mathbf{i} & \mathbf{j} \end{array}} \\
 \end{array} \\
 \hat{P}_{id} \hat{P}_{ja} c_{jb}^\dagger c_{ib} \hat{P}_{ib} \hat{P}_{jd} \Rightarrow \hat{P}_{jd} c_{jb}^\dagger c_{ib} \hat{P}_{id} \quad (2.44)
 \end{array}$$

$$\begin{array}{ccc}
 \begin{array}{c} \overbrace{\hspace{2cm}}^{t_{bb}} \\ \boxed{\begin{array}{|c|c|} \hline \mathbf{b} & \mathbf{0} \\ \hline \mathbf{i} & \mathbf{j} \end{array}} & \longrightarrow & \boxed{\begin{array}{|c|c|} \hline \mathbf{0} & \mathbf{b} \\ \hline \mathbf{i} & \mathbf{j} \end{array}} \\
 \end{array} \\
 \hat{P}_{ib} \hat{P}_{j0} c_{jb}^\dagger c_{ib} \hat{P}_{i0} \hat{P}_{jb} \Rightarrow \hat{P}_{jb} c_{jb}^\dagger c_{ib} \hat{P}_{ib} \quad (2.45)
 \end{array}$$

$$\begin{array}{ccc}
 \begin{array}{|c|c|} \hline & t_{ab} \\ \hline \text{d} & \text{a} \\ \hline \text{i} & \text{j} \\ \hline \end{array} & \longrightarrow & \begin{array}{|c|c|} \hline \text{b} & \text{d} \\ \hline \text{i} & \text{j} \\ \hline \end{array} \\
 \hat{P}_{id}\hat{P}_{ja}c_{jb}^\dagger c_{ia}\hat{P}_{ib}\hat{P}_{jd} & \Rightarrow & \hat{P}_{jd}c_{jb}^\dagger c_{ia}\hat{P}_{id}
 \end{array} \quad (2.46)$$

$$\begin{array}{ccc}
 \begin{array}{|c|c|} \hline & t_{ab} \\ \hline \text{a} & \text{0} \\ \hline \text{i} & \text{j} \\ \hline \end{array} & \longrightarrow & \begin{array}{|c|c|} \hline \text{0} & \text{b} \\ \hline \text{i} & \text{j} \\ \hline \end{array} \\
 \hat{P}_{ia}\hat{P}_{j0}c_{jb}^\dagger c_{ia}\hat{P}_{i0}\hat{P}_{jb} & \Rightarrow & \hat{P}_{jb}c_{jb}^\dagger c_{ia}\hat{P}_{ia}
 \end{array} \quad (2.47)$$

$$\begin{array}{ccc}
 \begin{array}{|c|c|} \hline & t_{ba} \\ \hline \text{d} & \text{b} \\ \hline \text{i} & \text{j} \\ \hline \end{array} & \longrightarrow & \begin{array}{|c|c|} \hline \text{a} & \text{d} \\ \hline \text{i} & \text{j} \\ \hline \end{array} \\
 \hat{P}_{id}\hat{P}_{jb}c_{ja}^\dagger c_{ib}\hat{P}_{ia}\hat{P}_{jd} & \Rightarrow & \hat{P}_{jd}c_{ja}^\dagger c_{ib}\hat{P}_{id}
 \end{array} \quad (2.48)$$

$$\begin{array}{ccc}
 \begin{array}{|c|c|} \hline & t_{ba} \\ \hline \text{b} & \text{0} \\ \hline \text{i} & \text{j} \\ \hline \end{array} & \longrightarrow & \begin{array}{|c|c|} \hline \text{0} & \text{a} \\ \hline \text{i} & \text{j} \\ \hline \end{array} \\
 \hat{P}_{ib}\hat{P}_{j0}c_{ja}^\dagger c_{ib}\hat{P}_{i0}\hat{P}_{ja} & \Rightarrow & \hat{P}_{jd}c_{ja}^\dagger c_{ib}\hat{P}_{id}
 \end{array} \quad (2.49)$$

These processes can be written in term of projected hopping terms as

สถาบันวิทยบริการ  
จุฬาลงกรณ์มหาวิทยาลัย

$$\hat{P}_{jd}c_{ja}^\dagger c_{ia}\hat{P}_{id} = \hat{n}_{ja}\hat{n}_{jb}c_{ja}^\dagger c_{ia}\hat{n}_{ia}\hat{n}_{ib} = \hat{n}_{jb}c_{ja}^\dagger c_{ia}\hat{n}_{ib}, \quad (2.50)$$

$$\hat{P}_{ja}c_{ja}^\dagger c_{ia}\hat{P}_{ia} = \hat{n}_{ja}(1 - \hat{n}_{jb})c_{ja}^\dagger c_{ia}\hat{n}_{ia}(1 - \hat{n}_{ib}) = (1 - \hat{n}_{jb})c_{ja}^\dagger c_{ia}(1 - \hat{n}_{ib}), \quad (2.51)$$

$$\hat{P}_{jd}c_{jb}^\dagger c_{ib}\hat{P}_{id} = \hat{n}_{ja}\hat{n}_{jb}c_{jb}^\dagger c_{ib}\hat{n}_{ia}\hat{n}_{ib} = \hat{n}_{ja}c_{jb}^\dagger c_{ib}\hat{n}_{ia}, \quad (2.52)$$

$$\hat{P}_{jb}c_{jb}^\dagger c_{ib}\hat{P}_{ib} = \hat{n}_{jb}(1 - \hat{n}_{ja})c_{jb}^\dagger c_{ib}\hat{n}_{ib}(1 - \hat{n}_{ia}) = (1 - \hat{n}_{ja})c_{jb}^\dagger c_{ib}(1 - \hat{n}_{ia}), \quad (2.53)$$

$$\hat{P}_{ja}c_{jb}^\dagger c_{ia}\hat{P}_{id} = \hat{n}_{ja}\hat{n}_{jb}c_{jb}^\dagger c_{ia}\hat{n}_{ia}\hat{n}_{ib} = \hat{n}_{ja}c_{jb}^\dagger c_{ia}\hat{n}_{ib}, \quad (2.54)$$

$$\hat{P}_{jb}c_{jb}^\dagger c_{ia}\hat{P}_{ia} = \hat{n}_{jb}(1 - \hat{n}_{ja})c_{jb}^\dagger c_{ia}\hat{n}_{ia}(1 - \hat{n}_{ib}) = (1 - \hat{n}_{ja})c_{jb}^\dagger c_{ia}(1 - \hat{n}_{ib}), \quad (2.55)$$

$$\hat{P}_{jd}c_{ja}^\dagger c_{ib}\hat{P}_{id} = \hat{n}_{ja}\hat{n}_{jb}c_{ja}^\dagger c_{ib}\hat{n}_{ia}\hat{n}_{ib} = \hat{n}_{jb}c_{ja}^\dagger c_{ib}\hat{n}_{ia}, \quad (2.56)$$

$$\hat{P}_{ja}c_{ja}^\dagger c_{ib}\hat{P}_{ib} = \hat{n}_{ja}(1 - \hat{n}_{jb})c_{ja}^\dagger c_{ib}\hat{n}_{ib}(1 - \hat{n}_{ia}) = (1 - \hat{n}_{jb})c_{ja}^\dagger c_{ib}(1 - \hat{n}_{ia}). \quad (2.57)$$

Moreover, they can be written in form of the Hamiltonian as

$$H_{taa}^0 = -t_{aa} \sum_{\langle ij \rangle} \{ \hat{n}_{ib}c_{ia}^\dagger c_{ja}\hat{n}_{jb} + (1 - \hat{n}_{ib})c_{ia}^\dagger c_{ja}(1 - \hat{n}_{jb}) + H.c. \}, \quad (2.58)$$

$$H_{tbb}^0 = -t_{bb} \sum_{\langle ij \rangle} \{ \hat{n}_{ia}c_{ib}^\dagger c_{jb}\hat{n}_{ja} + (1 - \hat{n}_{ia})c_{ib}^\dagger c_{jb}(1 - \hat{n}_{ja}) + H.c. \}, \quad (2.59)$$

$$H_{tab}^0 = -t_{ab} \sum_{\langle ij \rangle} \{ \hat{n}_{ib}c_{ia}^\dagger c_{jb}\hat{n}_{ja} + (1 - \hat{n}_{ib})c_{ia}^\dagger c_{jb}(1 - \hat{n}_{ja}) \\ + \hat{n}_{ja}c_{jb}^\dagger c_{ia}\hat{n}_{ib} + (1 - \hat{n}_{ja})c_{jb}^\dagger c_{ia}(1 - \hat{n}_{ib}) \}, \quad (2.60)$$

$$H_{tba}^0 = -t_{ba} \sum_{\langle ij \rangle} \{ \hat{n}_{ia}c_{ib}^\dagger c_{ja}\hat{n}_{jb} + (1 - \hat{n}_{ia})c_{ib}^\dagger c_{ja}(1 - \hat{n}_{jb}) \\ + \hat{n}_{jb}c_{ja}^\dagger c_{ib}\hat{n}_{ia} + (1 - \hat{n}_{jb})c_{ja}^\dagger c_{ib}(1 - \hat{n}_{ia}) \}. \quad (2.61)$$

Finally, the general cases are given by

$$H_{t\sigma,\sigma}^0 = - \sum_{\langle ij \rangle} \sum_{\sigma} t_{\sigma,\sigma} \{ \hat{n}_{i,-\sigma}c_{i\sigma}^\dagger c_{j\sigma}\hat{n}_{j,-\sigma} + (1 - \hat{n}_{i,-\sigma})c_{i\sigma}^\dagger c_{j\sigma}(1 - \hat{n}_{j,-\sigma}) + H.c. \}, \quad (2.62)$$

$$H_{t\sigma,-\sigma}^0 = - \sum_{\langle ij \rangle} \sum_{\sigma} t_{\sigma,-\sigma} \{ \hat{n}_{i,-\sigma}c_{i\sigma}^\dagger c_{j,-\sigma}\hat{n}_{j\sigma} + (1 - \hat{n}_{i,-\sigma})c_{i\sigma}^\dagger c_{j,-\sigma}(1 - \hat{n}_{j\sigma}) \\ + \hat{n}_{j\sigma}c_{j,-\sigma}^\dagger c_{i\sigma}\hat{n}_{i,-\sigma} + (1 - \hat{n}_{j\sigma})c_{j,-\sigma}^\dagger c_{i\sigma}(1 - \hat{n}_{i,-\sigma}) \}. \quad (2.63)$$

To sum up, all possible types of hopping events can be written as

$$H_{\text{hop}} = \sum_{\sigma} \{ H_{t\sigma,\sigma}^+ + H_{t\sigma,-\sigma}^+ + H_{t\sigma,\sigma}^- + H_{t\sigma,-\sigma}^- + H_{t\sigma,\sigma}^0 + H_{t\sigma,-\sigma}^0 \}. \quad (2.64)$$



### 2.2.5 Canonical transformation

When the strongly correlated electrons system are considered, the mixed states between the two subbands, doubly occupied and singly occupied subbands, will appear due to the hopping Hamiltonian; creating and annihilating the doubly occupied states respectively as shown in Eqs. (2.26) - (2.27) and (2.40) - (2.41). We need to separate these mix states . Therefore the canonical transformation method [8, 12] is introduced to solve this problem. The unmixed states can be found by rotating to such a new suitable basis. According to Eqs. (2.2) and (2.64) in the orbital basis, the two-orbitals Hubbard Hamiltonian can be written as

$$H = \sum_{\sigma} (H_{t_{\sigma,\sigma}}^+ + H_{t_{\sigma,-\sigma}}^+ + H_{t_{\sigma,\sigma}}^- + H_{t_{\sigma,-\sigma}}^- + H_{t_{\sigma,\sigma}}^0 + H_{t_{\sigma,-\sigma}}^0) + H_U, \quad (2.65)$$

when index  $\sigma$  refers to two orbitals ( $a$  and  $b$ ). It can be written as

$$\begin{aligned} H = & H_{t_{aa}}^+ + H_{t_{ab}}^+ + H_{t_{ba}}^+ + H_{t_{bb}}^+ + H_{t_{aa}}^- + H_{t_{ab}}^- + H_{t_{ba}}^- + H_{t_{bb}}^- \\ & + H_{t_{aa}}^0 + H_{t_{ab}}^0 + H_{t_{ba}}^0 + H_{t_{bb}}^0 + H_U. \end{aligned} \quad (2.66)$$

For convenience, the hopping Hamiltonian can be written as

$$H_t^+ = H_{t_{aa}}^+ + H_{t_{ab}}^+ + H_{t_{ba}}^+ + H_{t_{bb}}^+, \quad (2.67)$$

$$H_t^- = H_{t_{aa}}^- + H_{t_{ab}}^- + H_{t_{ba}}^- + H_{t_{bb}}^-, \quad (2.68)$$

$$H_t^0 = H_{t_{aa}}^0 + H_{t_{ab}}^0 + H_{t_{ba}}^0 + H_{t_{bb}}^0. \quad (2.69)$$

Then, the Hubbard model can be rewritten as

$$H = H_t^+ + H_t^- + H_t^0 + H_U. \quad (2.70)$$

Hamiltonian in Eq. (2.70) is used to find the Hamiltonian which have two conditions: large- $U$  limit and half-filling. This Hamiltonian is called *effective Hamiltonian*

$$H_{\text{eff}} = e^{iS} H e^{-iS} = H + i[S, H] + \frac{i^2}{2}[S, [S, H]] + \dots \quad (2.71)$$

$$\begin{aligned}
H_{\text{eff}} &= H_U + H_t^+ + H_t^- + H_t^0 + i[S, H_U] \\
&+ i[S, H_t^+ + H_t^- + H_t^0] + \frac{i^2}{2}[S, [S, H]] + \dots
\end{aligned} \tag{2.72}$$

The generator  $S$  is chosen as to assure that  $H_{\text{eff}}$  does not connect to different subbands. The largest cross-terms,  $H_t^+$  and  $H_t^-$ , should be eliminated. They are canceled from the commuted term,  $i[S, H_U]$ . This condition will be brought to find the suitable generator  $S$ . Terms with orders of  $t$  higher than 2 are neglected. The generator  $S$  is separated into two parts being  $S = S' + S''$ . We will let that  $S'$  and  $S''$  are in the order of  $t$  and  $t^2$  respectively where  $t$  is the hopping amplitude in all cases of an electron hopping between two sites. From Appendix. B, operator  $S'$  can be chosen to be

$$S' = \frac{-i}{U}(H_t^+ - H_t^-), \tag{2.73}$$

From Eq. (2.73) term of  $i[S, H_U]$  which is replaced by  $S = S' + S''$ , becomes

$$i[S, H_U] = i[S', H_U] + i[S'', H_U]. \tag{2.74}$$

The first term of the right-hand side is demonstrated in Appendix. B as being

$$i[S', H_U] = -(H_t^+ + H_t^-). \tag{2.75}$$

While, the second term of the right-hand side comes from the definition of operator  $i[S'', H_U]$  as

$$i[S'', H_U] = -\frac{1}{U}[H_t^+ - H_t^-, H_t^0]. \tag{2.76}$$

Moreover, we get

$$i[S, H_t^+ + H_t^- + H_t^0] = i[S', H_t^+ + H_t^- + H_t^0] + i[S'', H_t^+ + H_t^- + H_t^0]. \tag{2.77}$$

The first term of the right-hand side which is the order of  $t^2$  can be separated into two parts. They become

$$i[S', H_t^+ + H_t^-] = \frac{2}{U}[H_t^+, H_t^-], \tag{2.78}$$

and

$$i[S', H_t^0] = \frac{1}{U}[H_t^+ - H_t^-, H_t^0], \tag{2.79}$$

where Eq. (2.79) is canceled by Eq. (2.76). Moreover, the second term of the right hand side in Eq. (2.77) has disappeared because it is of the order  $t^3$ .

Besides, the term of  $\frac{i^2}{2}[S, [S, H_U]]$  is demonstrated in Appendix. B as

$$\frac{i^2}{2}[S, [S, H_U]] = -\frac{1}{U}[H_t^+, H_t^-]. \quad (2.80)$$

Finally, substituting Eqs. (2.75), (2.76), (2.78), (2.79) and (2.80) into Eq. (2.72), the effective Hamiltonian to the order of  $t^2$  can be written as

$$H_{\text{eff}} = H_t^0 + H_U + \frac{1}{U}[H_t^+, H_t^-]. \quad (2.81)$$

When  $H_t^+$ ,  $H_t^-$  and  $H_t^0$  in Eq. (2.81) are replaced with the full terms from Eqs. (2.67)- (2.69), the effective Hamiltonian is rewritten as

$$\begin{aligned} H_{\text{eff}} &= H_{t_{aa}}^0 + H_{t_{ab}}^0 + H_{t_{ba}}^0 + H_{t_{bb}}^0 + H_U \\ &+ \frac{1}{U}[H_{t_{aa}}^+ + H_{t_{ab}}^+ + H_{t_{ba}}^+ + H_{t_{bb}}^+, H_{t_{aa}}^- + H_{t_{ab}}^- + H_{t_{ba}}^- + H_{t_{bb}}^-]. \end{aligned} \quad (2.82)$$

This model is the two orbital Hubbard model.

In this thesis, the orbital Hubbard model for the ground state is considered in the large- $U$  limit and half-filled. Therefore, the term of  $H_t^0$  and  $H_U$ , which be up against these conditions, are neglected. Then, we will only evaluate  $\frac{1}{U}[H_{t_{aa}}^+ + H_{t_{ab}}^+ + H_{t_{ba}}^+ + H_{t_{bb}}^+, H_{t_{aa}}^- + H_{t_{ab}}^- + H_{t_{ba}}^- + H_{t_{bb}}^-]$  by replacing with Eqs. (2.22) - (2.23) and (2.36) - (2.37). For convenience, the suitable tool so-called Hubbard operators are used for this evaluation. The Hubbard operator properties are shown in Appendix. A. For example, the operator  $\hat{n}_{ib}c_{ia}^\dagger c_{ja}(1 - \hat{n}_{jb})$ , when replaced by the Hubbard operators, is written as

$$\begin{aligned} &X_i^{b\leftarrow b} X_j^{a\leftarrow a} (X_i^{a\leftarrow 0} + X_i^{d\leftarrow b})(X_j^{0\leftarrow a} + X_j^{b\leftarrow d}) X_j^{a\leftarrow a} X_i^{b\leftarrow b} \\ &= X_i^{d\leftarrow b} X_j^{0\leftarrow a}. \end{aligned} \quad (2.83)$$

As results from Eqs. (A.4) - (A.7), the hopping Hamiltonian in Eqs. (2.22) - (2.25) can be written as

$$H_{t_{aa}}^+ = -t_{aa} \sum_{\langle ij \rangle} \{X_i^{d\leftarrow b} X_j^{0\leftarrow a} + X_j^{d\leftarrow b} X_i^{0\leftarrow a}\}, \quad (2.84)$$

$$H_{tab}^+ = -t_{ab} \sum_{\langle ij \rangle} \{X_i^{d \leftarrow b} X_j^{0 \leftarrow b} - X_j^{d \leftarrow a} X_i^{0 \leftarrow a}\}, \quad (2.85)$$

$$H_{tba}^+ = -t_{ba} \sum_{\langle ij \rangle} \{-X_i^{d \leftarrow a} X_j^{0 \leftarrow a} + X_j^{d \leftarrow b} X_i^{0 \leftarrow b}\}, \quad (2.86)$$

$$H_{tbb}^+ = -t_{bb} \sum_{\langle ij \rangle} \{-(X_i^{d \leftarrow a} X_j^{0 \leftarrow b} + X_j^{d \leftarrow a} X_i^{0 \leftarrow b})\}. \quad (2.87)$$

Using the function  $\eta(\sigma)$  defined in Eq. (A.10), we get

$$H_t^+ = H_{taa}^+ + H_{tab}^+ + H_{tba}^+ + H_{tbb}^+ \quad (2.88)$$

$$\begin{aligned} H_t^+ &= - \sum_{\langle ij \rangle} \sum_{\sigma} \{t_{\sigma\sigma} \eta(\sigma) (X_i^{d \leftarrow -\sigma} X_j^{0 \leftarrow -\sigma} + X_j^{d \leftarrow -\sigma} X_i^{0 \leftarrow -\sigma}) \\ &+ t_{\sigma-\sigma} (\eta(\sigma) X_i^{d \leftarrow -\sigma} X_j^{0 \leftarrow -\sigma} + \eta(-\sigma) X_j^{d \leftarrow \sigma} X_i^{0 \leftarrow \sigma})\}. \end{aligned} \quad (2.89)$$

Similarly, the Hamiltonians that decrease the number of doubly occupied site is written as

$$H_{taa}^- = -t_{aa} \sum_{\langle ij \rangle} \{X_i^{a \leftarrow 0} X_j^{b \leftarrow d} + X_j^{a \leftarrow 0} X_i^{b \leftarrow d}\}, \quad (2.90)$$

$$H_{tab}^- = -t_{ab} \sum_{\langle ij \rangle} \{-X_i^{a \leftarrow 0} X_j^{a \leftarrow d} + X_j^{b \leftarrow 0} X_i^{b \leftarrow d}\}, \quad (2.91)$$

$$H_{tba}^- = -t_{ba} \sum_{\langle ij \rangle} \{X_i^{b \leftarrow 0} X_j^{b \leftarrow d} - X_j^{a \leftarrow 0} X_i^{a \leftarrow d}\}, \quad (2.92)$$

$$H_{tbb}^- = -t_{bb} \sum_{\langle ij \rangle} \{-(X_i^{b \leftarrow 0} X_j^{a \leftarrow d} + X_j^{b \leftarrow 0} X_i^{a \leftarrow d})\}. \quad (2.93)$$

Finally we get

$$H_t^- = H_{taa}^- + H_{tab}^- + H_{tba}^- + H_{tbb}^- \quad (2.94)$$

$$\begin{aligned} H_t^- &= - \sum_{\langle ij \rangle} \sum_{\sigma} \{t_{\sigma\sigma} \eta(\sigma) (X_i^{\sigma \leftarrow 0} X_j^{-\sigma \leftarrow d} + X_j^{\sigma \leftarrow 0} X_i^{-\sigma \leftarrow d}) \\ &+ t_{\sigma-\sigma} (\eta(-\sigma) X_i^{\sigma \leftarrow 0} X_j^{\sigma \leftarrow d} + \eta(\sigma) X_j^{-\sigma \leftarrow 0} X_i^{-\sigma \leftarrow d})\}. \end{aligned} \quad (2.95)$$

The important term in the large- $U$  limit and half-filling of  $H_{\text{eff}}$  is  $\frac{1}{U}[H_t^+, H_t^-]$ , this is  $H_t^+ H_t^- - H_t^- H_t^+$ . Since we are interested in half filling, the Hilbert of the effective Hamiltonian will contain only single occupied state. The  $H_t^+ H_t^-$  term is neglected since the value of operator  $H_t^+ H_t^-$  operates on this Hilbert space will

be zero. So, the remaining term which becomes the effective Hamiltonian is only  $H_t^- H_t^+$ . We will replace the index  $\sigma'$  into  $\sigma$  in Eq. (2.95) as

$$\begin{aligned} H_t^- &= - \sum_{\langle ij \rangle} \sum_{\sigma'} \{ t_{\sigma' \sigma'} \eta(\sigma') (X_i^{\sigma' \leftarrow 0} X_j^{-\sigma' \leftarrow d} + X_j^{\sigma' \leftarrow 0} X_i^{-\sigma' \leftarrow d}) \\ &+ t_{\sigma' -\sigma'} (\eta(-\sigma') X_i^{\sigma' \leftarrow 0} X_j^{\sigma' \leftarrow d} + \eta(\sigma') X_j^{-\sigma' \leftarrow 0} X_i^{-\sigma' \leftarrow d}) \}. \end{aligned} \quad (2.96)$$

We use Eqs. (2.96) and (2.89) for substituting in  $-\frac{1}{U} H_t^- H_t^+$  to get

$$\begin{aligned} -\frac{1}{U} H_t^- H_t^+ &= - \sum_{\langle ij \rangle} \sum_{\sigma'} \sum_{\sigma} \left\{ \frac{t_{\sigma' \sigma'} t_{\sigma \sigma}}{U} \eta(\sigma') \eta(\sigma) (X_j^{\sigma' \leftarrow 0} X_i^{-\sigma' \leftarrow d} X_i^{d \leftarrow -\sigma} X_j^{0 \leftarrow \sigma}) \right. \\ &+ \frac{t_{\sigma' \sigma'} t_{\sigma -\sigma}}{U} \eta(\sigma') \eta(\sigma) (X_j^{\sigma' \leftarrow 0} X_i^{-\sigma' \leftarrow d} X_i^{d \leftarrow -\sigma} X_j^{0 \leftarrow -\sigma}) \\ &+ \frac{t_{\sigma' -\sigma'} t_{\sigma \sigma}}{U} \eta(\sigma') \eta(\sigma) (X_j^{-\sigma' \leftarrow 0} X_i^{-\sigma' \leftarrow d} X_i^{d \leftarrow -\sigma} X_j^{0 \leftarrow \sigma}) \\ &+ \frac{t_{\sigma' -\sigma'} t_{\sigma -\sigma}}{U} \eta(\sigma') \eta(\sigma) (X_j^{-\sigma' \leftarrow 0} X_i^{-\sigma' \leftarrow d} X_i^{d \leftarrow -\sigma} X_j^{0 \leftarrow -\sigma}) \\ &+ \frac{t_{\sigma' \sigma'} t_{\sigma \sigma}}{U} \eta(\sigma') \eta(\sigma) (X_i^{\sigma' \leftarrow 0} X_j^{-\sigma' \leftarrow d} X_j^{d \leftarrow -\sigma} X_i^{0 \leftarrow \sigma}) \\ &+ \frac{t_{\sigma' \sigma'} t_{\sigma -\sigma}}{U} \eta(\sigma') \eta(-\sigma) (X_i^{\sigma' \leftarrow 0} X_j^{-\sigma' \leftarrow d} X_j^{d \leftarrow \sigma} X_i^{0 \leftarrow \sigma}) \\ &+ \frac{t_{\sigma' -\sigma'} t_{\sigma \sigma}}{U} \eta(-\sigma') \eta(\sigma) (X_i^{\sigma' \leftarrow 0} X_j^{\sigma' \leftarrow d} X_j^{d \leftarrow -\sigma} X_i^{0 \leftarrow \sigma}) \\ &+ \left. \frac{t_{\sigma' -\sigma'} t_{\sigma -\sigma}}{U} \eta(-\sigma') \eta(-\sigma) (X_i^{\sigma' \leftarrow 0} X_j^{\sigma' \leftarrow d} X_j^{d \leftarrow \sigma} X_i^{0 \leftarrow \sigma}) \right\}. \end{aligned} \quad (2.97)$$

Eq. (2.97) can be solved from Eq. (A.3) as

$$\begin{aligned} -\frac{1}{U} H_t^- H_t^+ &= - \sum_{\langle ij \rangle} \sum_{\sigma'} \sum_{\sigma} \left\{ \frac{t_{\sigma' \sigma'} t_{\sigma \sigma}}{U} \eta(\sigma') \eta(\sigma) (X_i^{-\sigma' \leftarrow -\sigma} X_j^{\sigma' \leftarrow \sigma}) \right. \\ &+ \frac{t_{\sigma' \sigma'} t_{\sigma -\sigma}}{U} \eta(\sigma') \eta(-\sigma) (X_i^{-\sigma' \leftarrow \sigma} X_j^{\sigma' \leftarrow \sigma}) \\ &+ \frac{t_{\sigma' -\sigma'} t_{\sigma \sigma}}{U} \eta(\sigma') \eta(\sigma) (X_i^{-\sigma' \leftarrow -\sigma} X_j^{-\sigma' \leftarrow \sigma}) \\ &+ \frac{t_{\sigma' -\sigma'} t_{\sigma -\sigma}}{U} \eta(\sigma') \eta(-\sigma) (X_i^{-\sigma' \leftarrow \sigma} X_j^{-\sigma' \leftarrow \sigma}) \\ &+ \frac{t_{\sigma' \sigma'} t_{\sigma \sigma}}{U} \eta(\sigma') \eta(\sigma) (X_i^{\sigma' \leftarrow \sigma} X_j^{-\sigma' \leftarrow -\sigma}) \\ &+ \frac{t_{\sigma' \sigma'} t_{\sigma -\sigma}}{U} \eta(\sigma') \eta(-\sigma) (X_i^{\sigma' \leftarrow \sigma} X_j^{-\sigma' \leftarrow \sigma}) \\ &+ \frac{t_{\sigma' -\sigma'} t_{\sigma \sigma}}{U} \eta(-\sigma') \eta(\sigma) (X_i^{\sigma' \leftarrow -\sigma} X_j^{\sigma' \leftarrow -\sigma}) \\ &+ \left. \frac{t_{\sigma' -\sigma'} t_{\sigma -\sigma}}{U} \eta(-\sigma') \eta(-\sigma) (X_i^{\sigma' \leftarrow \sigma} X_j^{\sigma' \leftarrow \sigma}) \right\}. \end{aligned} \quad (2.98)$$

We will replace  $\sigma' = \sigma$  and  $\sigma' = -\sigma$  in Eq. (2.98)

$$\begin{aligned}
-\frac{1}{U}H_t^-H_t^+ &= \sum_{\langle ij \rangle} \left\{ -\sum_{\sigma} \frac{t_{\sigma\sigma}^2}{U} X_i^{\sigma\leftarrow-\sigma} X_j^{\sigma\leftarrow\sigma} + \sum_{\sigma} \frac{t_{\sigma\sigma} t_{\sigma-\sigma}}{U} X_i^{\sigma\leftarrow\sigma} X_j^{\sigma\leftarrow\sigma} \right. \\
&- \sum_{\sigma} \frac{t_{\sigma-\sigma} t_{\sigma\sigma}}{U} X_i^{\sigma\leftarrow-\sigma} X_j^{\sigma\leftarrow\sigma} + \sum_{\sigma} \frac{t_{\sigma-\sigma}^2}{U} X_i^{\sigma\leftarrow\sigma} X_j^{\sigma\leftarrow\sigma} \\
&+ \sum_{\sigma} \frac{t_{\sigma-\sigma} t_{\sigma\sigma}}{U} X_i^{\sigma\leftarrow-\sigma} X_j^{\sigma\leftarrow\sigma} - \sum_{\sigma} \frac{t_{\sigma-\sigma} t_{\sigma-\sigma}}{U} X_i^{\sigma\leftarrow\sigma} X_j^{\sigma\leftarrow\sigma} \\
&+ \sum_{\sigma} \frac{t_{\sigma\sigma} t_{\sigma\sigma}}{U} X_i^{\sigma\leftarrow-\sigma} X_j^{\sigma\leftarrow\sigma} - \sum_{\sigma} \frac{t_{\sigma\sigma} t_{\sigma-\sigma}}{U} X_i^{\sigma\leftarrow\sigma} X_j^{\sigma\leftarrow\sigma} \\
&- \sum_{\sigma} \frac{t_{\sigma\sigma}^2}{U} X_i^{\sigma\leftarrow\sigma} X_j^{\sigma\leftarrow-\sigma} + \sum_{\sigma} \frac{t_{\sigma\sigma} t_{\sigma-\sigma}}{U} X_i^{\sigma\leftarrow\sigma} X_j^{\sigma\leftarrow\sigma} \\
&+ \sum_{\sigma} \frac{t_{\sigma-\sigma} t_{\sigma\sigma}}{U} X_i^{\sigma\leftarrow\sigma} X_j^{\sigma\leftarrow-\sigma} - \sum_{\sigma} \frac{t_{\sigma-\sigma}^2}{U} X_i^{\sigma\leftarrow\sigma} X_j^{\sigma\leftarrow\sigma} \\
&+ \sum_{\sigma} \frac{t_{\sigma-\sigma} t_{\sigma\sigma}}{U} X_i^{\sigma\leftarrow\sigma} X_j^{\sigma\leftarrow-\sigma} - \sum_{\sigma} \frac{t_{\sigma-\sigma} t_{\sigma-\sigma}}{U} X_i^{\sigma\leftarrow\sigma} X_j^{\sigma\leftarrow\sigma} \\
&\left. - \sum_{\sigma} \frac{t_{\sigma\sigma} t_{\sigma\sigma}}{U} X_i^{\sigma\leftarrow\sigma} X_j^{\sigma\leftarrow-\sigma} + \sum_{\sigma} \frac{t_{\sigma\sigma} t_{\sigma-\sigma}}{U} X_i^{\sigma\leftarrow\sigma} X_j^{\sigma\leftarrow\sigma} \right\}. \quad (2.99)
\end{aligned}$$

When the *effective Hamiltonian* is considered by replacing  $\sigma$  with  $a$  and  $b$  orbital; therefore  $H_{\text{eff}}$  is written as

$$\begin{aligned}
H_{\text{eff}} &= \sum_{\langle ij \rangle} \left\{ -\frac{t_{aa}^2}{U} X_i^{b\leftarrow b} X_j^{a\leftarrow a} - \frac{t_{bb}^2}{U} X_i^{a\leftarrow a} X_j^{b\leftarrow b} \right. \\
&+ \frac{t_{aa} t_{ab}}{U} X_i^{b\leftarrow a} X_j^{a\leftarrow a} + \frac{t_{bb} t_{ba}}{U} X_i^{a\leftarrow b} X_j^{b\leftarrow b} \\
&- \frac{t_{ab} t_{aa}}{U} X_i^{b\leftarrow b} X_j^{b\leftarrow a} - \frac{t_{ba} t_{bb}}{U} X_i^{a\leftarrow a} X_j^{a\leftarrow b} \\
&+ \frac{t_{ab}^2}{U} X_i^{b\leftarrow a} X_j^{b\leftarrow a} + \frac{t_{ba}^2}{U} X_i^{a\leftarrow b} X_j^{a\leftarrow b} \\
&+ \frac{t_{bb} t_{aa}}{U} X_i^{a\leftarrow b} X_j^{b\leftarrow a} + \frac{t_{aa} t_{bb}}{U} X_i^{b\leftarrow a} X_j^{a\leftarrow b} \\
&- \frac{t_{bb} t_{ab}}{U} X_i^{a\leftarrow a} X_j^{b\leftarrow a} - \frac{t_{aa} t_{ba}}{U} X_i^{b\leftarrow b} X_j^{a\leftarrow b} \\
&+ \frac{t_{ba} t_{aa}}{U} X_i^{a\leftarrow b} X_j^{a\leftarrow a} + \frac{t_{ab} t_{bb}}{U} X_i^{b\leftarrow a} X_j^{b\leftarrow b} \\
&- \frac{t_{ba} t_{ab}}{U} X_i^{a\leftarrow a} X_j^{a\leftarrow a} - \frac{t_{ab} t_{ba}}{U} X_i^{b\leftarrow b} X_j^{b\leftarrow b} \\
&\left. - \frac{t_{aa}^2}{U} X_i^{a\leftarrow a} X_j^{b\leftarrow b} - \frac{t_{bb}^2}{U} X_i^{b\leftarrow b} X_j^{a\leftarrow a} \right\}
\end{aligned}$$

$$\begin{aligned}
& + \frac{t_{aa}t_{ab}}{U} X_i^{a\leftarrow a} X_j^{b\leftarrow a} + \frac{t_{bb}t_{ba}}{U} X_i^{b\leftarrow b} X_j^{a\leftarrow b} \\
& + \frac{t_{ab}t_{aa}}{U} X_i^{a\leftarrow a} X_j^{a\leftarrow b} + \frac{t_{ba}t_{bb}}{U} X_i^{b\leftarrow b} X_j^{b\leftarrow a} \\
& + \frac{t_{ab}^2}{U} X_i^{a\leftarrow a} X_j^{a\leftarrow a} + \frac{t_{ba}^2}{U} X_i^{b\leftarrow b} X_j^{b\leftarrow b} \\
& + \frac{t_{bb}t_{aa}}{U} X_i^{b\leftarrow a} X_j^{a\leftarrow b} + \frac{t_{aa}t_{bb}}{U} X_i^{a\leftarrow b} X_j^{b\leftarrow a} \\
& - \frac{t_{bb}t_{ab}}{U} X_i^{b\leftarrow a} X_j^{a\leftarrow a} - \frac{t_{aa}t_{ba}}{U} X_i^{a\leftarrow b} X_j^{b\leftarrow b} \\
& - \frac{t_{ba}t_{aa}}{U} X_i^{b\leftarrow a} X_j^{b\leftarrow b} - \frac{t_{ab}t_{bb}}{U} X_i^{a\leftarrow b} X_j^{a\leftarrow a} \\
& + \frac{t_{ba}t_{ab}}{U} X_i^{b\leftarrow a} X_j^{b\leftarrow a} + \frac{t_{ab}t_{ba}}{U} X_i^{a\leftarrow b} X_j^{a\leftarrow b} \}. \tag{2.100}
\end{aligned}$$

Substituting Eqs. (2.13) and (A.11) into Eq. (2.100), after some rearrangements the effective Hamiltonian can be written in terms of pseudo-spin operators ,

$$\begin{aligned}
H_{\text{eff}} & = \sum_{\langle ij \rangle} \left\{ \frac{2}{U} (t_{aa}^2 + t_{bb}^2) (\hat{\tau}_i^z \hat{\tau}_j^z - \frac{\hat{n}_i \hat{n}_j}{4}) - \frac{2(t_{ab}^2 + t_{ba}^2)}{U} (\hat{\tau}_i^z \hat{\tau}_j^z + \frac{\hat{n}_i \hat{n}_j}{4}) \right. \\
& + \frac{2t_{ab}t_{ba}}{U} (\hat{\tau}_i^+ \hat{\tau}_j^+ + \hat{\tau}_i^- \hat{\tau}_j^-) + \frac{2t_{aa}t_{bb}}{U} (\hat{\tau}_i^+ \hat{\tau}_j^- + \hat{\tau}_i^- \hat{\tau}_j^+) \\
& + 2 \left( \frac{t_{aa}t_{ab}}{U} - \frac{t_{bb}t_{ba}}{U} \right) \{ (\hat{\tau}_i^z \hat{\tau}_j^+ + \hat{\tau}_i^z \hat{\tau}_j^-) \} \\
& \left. + 2 \left( \frac{t_{aa}t_{ba}}{U} - \frac{t_{bb}t_{ab}}{U} \right) \{ (\hat{\tau}_i^+ \hat{\tau}_j^z + \hat{\tau}_i^- \hat{\tau}_j^z) \} \right\}, \tag{2.101}
\end{aligned}$$

where  $\hat{\tau}_{i(j)}^z$ ,  $\hat{\tau}_{i(j)}^+$  and  $\hat{\tau}_{i(j)}^-$  are the pseudo-spin operators at site  $i(j)$ . This Hamiltonian will be used to calculate the ground state in the next chapter.

สถาบันวิทยบริการ  
จุฬาลงกรณ์มหาวิทยาลัย

# CHAPTER III

## DENSITY MATRIX RENORMALIZATION GROUP

In this chapter, the Density Matrix Renormalization Group (DMRG) algorithm, which is the main method to find the ground-state properties of the spinless two orbital Hubbard model from Chapter two in this work, is described. We begin with the basic idea of DMRG. This idea is used to the study of low-dimensional quantum systems. In the second section, the infinite system algorithm, which is one of the algorithm of DMRG used in this work, is explained. Next, the DMRG method is applied to a simple model (the Heisenberg spin chain model). In the last section, the measured parameters associated with the ground state of the system obtained by DMRG method are described.

### 3.1 Concept of DMRG

In the study of real space lattice systems in which the number of included basis states depend on the system size, if the system size is large, more number of the included basis states are needed. Many approaches have been used for studying these systems, one of them is the numerical methods. However, the problems of calculation are found when the number of bases increases exponentially as the system size is increased. Consequently, the studying of lattice systems approaching to the thermodynamic limits are impossible as a results of the memory restriction



and the computer run time. The Density Matrix Renormalization Group (DMRG) is one method which rectifies this problem. It was invented by White [9] in 1992. The main idea of DMRG methods is to calculate some target states (e.g. ground state) of the lattice system using only some of the basis states. These basis states extremely affect the target state. Thus, if we keep only the most relevant basis states by neglecting the less influential ones, this method provides highly accurate results. Therefore, the number of basis states used in this method is smaller than the exact number of the basis states in the system. As a result the related dimension of effective Hilbert space is restricted even if we increase the system size. In order to choose the relevant basis states, the density matrix is used. This approach is proposed by White and Noack [10].

The original DMRG is used to solve 1D lattices models to find the ground-state properties in the real space [15, 16, 17, 18]. In recent years, the DMRG has been used successfully and adopted to solve various 1D and coupled chain problems, such as the spin chain [19], strongly correlated electron systems and Hubbard models [20].

The procedure of the DMRG method starts with system with small number of sites, in this case only 2 sites are considered. One is called "from system site" and the other is called "added site". These two sites are combined to be the left enlarged block. From the symmetric properties of the left enlarged block, the right enlarged block is defined. Then the left and right enlarged blocks are merged to be the superblock. The target state, which is one of all states in the superblock, is therefore can be calculated from the superblock. The next step after the target state is obtained, the density matrix is formed from the target state. The density matrix is used to consider the importance of basis states. Some basis states, which are not importance, are neglected. Then, the number of basis states, which correspond with calculation in ground state, are reduced. However, if the number of kept states are large, the error will be small. However, the large number of basis leads to the higher dimension of the Hilbert space. As a result, the restriction of

memory and time evidently affect the calculations. Therefore, the suitable kept number of bases are important.

These important bases will be used to create a new system block in the next iteration. Accordingly, the number of lattice site of the next system block will be two. In the next iteration, the number of system sites will be gradually increased by adding one lattice site to the system block in the left enlarged block. The iterative process has finished when the error is below a threshold or a desired number of lattice size. The DMRG details of process will be thoroughly explained in the next section.

The DMRG algorithm is used in two different systems, infinite and finite system [15, 16, 17, 18, 19, 20]. In this thesis, we will use only the infinite system in one dimension. Schematically, the algorithm can be described as follows:

1. Construct the left enlarged block  $B_l^M \bullet^d$ , consisting of the system block and one added site. The system block is denoted by  $B_l^M$  where  $l$  is lattice sites and  $M$  is the number of states. Moreover, if  $d$  denote the number of states at a single site, the system block of  $l$  sites has  $M = d^l$  states and denoted by  $B_l^{d^l}$ . While, the added site is denoted as  $\bullet^d$  where  $d$  is the number of states. The left enlarged block is shown in Figure 3.1.

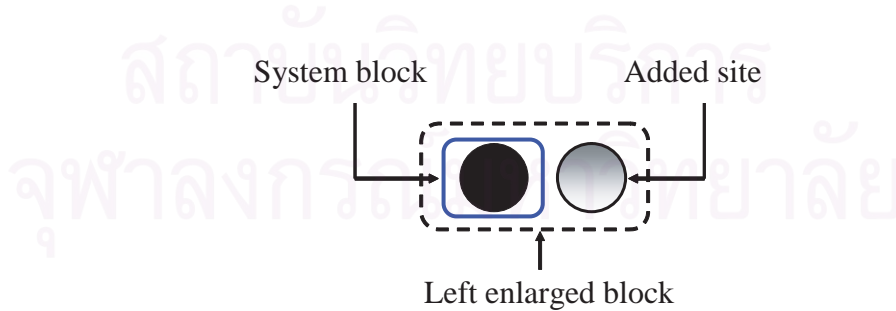


Figure 3.1: The left enlarged block

Consequently, the Hamiltonian and the operator only associated with the system block can be written as matrices  $H_{S(M \times M)}$  and  $A_{S(M \times M)}$  of  $M \times M$  dimension. The left enlarged block  $B_l^M \bullet^d$  is created by joining the system block  $B_l^M$  to the added single site  $\bullet^d$ . Consequently, it has  $Md$  states. Then, the Hamiltonian of the left enlarged block is denoted as

$$H_{E(Md \times Md)}^L = H_{S(M \times M)} \otimes \delta_{d \times d} + A_{S(M \times M)} \otimes A_{\bullet(d \times d)}, \quad (3.1)$$

where  $A_{\bullet(d \times d)}$  is the operator of the added site and  $\delta_{d \times d}$  is the unit matrix which has the same dimension as the operator in the added site. while the operator at the added site of the enlarged block is denoted as

$$(A_{\bullet})_{E(Md \times Md)}^L = \delta_{M \times M} \otimes A_{\bullet(d \times d)}, \quad (3.2)$$

where superscript  $L$  and subscript  $E$  indicate that these operators are in the left (L) enlarged (E) block. Besides,  $A_{\bullet(d \times d)}$  is the operator at added site. In Eq. (3.1), the first term of the right-hand side show that the dimension of Hamiltonian matrix of system block is expanded to agree with the dimension of the enlarged block. While, the second term defines the interaction between a site in the system block and the added site. In Eq. (3.2),  $\delta_{M \times M}$  is the unit matrix which has the same dimension as the operator in the system block. Accordingly, the Hamiltonian and the operator operated in  $B_l^M \bullet^d$  will be matrices of  $Md \times Md$  dimensions. These matrices are formed as a direct product of the matrix representation of Hamiltonian and operator of system block and a single site.

2. Construct the superblock by connecting two enlarge blocks, left enlarged block and right enlarged block. Right enlarged block is constructed by using the reflection symmetry of the left enlarged block. Therefore, we can define that

$$H_{E(Md \times Md)}^R = \delta_{d \times d} \otimes H_{S(M \times M)} + A_{\bullet(d \times d)} \otimes A_{S(M \times M)}, \quad (3.3)$$

then it is given by

$$H_{E(Md \times Md)}^R = (H_{E(Md \times Md)}^L)^\dagger, \quad (3.4)$$

which is the Hamiltonian of the right enlarged block. While, the operator of the right enlarged block is given by

$$(A_{\bullet})_{E(Md \times Md)}^R = A_{\bullet(d \times d)} \otimes \delta_{(M \times M)}. \quad (3.5)$$

Due to Eq. (3.2), the reflection symmetry, the operator of the right enlarged block can be written as

$$(A_{\bullet})_{E(Md \times Md)}^R = (A_{E(Md \times Md)}^L)^\dagger. \quad (3.6)$$

The Hamiltonian of the superblock is constructed by connecting two enlarged blocks via operator  $(A_{\bullet})_E^L$  and  $(A_{\bullet})_E^R$  which are defined as the operator of the added sites belonging to left and right enlarged blocks respectively.

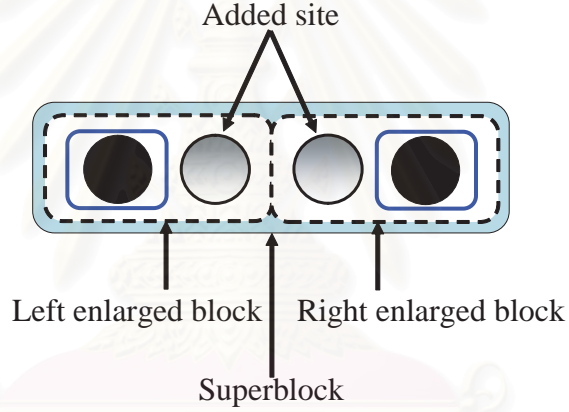


Figure 3.2: The superblock

In Figure 3.2, the notation of the superblock will be  $B_i^M \bullet^d \bullet^d B_i^M$ . The matrix representation of the Hamiltonian of the superblock is written as

$$\begin{aligned} H_{((Md)^2 \times (Md)^2)}^{\text{super}} &= H_{E(Md \times Md)}^L \otimes \delta_{(Md \times Md)} + \delta_{(Md \times Md)} \otimes H_{E(Md \times Md)}^R \\ &+ (A_{\bullet})_{E(Md \times Md)}^L \otimes (A_{\bullet})_{E(Md \times Md)}^R, \end{aligned} \quad (3.7)$$

where  $\delta_{(Md \times Md)}$  is the unit matrix which has the same dimension as the operator in the right and left enlarged block. The contact of the two enlarged blocks in Eq. (3.7) is  $(A_{\bullet})_{E(Md \times Md)}^L \otimes (A_{\bullet})_{E(Md \times Md)}^R$ . Next, this Hamiltonian is diagonalized to find ground state (target state) in the next step.

3. Construct the density matrix from the ground state. The ground state can be written as

$$|\psi\rangle = \sum_{i=1}^{Md} \sum_{j=1}^{Md} \psi_{ij} |i\rangle |j\rangle, \quad (3.8)$$

where  $|i\rangle$  and  $|j\rangle$  are the bases from the left enlarged block and the right enlarged block, respectively. The coefficient is  $\psi_{ij} = \langle i|\langle j|\psi\rangle$  which is the representation of bases in the left and the right enlarged block on the ground state in the superblock. The density matrix can be written as

$$\rho_{ii'} = \sum_j \psi_{ij} \psi_{ji'}^\dagger \quad (3.9)$$

where  $\rho_{ii'}$  are the value of matrix element in the density matrix at row  $i$  and column  $i'$ . The construction of the density matrix can be illustrated as follows: For example, if  $Md = 4$ , the coefficients of the ground state of the superblock is written in the vector form  $|\psi\rangle$  as

$$|\psi\rangle = \begin{pmatrix} v_1 \\ v_2 \\ \vdots \\ v_{16} \end{pmatrix}_{16 \times 1}. \quad (3.10)$$

The ground state can be transformed from  $16 \times 1$  matrix by new alignment of all matrix elements to  $4 \times 4$  matrix [20]. The square matrix of the ground states can be written as

$$|\psi\rangle = \begin{pmatrix} v_1 & v_2 & v_3 & v_4 \\ v_5 & v_6 & v_7 & v_8 \\ v_9 & v_{10} & v_{11} & v_{12} \\ v_{13} & v_{14} & v_{15} & v_{16} \end{pmatrix}_{4 \times 4}, \quad (3.11)$$

where the rows correspond to the complete basis of the left enlarged block, and the columns correspond to the complete basis of the right enlarged block. Then,

it can be transposed as

$$|\psi\rangle^\dagger = \begin{pmatrix} v_1 & v_5 & v_9 & v_{13} \\ v_2 & v_6 & v_{10} & v_{14} \\ v_3 & v_7 & v_{11} & v_{15} \\ v_4 & v_8 & v_{12} & v_{16} \end{pmatrix}_{4 \times 4}. \quad (3.12)$$

The density matrix for the left enlarged block is given by

$$\rho = \psi\psi^\dagger. \quad (3.13)$$

Therefore from Eqs. (3.11) and (3.12),  $\rho$  is a  $4 \times 4$  matrix corresponding to with Eq. (3.9).

4. Diagonalize the density matrix to find the important states. From above, when the density matrix is diagonalized, eigenvalue and eigenvector are  $w_\alpha$  and  $|u_\alpha\rangle$  respectively, with  $\alpha = 1, \dots, Md$ . Each  $w_\alpha$  represents the possibility of the left enlarged block being in the state  $|u_\alpha\rangle$ , with  $\sum_{\alpha=1}^{Md} w_\alpha = 1$ . Therefore, the accuracy of the DMRG approximation method depends on the number of kept states being the largest density matrix eigenvalue. If  $m$  states will be kept and  $w_1 > w_2 > \dots > w_m$ , the corresponding kept states being  $|u_1\rangle, |u_2\rangle, \dots, |u_m\rangle$  respectively. If  $m = Md$ , it means that all the states are kept. Therefore, an error cannot occurs in this process. But if  $m < Md$ , the error will occur.

For example in the previous step as  $Md = 4$ , if we choose  $m = Md$  and  $w_1 > w_2 > w_3 > w_4$ , we will get  $|u_1\rangle, |u_2\rangle, |u_3\rangle$  and  $|u_4\rangle$  which are shown in the matrix from for the important states in chronological order as

$$|u_1\rangle = \begin{pmatrix} a_1 \\ a_2 \\ a_3 \\ a_4 \end{pmatrix}, |u_2\rangle = \begin{pmatrix} b_1 \\ b_2 \\ b_3 \\ b_4 \end{pmatrix}, |u_3\rangle = \begin{pmatrix} c_1 \\ c_2 \\ c_3 \\ c_4 \end{pmatrix}, |u_4\rangle = \begin{pmatrix} e_1 \\ e_2 \\ e_3 \\ e_4 \end{pmatrix}. \quad (3.14)$$

5. Form the truncation matrix  $O$  by keeping the finite states of the density

matrix. The truncation matrix is

$$O = \begin{pmatrix} |u_1\rangle^\dagger \\ |u_2\rangle^\dagger \\ |u_3\rangle^\dagger \\ |u_4\rangle^\dagger \end{pmatrix}. \quad (3.15)$$

Obviously, the order of the important state is considered to construct truncation matrix. From Eq. (3.14), it becomes

$$O = \begin{pmatrix} a_1 & a_2 & a_3 & a_4 \\ b_1 & b_2 & b_3 & b_4 \\ c_1 & c_2 & c_3 & c_4 \\ e_1 & e_2 & e_3 & e_4 \end{pmatrix}_{4 \times 4}. \quad (3.16)$$

Evidently, the number of rows of  $O$  matrix depend on the number of kept states. This point effects the size of Hilbert space in the next iteration. In the general case, the matrix  $O$  will be  $m \times Md$ . Accordingly, the truncation matrix  $O$  can be written as  $O_{m \times Md}$ .

6. Truncate the left enlarged block to create the new system block. This new system block consists of system block from the previous step and the added site. All corresponding operators in the left enlarged block are truncated by the truncation matrix  $O$ . For example, when  $H_{Md \times Md}^L$  and  $(A_\bullet)_{Md \times Md}^L$  are the Hamiltonian and  $\hat{A}$  operators on the left enlarged block having the dimension being  $Md \times Md$ , they are truncated by

$$\begin{aligned} H_{S(m \times m)}^{\text{new}} &= O_{m \times Md} H_{E(Md \times Md)}^L O_{Md \times m}^\dagger, \\ A_{S(m \times m)}^{\text{new}} &= O_{m \times Md} (A_\bullet)_{E(Md \times Md)}^L O_{Md \times m}^\dagger, \end{aligned} \quad (3.17)$$

where  $H_{S(m \times m)}^{\text{new}}$  and  $A_{S(m \times m)}^{\text{new}}$  are the Hamiltonian and  $\hat{A}$  operator of the new system block having  $m \times m$  dimension.

7. Define the new system block. After we get a new Hamiltonian and an operator  $\hat{A}$  from truncation, we will use them for the new system block, shown as

$$H_{S(m \times m)} = H_{S(m \times m)}^{\text{new}},$$

$$A_{S(m \times m)} = A_{S(m \times m)}^{\text{new}}. \quad (3.18)$$

Consequently, the dimension of the Hamiltonian and operators in the system block is  $m \times m$ , which will be constant because the number of the kept states  $m$  has been defined before the iteration. This process leads to the limited size of the Hilbert space. In Figure 3.3, it looks as if we expand the system block to cover the added site.

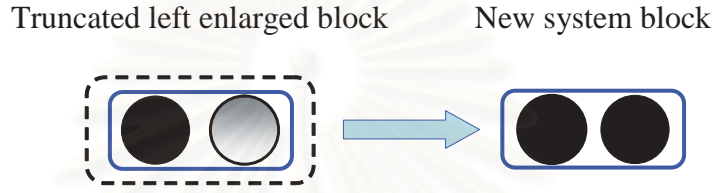


Figure 3.3: Constructing the new system block

8. Add one site on the right-hand side of the system block to form the new left enlarged block, Figure 3.4. The Hamiltonian of enlarged block in Figure 3.4 is written as

New left enlarged block

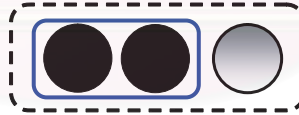


Figure 3.4: Constructing the new left enlarged block

$$\begin{aligned} H_{E(md \times md)}^{L(\text{new})} &= H_{S(m \times m)} \otimes \delta_{d \times d} + A_{S(m \times m)} \otimes A_{\bullet(d \times d)} \\ (A_{\bullet})_{E(md \times md)}^{L(\text{new})} &= \delta_{m \times m} \otimes A_{\bullet d \times d} \end{aligned} \quad (3.19)$$

After we get the Hamiltonian and operators of the new left enlarged block, we will replace them in  $H_{E(Md \times Md)}^L$  and  $(A_{\bullet})_{E(Md \times Md)}^L$ , i.e.

$$\begin{aligned} H_{E(md \times md)}^L &= H_{E(md \times md)}^{L(\text{new})} \\ (A_{\bullet})_{E(md \times md)}^L &= (A_{\bullet})_{E(md \times md)}^{L(\text{new})}. \end{aligned} \quad (3.20)$$



From Eq. (3.1), the process has the dimension of the enlarged block not exceeding  $(md \times md)$ .

9. Go to step 2 for creating the new superblock. We will use  $H_{E(md \times md)}^L$  and  $(A_{\bullet})_{E(md \times md)}^L$  in step 8 to compute in step 2 for the next iteration process. Some of the operators and truncation matrices in each loop will be kept for the calculation of the parameters such as correlation and expectation values. This part will be explained again in the next section. The process will finish, when convergence of the target state eigenvalue of the superblock is reached.

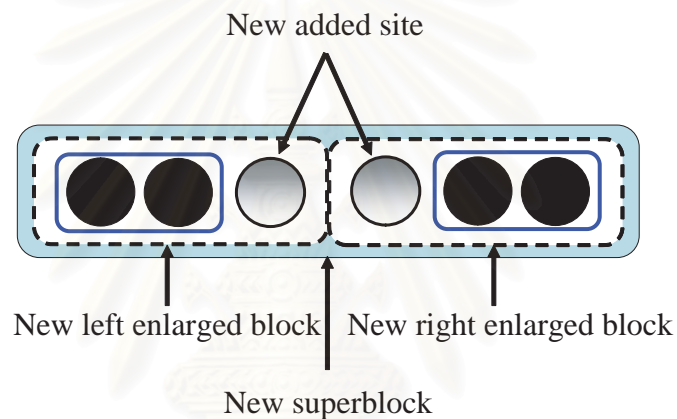


Figure 3.5: Constructing the new superblock

## 3.2 Example: The Heisenberg Model

In this section, the infinite DMRG approach is implemented to calculate the ground-state energy and spin correlation of antiferromagnetic Heisenberg spin-1/2 chain.

The Heisenberg spin chain [21] is used to describe magnetic systems with interacting spins. In the antiferromagnetic phase, which the spin favors antiparallel

arrangement, the Hamiltonian is given by

$$H = J \sum_{\langle ij \rangle} \vec{S}_i \cdot \vec{S}_j \quad (3.21)$$

where  $\langle ij \rangle$  means that the summation is to be taken over pair of nearest neighbor sites only and  $J > 0$ . While,  $\vec{S}_{i(j)}$  is the total spin operator at site  $i(j)$ . Consequently, The Hamiltonian becomes

$$H = J \sum_{i=1}^{\mathcal{L}-1} \vec{S}_i \cdot \vec{S}_{i+1}, \quad (3.22)$$

when we consider in one-dimension with  $\mathcal{L}$  length. Furthermore, the spin operators can be written as

$$\begin{aligned} \vec{S} &= \hat{S}^x + \hat{S}^y + \hat{S}^z, \\ \hat{S}^+ &= \hat{S}^x + i\hat{S}^y, \\ \hat{S}^- &= \hat{S}^x - i\hat{S}^y, \end{aligned} \quad (3.23)$$

where  $\hat{S}^+$  and  $\hat{S}^-$  are the raising and lowering operators respectively. They affect on the  $z$  component of the spin angular momentum by  $\hbar$ .

Let  $|\uparrow\rangle$  ( $|\downarrow\rangle$ ) be the eigenstate of operator  $\hat{S}^z$  with eigenvalue  $\frac{1}{2}$  ( $-\frac{1}{2}$ ), i.e.  $\hat{S}^z|\uparrow\rangle = \frac{1}{2}|\uparrow\rangle$  and  $\hat{S}^z|\downarrow\rangle = -\frac{1}{2}|\downarrow\rangle$ . The raising and lowering operators operate on these bases can be written as

$$\begin{aligned} \hat{S}^+|\uparrow\rangle &= 0, \quad \hat{S}^+|\downarrow\rangle = \hbar|\uparrow\rangle, \\ \hat{S}^-|\downarrow\rangle &= 0, \quad \hat{S}^-|\uparrow\rangle = \hbar|\downarrow\rangle. \end{aligned} \quad (3.24)$$

The commutation relations are

$$[\hat{S}^+, \hat{S}^-] = 2\hat{S}^z, \quad (3.25)$$

$$[\hat{S}^z, \hat{S}^\pm] = \pm\hat{S}^\pm, \quad (3.26)$$

and

$$[\vec{S}^2, \hat{S}^\pm] = 0. \quad (3.27)$$

From the above equations, the scalar product of the spin operators becomes

$$\vec{S}_i \cdot \vec{S}_{i+1} = \hat{S}_i^z \cdot \hat{S}_{i+1}^z + \frac{1}{2}(\hat{S}_i^+ \cdot \hat{S}_{i+1}^- + \hat{S}_i^- \cdot \hat{S}_{i+1}^+). \quad (3.28)$$

In this model for spin 1/2, each site has spin  $S = 1/2$ , so the number of states per site is  $2S + 1 = 2$ . Therefore, all the corresponding on-site spin operators can be expressed as  $2 \times 2$  matrices as

$$\hat{S}^+ = \begin{pmatrix} 0 & 1 \\ 0 & 0 \end{pmatrix}, \quad \hat{S}^- = \begin{pmatrix} 0 & 0 \\ 1 & 0 \end{pmatrix}, \quad \hat{S}^z = \frac{1}{2} \begin{pmatrix} 1 & 0 \\ 0 & -1 \end{pmatrix}, \quad (3.29)$$

where we put  $\hbar = 1$ . A unit matrix in one site is

$$\delta = \begin{pmatrix} 1 & 0 \\ 0 & 1 \end{pmatrix}, \quad (3.30)$$

which is used to expand the system for the DMRG algorithm. To demonstrate the calculation using the DMRG algorithm, we will follow Section 3.2.

**Step 1** We construct the left enlarged block having one site from the system block and one site from added site. The on-site Hamiltonian matrix can be enlarged by performing direct product with a unit matrix,  $H_{S(2 \times 2)} \otimes \delta_{2 \times 2}$ . The Hamiltonian of the left enlarged block is written as

$$H_{E(4 \times 4)}^L = H_{S(2 \times 2)} \otimes \delta_{(2 \times 2)} + \hat{S}_{S(2 \times 2)}^z \otimes \hat{S}_{\bullet(2 \times 2)}^z + \frac{1}{2}(\hat{S}_{S(2 \times 2)}^+ \otimes \hat{S}_{\bullet(2 \times 2)}^- + \hat{S}_{S(2 \times 2)}^- \otimes \hat{S}_{\bullet(2 \times 2)}^+) \quad (3.31)$$

where subscript  $\bullet$ ,  $S$  and  $E$  of each operators indicate where operators act to the added site, the system block and the enlarged block, respectively. Furthermore, the dimension of them are shown in bracket subscripts. Eq. (3.31) is shown in a matrix form as

$$\begin{aligned} H_E^L &= \begin{pmatrix} 0 & 0 \\ 0 & 0 \end{pmatrix} \otimes \begin{pmatrix} 1 & 0 \\ 0 & 1 \end{pmatrix} \\ &+ \frac{1}{4} \left[ \begin{pmatrix} 1 & 0 \\ 0 & -1 \end{pmatrix} \otimes \begin{pmatrix} 1 & 0 \\ 0 & -1 \end{pmatrix} \right] \\ &+ \frac{1}{2} \left[ \begin{pmatrix} 0 & 1 \\ 0 & 0 \end{pmatrix} \otimes \begin{pmatrix} 0 & 0 \\ 1 & 0 \end{pmatrix} + \begin{pmatrix} 0 & 0 \\ 1 & 0 \end{pmatrix} \otimes \begin{pmatrix} 0 & 1 \\ 0 & 0 \end{pmatrix} \right] \quad (3.32) \end{aligned}$$

then we get

$$H_E^L = \frac{1}{4} \begin{pmatrix} 1 & 0 & 0 & 0 \\ 0 & -1 & 2 & 0 \\ 0 & 2 & -1 & 0 \\ 0 & 0 & 0 & 1 \end{pmatrix}. \quad (3.33)$$

In Eq. (3.31),  $H_S$  is a zero matrix owing to the system block having only one site. Accordingly, the interaction of two spins has never occurred.

**Step 2** The superblock Hamiltonian is constructed by the left and right enlarged block. Before starting this process, we will define the right enlarged block  $H_E^R$  from the left enlarged block  $H_E^L$  as

$$H_E^R = (H_E^L)^\dagger. \quad (3.34)$$

To link two enlarged blocks for creating the superblock, the sites at the edge of two enlarge blocks are considered. They are the added sites of the left enlarged block and the right enlarged block. The corresponding operators of the added site of the left enlarged block can be obtained by

$$\begin{aligned} (\hat{S}_\bullet^+)_{E(4 \times 4)}^L &= \delta_{(2 \times 2)} \otimes \hat{S}_{\bullet(2 \times 2)}^+, \\ (\hat{S}_\bullet^-)_{E(4 \times 4)}^L &= \delta_{(2 \times 2)} \otimes \hat{S}_{\bullet(2 \times 2)}^-, \\ (\hat{S}_\bullet^z)_{E(4 \times 4)}^L &= \delta_{(2 \times 2)} \otimes \hat{S}_{\bullet(2 \times 2)}^z. \end{aligned} \quad (3.35)$$

Similarly in Eq. (3.34), we can generate the operators which belong to the added site of the right enlarged block, being

$$\begin{aligned} (\hat{S}_\bullet^+)_{E(4 \times 4)}^R &= \{(\hat{S}_\bullet^+)_{E(4 \times 4)}^L\}^\dagger, \\ (\hat{S}_\bullet^-)_{E(4 \times 4)}^R &= \{(\hat{S}_\bullet^-)_{E(4 \times 4)}^L\}^\dagger, \\ (\hat{S}_\bullet^z)_{E(4 \times 4)}^R &= \{(\hat{S}_\bullet^z)_{E(4 \times 4)}^L\}^\dagger. \end{aligned} \quad (3.36)$$

The superblock Hamiltonian is constructed by Eqs. (3.34), (3.35) and (3.36). Then, it is defined as

$$H_{\text{super}(16 \times 16)} = H_{E(4 \times 4)}^L \otimes \delta_{(4 \times 4)} + \delta_{(4 \times 4)} \otimes H_{E(4 \times 4)}^R$$

$$\begin{aligned}
& + \frac{1}{4} \left[ (\hat{S}_{\bullet}^z)^L_{E(4 \times 4)} \otimes (\hat{S}_{\bullet}^z)^R_{E(4 \times 4)} \right] \\
& + \frac{1}{2} \left[ (\hat{S}_{\bullet}^+)^L_{E(4 \times 4)} \otimes (\hat{S}_{\bullet}^-)^R_{E(4 \times 4)} + (\hat{S}_{\bullet}^-)^L_{E(4 \times 4)} \otimes (\hat{S}_{\bullet}^+)^R_{E(4 \times 4)} \right].
\end{aligned} \tag{3.37}$$

The matrix form of the superblock Hamiltonian  $H_{\text{super}(16 \times 16)}$  is written as

$$\begin{pmatrix}
0.75 & 0 & 0 & 0 & 0 & 0 & 0 & 0 & 0 & 0 & 0 & 0 & 0 & 0 & 0 & 0 \\
0 & 0.25 & 0.5 & 0 & 0 & 0 & 0 & 0 & 0 & 0 & 0 & 0 & 0 & 0 & 0 & 0 \\
0 & 0.5 & -0.25 & 0 & 0.5 & 0 & 0 & 0 & 0 & 0 & 0 & 0 & 0 & 0 & 0 & 0 \\
0 & 0 & 0 & 0.25 & 0 & 0.5 & 0 & 0 & 0 & 0 & 0 & 0 & 0 & 0 & 0 & 0 \\
0 & 0 & 0.5 & 0 & -0.25 & 0 & 0 & 0 & 0.5 & 0 & 0 & 0 & 0 & 0 & 0 & 0 \\
0 & 0 & 0 & 0.5 & 0 & -0.75 & 0.5 & 0 & 0 & 0.5 & 0 & 0 & 0 & 0 & 0 & 0 \\
0 & 0 & 0 & 0 & 0 & 0.5 & -0.25 & 0 & 0 & 0 & 0.5 & 0 & 0 & 0 & 0 & 0 \\
0 & 0 & 0 & 0 & 0 & 0 & 0 & 0.25 & 0 & 0 & 0 & 0.5 & 0 & 0 & 0 & 0 \\
0 & 0 & 0 & 0 & 0.5 & 0 & 0 & 0 & 0.25 & 0 & 0 & 0 & 0 & 0 & 0 & 0 \\
0 & 0 & 0 & 0 & 0 & 0.5 & 0 & 0 & 0 & -0.25 & 0.5 & 0 & 0 & 0 & 0 & 0 \\
0 & 0 & 0 & 0 & 0 & 0 & 0.5 & 0 & 0 & 0.5 & -0.75 & 0 & 0.5 & 0 & 0 & 0 \\
0 & 0 & 0 & 0 & 0 & 0 & 0 & 0.5 & 0 & 0 & 0 & -0.25 & 0 & 0.5 & 0 & 0 \\
0 & 0 & 0 & 0 & 0 & 0 & 0 & 0 & 0 & 0 & 0.5 & 0 & 0.25 & 0 & 0 & 0 \\
0 & 0 & 0 & 0 & 0 & 0 & 0 & 0 & 0 & 0 & 0 & 0.5 & 0 & -0.25 & 0.5 & 0 \\
0 & 0 & 0 & 0 & 0 & 0 & 0 & 0 & 0 & 0 & 0 & 0 & 0 & 0.5 & 0.25 & 0 \\
0 & 0 & 0 & 0 & 0 & 0 & 0 & 0 & 0 & 0 & 0 & 0 & 0 & 0 & 0 & 0.75
\end{pmatrix}. \tag{3.38}$$

**Step 3** After  $H_{\text{super}}$ , Eq. (3.38), is diagonalized, we obtain the lowest eigenvalue which is the ground-state energy  $E_0$  as -1.616 eV, and corresponding eigenvector which is the ground-state wave function  $|\psi_0\rangle$ . The ground-state wave func-

สถาบันวิทยบริการ  
จุฬาลงกรณ์มหาวิทยาลัย

tion are expressed as

$$|\psi_0\rangle = \begin{pmatrix} 0 \\ 0 \\ 0 \\ -0.14943 \\ 0 \\ 0.55768 \\ -0.40825 \\ 0 \\ 0 \\ -0.40825 \\ 0.55768 \\ 0 \\ -0.14943 \\ 0 \\ 0 \\ 0 \end{pmatrix}. \quad (3.39)$$

Eq. (3.9), Eq. (3.39) is then transformed to a square matrix,

$$|\psi_0\rangle_{4 \times 4} = \begin{pmatrix} 0 & 0 & 0 & -0.14943 \\ 0 & 0.55768 & -0.40825 & 0 \\ 0 & -0.40825 & 0.55768 & 0 \\ -0.14943 & 0 & 0 & 0 \end{pmatrix}. \quad (3.40)$$

After we get  $|\psi_0\rangle_{4 \times 4}$ , it will be used to construct the density matrix from Eq. (3.9) as

$$\rho = \begin{pmatrix} 0.022329 & 0 & 0 & 0 \\ 0 & 0.47767 & -0.45534 & 0 \\ 0 & -0.45534 & 0.47767 & 0 \\ 0 & 0 & 0 & 0.022329 \end{pmatrix}. \quad (3.41)$$

**Step 4** In order to decide which states of the left enlarged block are the most important for the ground state of the superblock, one diagonalizes the density matrix Eq. (3.41). Then, we get  $w_\alpha$  and  $|u_\alpha\rangle$  being

$$|u_1\rangle = \begin{pmatrix} 0 \\ 0.70711 \\ -0.70711 \\ 0 \end{pmatrix}, \quad |u_2\rangle = \begin{pmatrix} -0.51873 \\ 0.48311 \\ 0.48311 \\ -0.51393 \end{pmatrix}, \quad |u_3\rangle = \begin{pmatrix} 0.27334 \\ -0.30904 \\ -0.30904 \\ -0.8569 \end{pmatrix}, \quad |u_4\rangle = \begin{pmatrix} 0.81006 \\ 0.41364 \\ 0.41364 \\ -0.039962 \end{pmatrix}. \quad (3.42)$$

Then, we get  $w_1 > w_2 > w_3 > w_4$ .

**Step 5** If assume that they are non-degenerate states and the truncation matrices are created by keeping only three states, then the error occurs because of the disappearing of  $|u_4\rangle$ . Therefore, from Eq. (3.15), the truncation matrix  $O$  for  $m = 3$  is given by

$$O_{3 \times 4} = \begin{pmatrix} 0 & 0.70711 & -0.70711 & 0 \\ -0.51873 & 0.48311 & 0.48311 & -0.51393 \\ 0.27334 & -0.30904 & -0.30904 & -0.8569 \end{pmatrix}. \quad (3.43)$$

For each iteration,  $O$  is kept and labeled with an index to be used to calculate the expectation value of operators such as spin correlation.

**Step 6** We will truncate all operators of the left enlarged block to make a new system block. The processes are

$$\begin{aligned} H_{S(3 \times 3)}^{L(\text{new})} &= O_{3 \times 4} H_{E(4 \times 4)}^L O_{4 \times 3}^\dagger, \\ (\hat{S}_\bullet^+)^{L(\text{new})}_{S(3 \times 3)} &= O_{3 \times 4} (\hat{S}_\bullet^+)^L_{E(4 \times 4)} O_{4 \times 3}^\dagger, \\ (\hat{S}_\bullet^-)^{L(\text{new})}_{S(3 \times 3)} &= O_{3 \times 4} (\hat{S}_\bullet^-)^L_{E(4 \times 4)} O_{4 \times 3}^\dagger, \\ (\hat{S}_\bullet^z)^{L(\text{new})}_{S(3 \times 3)} &= O_{3 \times 4} (\hat{S}_\bullet^z)^L_{E(4 \times 4)} O_{4 \times 3}^\dagger. \end{aligned} \quad (3.44)$$

Then, all of the corresponding operators become  $3 \times 3$  matrices, and the size of the Hilbert space is reduced from 4 to 3.

**Step 7** Construct the new system block which consists of 2 sites. The system block operators are replaced by the new system block operators which are obtained from step 6. Therefore, the operators of the system block become

$$\begin{aligned} H_{S(3 \times 3)}^L &= H_{S(3 \times 3)}^{L(\text{new})}, \\ (\hat{S}_\bullet^+)^L_{S(3 \times 3)} &= (\hat{S}_\bullet^+)^{L(\text{new})}_{S(3 \times 3)}, \\ (\hat{S}_\bullet^-)^L_{S(3 \times 3)} &= (\hat{S}_\bullet^-)^{L(\text{new})}_{S(3 \times 3)}, \\ (\hat{S}_\bullet^z)^L_{S(3 \times 3)} &= (\hat{S}_\bullet^z)^{L(\text{new})}_{S(3 \times 3)}. \end{aligned} \quad (3.45)$$

**Step 8** The system block of 2 sites combined with added site becomes the new enlarged block. The new left enlarged block operators are constructed as the

following,

$$\begin{aligned}
H_{E(6 \times 6)}^{L(\text{new})} &= H_{S(3 \times 3)}^L \otimes \delta_{(2 \times 2)}, \\
H_{E(6 \times 6)}^L &= H_{E(6 \times 6)}^{L(\text{new})}, \\
(\hat{S}_{\bullet}^+)^{L(\text{new})}_{E(6 \times 6)} &= \delta_{(3 \times 3)} \otimes \hat{S}_{\bullet(2 \times 2)}^+, \\
(\hat{S}_{\bullet}^+)^L_{E(6 \times 6)} &= (\hat{S}_{\bullet}^+)^{L(\text{new})}_{E(6 \times 6)}, \\
(\hat{S}_{\bullet}^-)^{L(\text{new})}_{E(6 \times 6)} &= \delta_{(3 \times 3)} \otimes \hat{S}_{\bullet(2 \times 2)}^-, \\
(\hat{S}_{\bullet}^-)^L_{E(6 \times 6)} &= (\hat{S}_{\bullet}^-)^{L(\text{new})}_{E(6 \times 6)}, \\
(\hat{S}_{\bullet}^z)^{L(\text{new})}_{E(6 \times 6)} &= \delta_{(3 \times 3)} \otimes \hat{S}_{\bullet(2 \times 2)}^z, \\
(\hat{S}_{\bullet}^z)^L_{E(6 \times 6)} &= (\hat{S}_{\bullet}^z)^{L(\text{new})}_{E(6 \times 6)}.
\end{aligned} \tag{3.46}$$

**Step 9** The process continues by repeating step 2 by using Eq. (3.46) to produce the superblock Hamiltonian. Since the operators belonging to the added site of the right enlarged block are

$$\begin{aligned}
H_E^R &= (H_E^L)^\dagger, \\
(\hat{S}_{\bullet}^+)^R_{E(6 \times 6)} &= \{(\hat{S}_{\bullet}^+)^L_{E(6 \times 6)}\}^\dagger, \\
(\hat{S}_{\bullet}^-)^R_{E(6 \times 6)} &= \{(\hat{S}_{\bullet}^-)^L_{E(6 \times 6)}\}^\dagger, \\
(\hat{S}_{\bullet}^z)^R_{E(6 \times 6)} &= \{(\hat{S}_{\bullet}^z)^L_{E(6 \times 6)}\}^\dagger.
\end{aligned} \tag{3.47}$$

Then, the superblock Hamiltonian resembles to Eq. (3.38). However, the dimension of the matrix has been changed according to the size of Hilbert space. Thus it becomes

$$\begin{aligned}
H_{\text{super}(36 \times 36)} &= H_{E(6 \times 6)}^L \otimes \delta_{(6 \times 6)} + \delta_{(6 \times 6)} \otimes H_{E(6 \times 6)}^R \\
&+ \frac{1}{4} \left[ (\hat{S}_{\bullet}^z)^L_{E(6 \times 6)} \otimes (\hat{S}_{\bullet}^z)^R_{E(6 \times 6)} \right] \\
&+ \frac{1}{2} \left[ (\hat{S}_{\bullet}^+)^L_{E(6 \times 6)} \otimes (\hat{S}_{\bullet}^-)^R_{E(6 \times 6)} + (\hat{S}_{\bullet}^-)^L_{E(6 \times 6)} \otimes (\hat{S}_{\bullet}^+)^R_{E(6 \times 6)} \right].
\end{aligned} \tag{3.48}$$

Hence in step 3, the ground state becomes  $|\psi_0\rangle_{36 \times 1}$  which is transformed to the square matrix being  $|\psi_0\rangle_{6 \times 6}$ . The density matrix equivalent to  $\rho_{6 \times 6}$ . When  $\rho$



is diagonalized, we will get  $w_\alpha$  and  $|u_\alpha\rangle_{6\times 1}$ , where  $\alpha = 1, \dots, 6$ . In step 5 three states are kept according to the number of kept states  $m=3$ . Therefore, the truncation matrix is equal to  $O_{3\times 6}$ . For this reason, the truncation in the next step affects to all of the operators of the system block having the matrix dimension being  $3 \times 3$ . Consequently, the dimension matrices of the enlarged block (being  $6 \times 6$ ) and superblock (being  $36 \times 36$ ) are constant in every loop until the end of the process. The iteration process will finish when convergence of the ground-state energy has been reached. Another way to stop iteration is that the define system size has been reached. However, the system size should large enough to ensure the convergence.

### 3.3 Measurement

In this section, measurement processes by using the DMRG algorithm are demonstrated. Both the ground-state energy and the spin correlation are described. Moreover, the measurement results from the Heisenberg spin chain model in the last chapter are represented. Furthermore, the results from the Matlab program have been compared with the exact result from the calculation of Bethe ansatz [19].

#### 3.3.1 Ground state energy

When the superblock Hamiltonian is diagonalized, the ground-state energy is determined every time. The convergence of ground-state energy of iteration process leads to the true ground-state energy of the total system. Above all, the accuracy of the ground-state energy depends on the number of kept states. From Figure 3.6, this calculation are calculated by the length of sites  $L$  as many as 2002 sites (from  $L=2i+2$  when  $i= 1000$  being number of iteration loop). Moreover, the kept

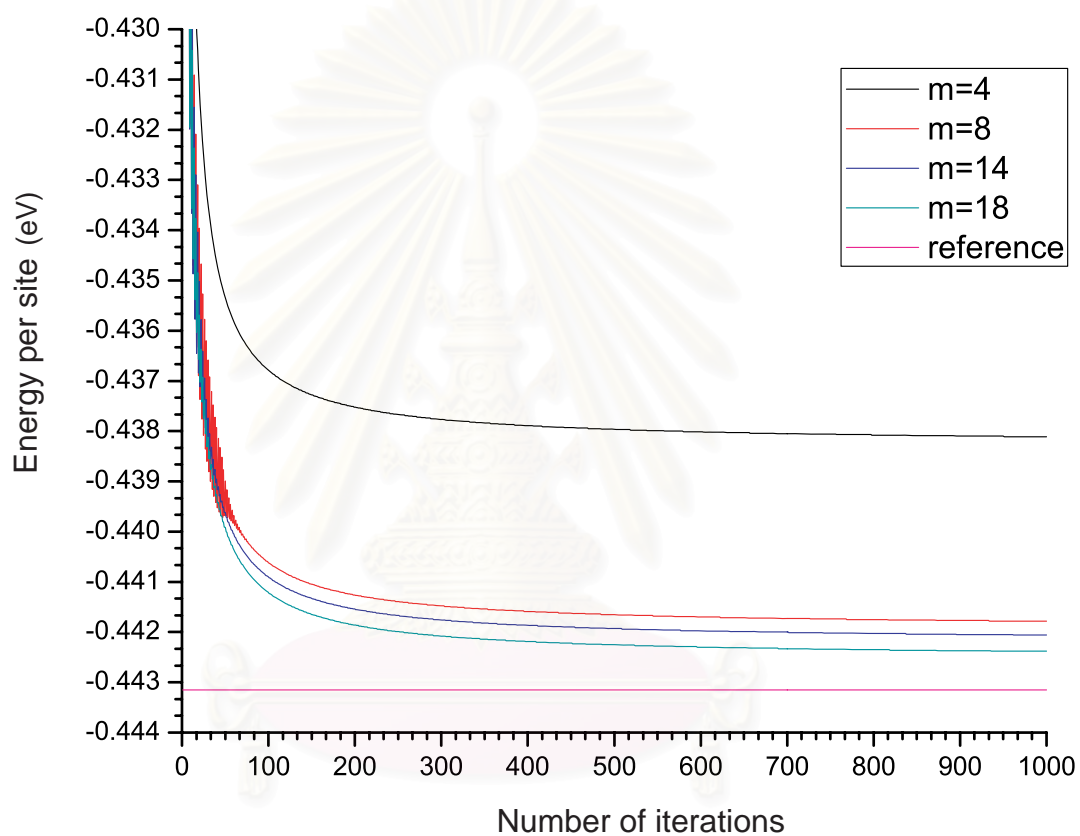


Figure 3.6: A DMRG calculation from The average ground energy per site for antiferromagnetic spin 1/2 Heisenberg chain keeping various number of kept states.

states are varied to be  $m = 4, 8, 14$  and  $18$ . We found that the ground-state energy will converge as the length goes to infinity. Furthermore, the result are in good agreement with the exact result as the number of kept state  $m$  is increased. The exact result [19] has been used to compare with these result. The difference between the exact and DMRG calculation have been demonstrated in Table 3.1 when *exact* refers to the ground-state energy from the exact solution.

m	Energy per site	$E_0^{DMRG} - E_0^{exact}$
4	-0.43811	$5.04 \times 10^{-3}$
8	-0.44178	$1.37 \times 10^{-3}$
14	-0.44206	$1.09 \times 10^{-3}$
18	-0.44238	$0.77 \times 10^{-3}$
<i>exact</i> [19]	-0.44315	

Table 3.1: Difference of the average ground-state energy per site for antiferromagnetic spin 1/2 Heisenberg chain between a DMRG calculation and the exact result keeping different number of kept states.

The ground-state energy and the error of the ground-state energy from DMRG algorithm at each number of kept states are shown in Table. (3.1). The error decreases with increasing the number of kept states ( $m$ ).

### 3.3.2 Correlations

Besides the groundstate energy, the expectation value of interested operators corresponding to the system can be found likewise, for example the spin correlation operator. The calculation of the correlation operators depends on the position of the spin in the left enlarged block as shown in Figure 3.7. When we compute the nearest neighbor spin correlation, spin at site  $i$  in the system block and spin at site  $i + 1$  being added site, are considered.

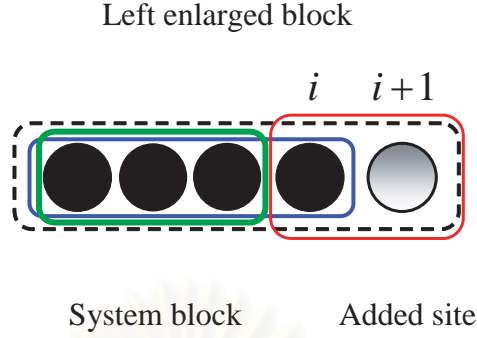


Figure 3.7: Different position of the two operators on the left enlarged block.

For example, the spin correlations are described with operators from two different sites of the left enlarged block. That is,  $\hat{S}_i^z$  operator acts on site  $i$  in the system block and  $\hat{S}_{i+1}^z$  operator acts on site  $i + 1$  in added site. Since, the ground state has been transformed every time in each iteration. Therefore, the truncation matrix is stored for every iteration.

To consider each operator,  $(\hat{S}_i^z)_{i+1}^e$  represents the  $\hat{S}^z$  operator on site  $i$  of the left enlarged block with total number of  $i + 1$  site.  $O_{i+1}$  represents truncate matrix. Spin-spin correlation can be found in subsequent calculations. If the left enlarged block has the chain size of  $i + 1$ , the local spin operator for site  $i$  can be written as

$$(\hat{S}_i^z)_{i+1}^e = (O_i(\delta_b \otimes S^z)O_i^\dagger) \otimes \delta_d, \quad (3.49)$$

where  $\delta_b$  and  $\delta_d$  are unit matrices corresponding to the system block and added sites matrix in each iteration respectively. Also the spin operator for added site is written as

$$(\hat{S}_{i+1}^z)_{i+1}^e = \delta_b \otimes S^z. \quad (3.50)$$

Then, the spin correlation is

$$(\hat{S}_i^z \hat{S}_{i+1}^z)_{i+1}^e = (O_i(\delta_b \otimes S^z)O_i^\dagger) \otimes \delta_d (\delta_b \otimes S^z). \quad (3.51)$$

Thus if  $|\psi_0\rangle$  is the ground state, the spin correlation can be calculated as

$$\langle \psi_0 | \hat{S}_i^z \hat{S}_j^z | \psi_0 \rangle \Rightarrow \langle \hat{S}_i^z \hat{S}_j^z \rangle. \quad (3.52)$$

After we get the operator at each site of the system, the correlation at the ground state can be calculated as

$$\langle S_i^z S_{i+1}^z \rangle = \langle \psi_0 | (S_i^z S_{i+1}^z)_{i+1}^e \otimes \delta_E^R | \psi_0 \rangle \quad (3.53)$$

where  $\delta_E^R$  is a unit matrix having size the same as the dimension of right enlarged block.



สถาบันวิทยบริการ  
จุฬาลงกรณ์มหาวิทยาลัย

# CHAPTER IV

## GROUND STATE PROPERTIES OF THE SPINLESS TWO-ORBITAL HUBBARD MODEL IN ONE DIMENSION

In this chapter the ground state of Hamiltonian in Chapter two, which is derived from Hubbard model in the large- $U$  limit at half-filling, has been calculated in one dimension by using infinite DMRG algorithm. We start with the definition of hopping amplitudes by introducing the condition of manganite compounds and using DMRG algorithm to calculate the ground state of the effective Hamiltonian for one-dimensional spinless orbital Hubbard model. A comparison between the Heisenberg spin chain and spinless orbital Hubbard chain is presented, including the calculation of ground-state energy of spinless orbital Hubbard at various axes (x-, y- and z- axis). Finally, the orbital orders and correlations of electronic ground state are described.

### 4.1 Definition of Hopping Amplitude

In this section, the parameters which correspond to the hopping terms are described. The processes of electronic hopping leading to the calculation of hopping

amplitudes for transition metal oxide have been explained by Slater and Koster in [23]. Especially, the hopping processes in manganite compound in Figure 2.1 with Perovkite structure in which the manganese ions are surrounded by oxygen ions, are investigated. The important phenomena occur when the orbital degrees of freedom of electron are considered. The exchange of electrons among neighbor sites of manganese ions occurs as the  $p$ -orbitals of the oxygen ions and  $d$ -orbitals of manganese ions overlap. Hence, one of the important parameters are the  $pd\sigma$  bond which is the overlap integral between the  $d\sigma$  and  $p\sigma$  orbitals. Additional information can be found in the original paper by Slater and Koster [23]. In this paper, the effective hopping amplitude of electrons between two nearest manganese ions via the oxygen ion orbitals along the  $x$ -axis,  $y$ -axis and  $z$ -axis can be written as

$$\begin{aligned} t_{aa}^x &= \frac{3}{4}(pd\sigma)^2, \\ t_{bb}^x &= \frac{1}{4}(pd\sigma)^2, \\ t_{ab}^x &= -\frac{\sqrt{3}}{4}(pd\sigma)^2, \end{aligned} \quad (4.1)$$

$$\begin{aligned} t_{aa}^y &= \frac{3}{4}(pd\sigma)^2, \\ t_{bb}^y &= \frac{1}{4}(pd\sigma)^2, \\ t_{ab}^y &= \frac{\sqrt{3}}{4}(pd\sigma)^2, \end{aligned} \quad (4.2)$$

$$\begin{aligned} t_{aa}^z &= 0, \\ t_{bb}^z &= (pd\sigma)^2, \\ t_{ab}^z &= 0, \end{aligned} \quad (4.3)$$

where  $a$  denotes  $x^2 - y^2$  orbital and  $b$  denotes  $3z^2 - r^2$  orbital. By using  $t_0$  which is defined as  $t_0 = (pd\sigma)^2$ , the hopping amplitude along the  $x$ - and  $y$ - axis can be rewritten as follows:

$x$ -axis

$$\begin{aligned} t_{ab}^x &= t_{ba}^x = -\frac{\sqrt{3}}{4}t_0, \\ t_{aa}^x &= \alpha t_{ab}^x = -\sqrt{3}t_{ab}^x, \end{aligned}$$

$$t_{bb}^x = \beta t_{ab}^x = -\frac{1}{\sqrt{3}}t_{ab}^x, \quad (4.4)$$

*y*-axis

$$\begin{aligned} t_{ab}^y &= t_{ba}^y = \frac{\sqrt{3}}{4}t_0, \\ t_{aa}^y &= \alpha t_{ab}^y = \sqrt{3}t_{ab}^y, \\ t_{bb}^y &= \beta t_{ab}^y = \frac{1}{\sqrt{3}}t_{ab}^y. \end{aligned} \quad (4.5)$$

We let  $t_{aa} = \alpha t_{ab}$  and  $t_{bb} = \beta t_{ab}$ , and  $t_{ab} = t_{ba} = t$  and the eigenvalue of  $\hat{n}$  is 1. Then Eq. (2.101) becomes

$$\begin{aligned} H_{\text{eff}} &= \sum_{\langle ij \rangle} \left\{ \frac{2t^2}{U} (\alpha^2 + \beta^2) (\hat{\tau}_i^z \hat{\tau}_j^z - \frac{1}{4}) - \frac{4t^2}{U} (\hat{\tau}_i^z \hat{\tau}_j^z + \frac{1}{4}) \right. \\ &+ \frac{2t^2}{U} (\hat{\tau}_i^- \hat{\tau}_j^- + \hat{\tau}_i^+ \hat{\tau}_j^+) + \frac{2t^2 \alpha \beta}{U} (\hat{\tau}_i^+ \hat{\tau}_j^- + \hat{\tau}_i^- \hat{\tau}_j^+) \\ &\left. + \frac{2t^2}{U} (\alpha - \beta) \{ \hat{\tau}_i^+ \hat{\tau}_j^z + \hat{\tau}_i^z \hat{\tau}_j^+ + \hat{\tau}_i^- \hat{\tau}_j^z + \hat{\tau}_i^z \hat{\tau}_j^- \} \right\}. \end{aligned} \quad (4.6)$$

However of the special case in *z*-axis,  $H_{\text{eff}}$  has been modified since  $t_{aa}^z = t_{ab}^z = t_{ba}^z = 0$  and  $t_{bb}^z = t_0$ , and it is given by

$$H_{\text{eff}} = \frac{2}{U} (t_{bb}^z)^2 (\hat{\tau}_i^z \hat{\tau}_j^z - \frac{\hat{n}_i \hat{n}_j}{4}). \quad (4.7)$$

## 4.2 DMRG for Spinless Orbital Hubbard Model

In this section, the DMRG for spinless orbital Hubbard model is described in the first loop. The effective Hamiltonian is separated into two cases; along *x*- or *y*- axis and along *z*- axis. For example, we begin with the construction of Hamiltonian for the left enlarge block which contains the system block and added site as in Figure 3.1. For the case of electrons hopping along *x*- or *y*- axis, it is written as

$$\begin{aligned} H_E^L &= H_S \otimes \delta_{\bullet} + \frac{2t^2}{U} (\alpha^2 + \beta^2) \{ \hat{\tau}_S^z \otimes \hat{\tau}_{\bullet}^z - \frac{1}{4} (\delta_S \otimes \delta_{\bullet}) \} + \frac{2t^2}{U} \{ \hat{\tau}_S^- \otimes \hat{\tau}_{\bullet}^- + \hat{\tau}_S^+ \otimes \hat{\tau}_{\bullet}^+ \} \\ &+ \frac{2t^2 \alpha \beta}{U} \{ \hat{\tau}_S^+ \otimes \hat{\tau}_{\bullet}^- + \hat{\tau}_S^- \otimes \hat{\tau}_{\bullet}^+ \} - \frac{4t^2}{U} \{ \hat{\tau}_S^z \otimes \hat{\tau}_{\bullet}^z + \frac{1}{4} (\delta_S \otimes \delta_{\bullet}) \} \\ &+ \frac{2t^2}{U} (\alpha - \beta) \{ \hat{\tau}_S^+ \otimes \hat{\tau}_{\bullet}^z + \hat{\tau}_S^z \otimes \hat{\tau}_{\bullet}^+ + \hat{\tau}_S^- \otimes \hat{\tau}_{\bullet}^z + \hat{\tau}_S^z \otimes \hat{\tau}_{\bullet}^- \}, \end{aligned} \quad (4.8)$$



which are shown in matrix form in the first loop of Matlab programming in Eqs. (D.1) and (D.2) following the direction of an electron hopping. For moving along z-axis it becomes

$$H_E^L = H_S \otimes \delta_{\bullet} + \frac{2}{U} (\hat{\tau}_{bb}^z)^2 \{ \hat{\tau}_S^z \otimes \hat{\tau}_{\bullet}^z + \frac{1}{4} (\delta_S \otimes \delta_{\bullet}) \}. \quad (4.9)$$

Where subscripts  $S$  and  $\bullet$  refer to the pseudo spin operator in the system block and the added site, respectively. Moreover from Eqs. (4.8) and (4.9),  $H_S$  is the Hamiltonian in the system block. The matrix form of the left enlarged block for an electron hopping along z-axis is denoted in Eq. (D.3).

To construct the superblock Hamiltonian, the Hamiltonian of two enlarged blocks, the left and right enlarged blocks, are considered. Hence, we will construct the connecting point between the left and right enlarged blocks via operators at the added sites. Then, operations at the added site of the left enlarged block are given by

$$\begin{aligned} (\hat{\tau}_{\bullet}^+)^R &= \delta_S \otimes \hat{\tau}_{\bullet}^+, \\ (\hat{\tau}_{\bullet}^-)^R &= \delta_S \otimes \hat{\tau}_{\bullet}^-, \\ (\hat{\tau}_{\bullet}^z)^R &= \delta_S \otimes \hat{\tau}_{\bullet}^z. \end{aligned} \quad (4.10)$$

According to Eqs. (3.4) and (3.5), the Hamiltonian and the operators at the added site of the right enlarged block can be written as

$$\begin{aligned} H_E^R &= \delta_{\bullet} \otimes H_S + \frac{2}{U} (\hat{\tau}_{bb}^z)^2 \{ \hat{\tau}_{\bullet}^z \otimes \hat{\tau}_S^z + \frac{1}{4} (\delta_{\bullet} \otimes \delta_S) \} \\ (\hat{\tau}_{\bullet}^+)^R &= \hat{\tau}_{\bullet}^+ \otimes \delta_S, \\ (\hat{\tau}_{\bullet}^-)^R &= \hat{\tau}_{\bullet}^- \otimes \delta_S, \\ (\hat{\tau}_{\bullet}^z)^R &= \hat{\tau}_{\bullet}^z \otimes \delta_S. \end{aligned} \quad (4.11)$$

So, they can be written in form of left enlarged block as

$$H_E^R = (H_E^L)^\dagger,$$

$$\begin{aligned}
(\hat{\tau}_{\bullet}^+)^R &= ((\hat{\tau}_{\bullet}^+)^L)^\dagger, \\
(\hat{\tau}_{\bullet}^-)^R &= ((\hat{\tau}_{\bullet}^-)^L)^\dagger, \\
(\hat{\tau}_{\bullet}^z)^R &= ((\hat{\tau}_{\bullet}^z)^L)^\dagger.
\end{aligned} \tag{4.12}$$

Consequently, the superblock Hamiltonian, which is created from two enlarged blocks for the case of electrons moving along x- or y-axis cases, is given by

$$\begin{aligned}
H_{\text{super}} &= H_E^L \otimes \delta_E^R + \delta_E^L \otimes H_E^R \\
&+ \frac{2t^2}{U}(\alpha^2 + \beta^2)\{(\hat{\tau}_{\bullet}^z)^L \otimes (\hat{\tau}_{\bullet}^z)^R - \frac{1}{4}(\delta_E^L \otimes \delta_E^R)\} \\
&+ \frac{2t^2}{U}\{(\hat{\tau}_{\bullet}^-)^L \otimes (\hat{\tau}_{\bullet}^-)^R + (\hat{\tau}_{\bullet}^+)^L \otimes (\hat{\tau}_{\bullet}^+)^R\} \\
&+ \frac{2t^2\alpha\beta}{U}\{(\hat{\tau}_{\bullet}^+)^L \otimes (\hat{\tau}_{\bullet}^-)^R + (\hat{\tau}_{\bullet}^-)^L \otimes (\hat{\tau}_{\bullet}^+)^R\} \\
&- \frac{4t^2}{U}\{(\hat{\tau}_{\bullet}^z)^L \otimes (\hat{\tau}_{\bullet}^z)^R + \frac{1}{4}(\delta_E^L \otimes \delta_E^R)\} \\
&+ \frac{2t^2}{U}(\alpha - \beta)\{(\hat{\tau}_{\bullet}^+)^L \otimes (\hat{\tau}_{\bullet}^z)^R + (\hat{\tau}_{\bullet}^z)^L \otimes (\hat{\tau}_{\bullet}^+)^R \\
&+ (\hat{\tau}_{\bullet}^-)^L \otimes (\hat{\tau}_{\bullet}^z)^R + (\hat{\tau}_{\bullet}^z)^L \otimes (\hat{\tau}_{\bullet}^-)^R\}.
\end{aligned} \tag{4.13}$$

When an electron hops in x- and y-axis, the matrices form of the superblock Hamiltonian are shown in Eqs. (D.4) and (D.5). For the case of electron moving along z-axis, the superblock Hamiltonian can be written as

$$\begin{aligned}
H_{\text{super}} &= H_E^L \otimes \delta_E^R + \delta_E^L \otimes H_E^R \\
&+ \frac{2t_{bb}^2}{U}\{(\hat{\tau}_{\bullet}^z)^L \otimes (\hat{\tau}_{\bullet}^z)^R - \frac{1}{4}(\delta_E^L \otimes \delta_E^R)\}.
\end{aligned} \tag{4.14}$$

The matrix form of the superblock in this case is shown in Eq. (D.6). When we get the superblock Hamiltonian, it is diagonalized to find the ground-state wave function and ground-state energy. After, the optimized states are found by using the density matrix method. The truncation matrix can be constructed by the optimized state. The truncation matrix is used to transform the operators in the left enlarged block:

$$H_S = O H_E^L O^\dagger,$$

$$\begin{aligned}
\hat{\tau}_S^+ &= O(\hat{\tau}_\bullet^+)^L_E O^\dagger, \\
\hat{\tau}_S^- &= O(\hat{\tau}_\bullet^-)^L_E O^\dagger, \\
\hat{\tau}_S^z &= O(\hat{\tau}_\bullet^z)^L_E O^\dagger.
\end{aligned} \tag{4.15}$$

Furthermore, these operators, which have been truncated, are used as the operators in the system block in the next iteration. When the convergence of ground-state energy (in the superblock) is reached, we will get the ground-state energy and ground-state wave function of the total system.

### 4.3 Comparing of Orbital and Spin Model

In this section, we will check the orbital model by defining its parameter similar to the case of the spin model. Evidently, the difference of the orbital and spin model are the off-diagonal hopping amplitudes. Moreover, the hopping amplitude of spin model is isotropic because the directions of spin do not effect the hopping amplitude while the hopping amplitude of orbital model is either isotropic or anisotropic depending on the occupation of electronic orbital. Obviously, the orbital model can be reduced to the spin model by defining hopping amplitude parameter as  $t_{aa} = t_{bb} = t$  and  $t_{ab} = t_{ba} = 0$ . Hence the effective  $H$  is written as

$$\begin{aligned}
H_{\text{eff}} &= \frac{4t^2}{U}(\hat{\tau}_i^z \hat{\tau}_j^z - \frac{1}{4}) + \frac{2t^2}{U}(\hat{\tau}_i^+ \hat{\tau}_j^- + \hat{\tau}_i^- \hat{\tau}_j^+) \\
&= \frac{4t^2}{U}(\hat{\tau}_i^z \hat{\tau}_j^z + \frac{1}{2}(\hat{\tau}_i^+ \hat{\tau}_j^- + \hat{\tau}_i^- \hat{\tau}_j^+) - \frac{1}{4}) \\
&= \frac{4t^2}{U}(\vec{\tau}_i \cdot \vec{\tau}_j - \frac{1}{4}).
\end{aligned} \tag{4.16}$$

Evidently, the effect of  $\frac{1}{4}$  in bracket can be neglected because it is constant. As a reason, the ground-state energy of the Heisenberg spin chain model and the orbital model can be compared as in Figure 4.1.

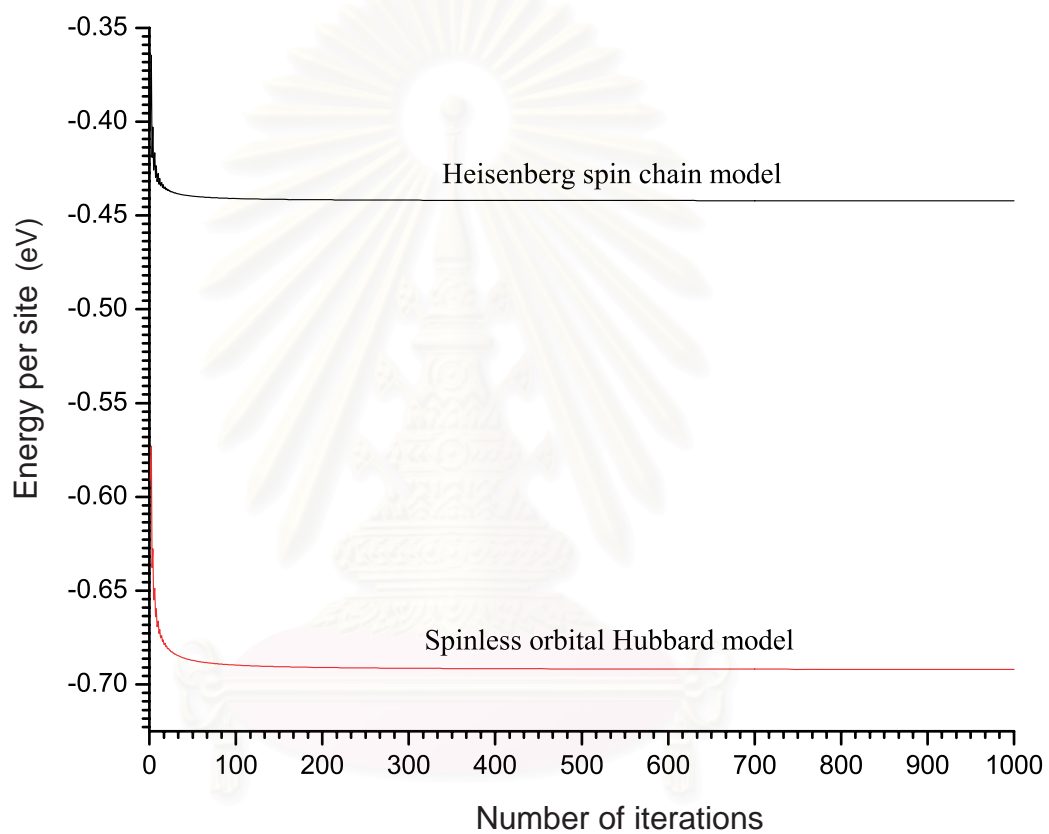


Figure 4.1: Comparison of ground state of Spin model and Orbital model using DMRG by keeping 16 states.

## 4.4 Ground State Energy

The ground-state energy of the spinless orbital Hubbard model with DMRG calculations are computed in each axis (x-, y- and z-axis). The conditions of hopping amplitudes are mentioned earlier. We have found that the calculated ground-state energies of all axes are equivalent. When we use  $pd\sigma$  bond to be  $-1.97$  eV and  $U = 4$  eV [25] and the number of sites to be 2002 ( $i=1000$  and  $\text{site}=2i+2$ ). This number of sites is large enough to ensure the convergence to the ground-state energy. The convergent to the ground state are reached which can be seen from Figure 4.2. Moreover, this result is extrapolated to the thermodynamic limit as  $\frac{1}{N} \rightarrow 0$  shown in Figure 4.3., which the ground-state energy is  $-3.7635$  eV.

## 4.5 Order Parameters

In this work we will focus on the change of orbital degrees of freedom in the ground state then the crucial considered parameters are the orbital correlation [6, 7]. Possible types of orbital ordering will be calculated by operator  $\hat{\tau}_i^z(\theta)$  in the ground state where index  $i$  indicates the site number in the chain and parameter  $\theta$  is the rotating angle of the new basis  $|\tilde{a}\rangle$  and  $|\tilde{b}\rangle$  from original starting basis  $|a\rangle$  and  $|b\rangle$ . Operator  $\hat{\tau}_i^z(\theta)$  is pseudo-spin operators correspond to the basis states  $|\tilde{a}\rangle$ ,  $|\tilde{b}\rangle$  and  $\hat{\tau}_i^z$  is pseudo-spin operators correspond to the  $|a\rangle$  and  $|b\rangle$ . The relation between new and old bases is

$$\begin{pmatrix} |\tilde{a}\rangle \\ |\tilde{b}\rangle \end{pmatrix} = \begin{pmatrix} \cos \theta & \sin \theta \\ -\sin \theta & \cos \theta \end{pmatrix} \begin{pmatrix} |a\rangle \\ |b\rangle \end{pmatrix}. \quad (4.17)$$

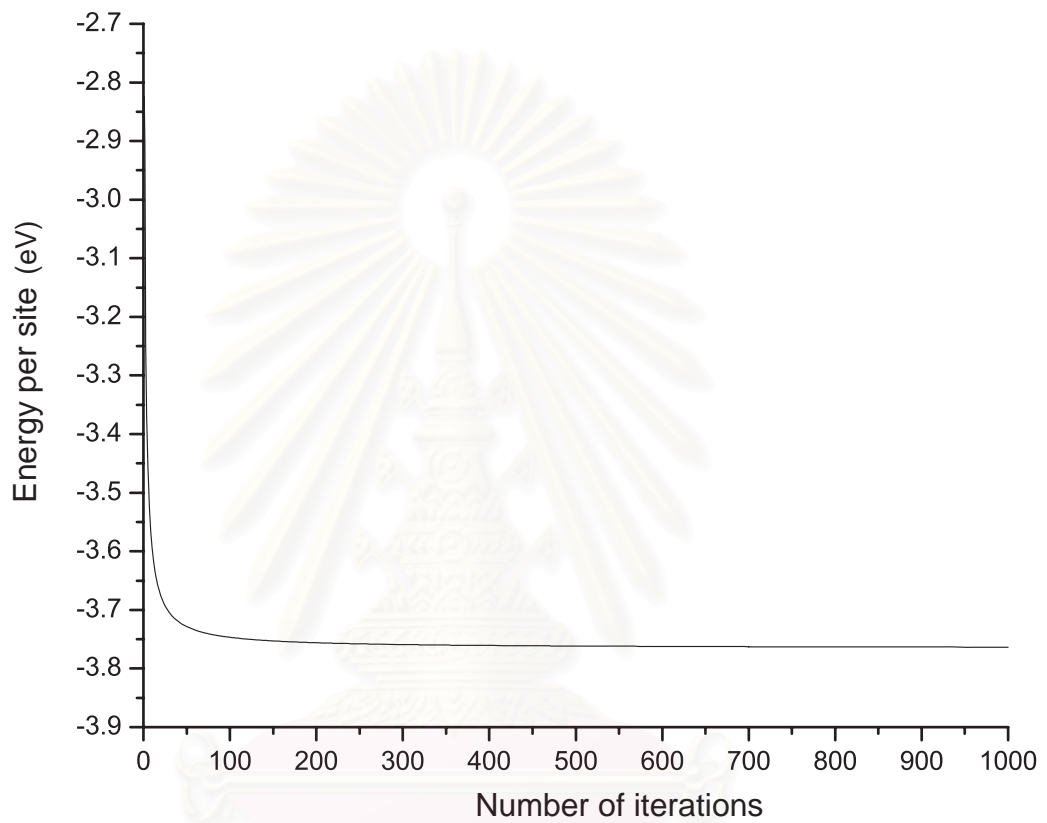


Figure 4.2: Ground-state energy per site of the one-dimension spinless orbital Hubbard model are plotted in three axis, namely x-, y- and z-axis with 16 kept states and 2002 sites of infinite DMRG algorithm. The optimum of a number of iteration are considered from the time of calculation and the convergence of ground-state energy.

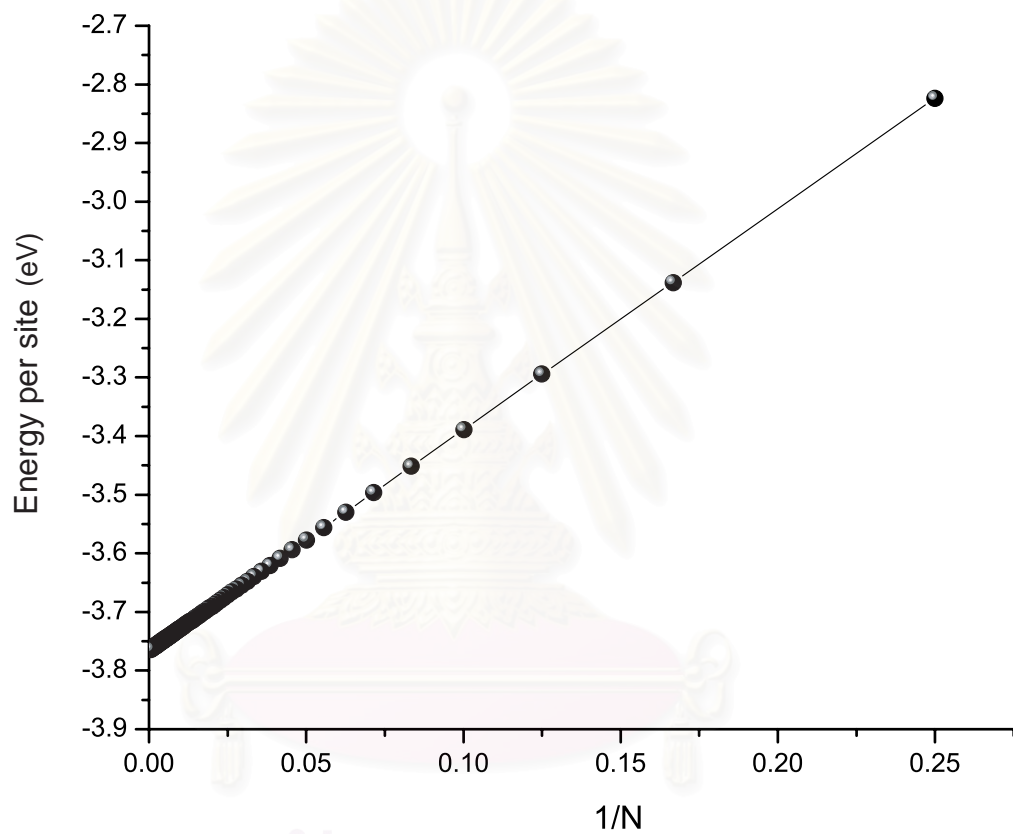


Figure 4.3: The extrapolation is used to finding the ground-state energy as  $N \rightarrow \infty$ .

The pseudo-spin operators are defined as

$$\hat{\tau}_i^z(\theta) = \hat{\tau}_i^z \cos 2\theta + \hat{\tau}_i^x \sin 2\theta, \quad (4.18)$$

$$\hat{\tau}_i^z = \frac{1}{2}(n_{ia} - n_{ib}), \quad (4.19)$$

$$\hat{\tau}_i^x = \frac{1}{2}(c_{ib}^\dagger c_{ia} + c_{ia}^\dagger c_{ib}). \quad (4.20)$$

We are interested in the orbital correlation. It is the expectation value of the operator  $\hat{\tau}_i^z(\theta_i)\hat{\tau}_j^z(\theta_j)$  which is defined as

$$\begin{aligned} \hat{\tau}_i^z(\theta_i)\hat{\tau}_j^z(\theta_j) &= \hat{\tau}_i^z \hat{\tau}_j^z \cos 2\theta_i \cos 2\theta_j + \hat{\tau}_i^x \hat{\tau}_j^x \sin 2\theta_i \sin 2\theta_j \\ &+ \hat{\tau}_i^z \hat{\tau}_j^x \cos 2\theta_i \sin 2\theta_j + \hat{\tau}_i^x \hat{\tau}_j^z \sin 2\theta_i \cos 2\theta_j. \end{aligned} \quad (4.21)$$

The event of strong orbital correlation between site  $i$  and  $j$  emerges when the expectation value of this operator is maximum or minimum. For maximum expectation value, it is highly possible that the electrons occupy the orbital  $|\tilde{a}_i\rangle(|\tilde{b}_i\rangle)$  at site  $i$  and orbital  $|\tilde{a}_j\rangle(|\tilde{b}_j\rangle)$  at site  $j$  simultaneously. Similarly, for the minimum expectation value this event should have electrons occupy on the orbital  $|\tilde{a}_i\rangle(|\tilde{b}_i\rangle)$  at site  $i$  and orbital  $|\tilde{b}_j\rangle(|\tilde{a}_j\rangle)$  at site  $j$  simultaneously.

## 4.6 Orbital Correlation

In this section we discuss the nearest-neighbor orbital correlations at position  $j - i = 1$ . This result is calculated by DMRG method and kept only 16 states which are shown in Figure 4.4, 4.5 and 4.6 in x-, y- and z- axis respectively. The hopping amplitudes are defined according to the electronic hopping on each axis and  $pd\sigma$  is set to be -1.97 eV [25], which is the value of  $pd\sigma$  bonding between  $d$ -orbital of Mn atom and  $p$ -orbital of O atom.

The expectation values  $\langle \hat{\tau}_i^z(\theta_i)\hat{\tau}_j^z(\theta_j) \rangle$  at ground state have been shown in Figure 4.4, 4.5 and 4.6 as the following. The results that appear in these graphs can be analyzed and discussed. For example in Figure 4.4, the maximum of the



expectation value of pseudo-spin correlation operator is 0.25. At this point, both  $\theta_i$  and  $\theta_j$  are found to be  $60^\circ$  and  $150^\circ$ , respectively. The linear combination of states  $|a\rangle$  and  $|b\rangle$  is calculated according to Eq. (4.17). They can be written as

$$\begin{aligned} |\tilde{a}_i\rangle &= \cos 60|a\rangle + \sin 60|b\rangle, \\ |\tilde{b}_i\rangle &= -\sin 60|a\rangle + \cos 60|b\rangle, \end{aligned} \quad (4.22)$$

and

$$\begin{aligned} |\tilde{a}_j\rangle &= \cos 150|a\rangle + \sin 150|b\rangle, \\ |\tilde{b}_j\rangle &= -\sin 150|a\rangle + \cos 150|b\rangle. \end{aligned} \quad (4.23)$$

Then, they are

$$\begin{aligned} |\tilde{a}_i\rangle &= \frac{1}{2}|a\rangle + \frac{\sqrt{3}}{2}|b\rangle, \\ |\tilde{b}_i\rangle &= -\frac{\sqrt{3}}{2}|a\rangle + \frac{1}{2}|b\rangle, \end{aligned} \quad (4.24)$$

and

$$\begin{aligned} |\tilde{a}_j\rangle &= -\frac{\sqrt{3}}{2}|a\rangle + \frac{1}{2}|b\rangle, \\ |\tilde{b}_j\rangle &= -\frac{1}{2}|a\rangle - \frac{\sqrt{3}}{2}|b\rangle. \end{aligned} \quad (4.25)$$

According to Eqs. (4.24) and (4.25) we found that

$$\begin{aligned} |\tilde{a}_j\rangle &= |\tilde{b}_i\rangle, \\ |\tilde{b}_j\rangle &= -|\tilde{a}_i\rangle. \end{aligned} \quad (4.26)$$

We can define the new notations as

$$\begin{aligned} |\tilde{a}_i\rangle &= -|\tilde{b}_j\rangle = |\uparrow\rangle, \\ |\tilde{b}_i\rangle &= |\tilde{a}_j\rangle = |\downarrow\rangle. \end{aligned} \quad (4.27)$$

The positive peak at  $\theta_i = 60^\circ$  and  $\theta_j = 150^\circ$  show that the electrons occupies two possible basis either  $|\tilde{a}_i\tilde{a}_j\rangle$  or  $|\tilde{b}_i\tilde{b}_j\rangle$ . When  $\uparrow$  and  $\downarrow$  are replaced in both  $|\tilde{a}_i\tilde{a}_j\rangle$  and  $|\tilde{b}_i\tilde{b}_j\rangle$ , it is shown that these states are antiferro-orbital state as

$$\begin{aligned} |\tilde{a}_i\tilde{a}_j\rangle &= |\uparrow\downarrow\rangle, \\ |\tilde{b}_i\tilde{b}_j\rangle &= -|\downarrow\uparrow\rangle. \end{aligned} \quad (4.28)$$

Thus, we can conclude that it has antiferro-orbital correlation between two nearest neighbor sites when we consider hopping of electrons along x-axis at the ground state.

Similarly, the orbital correlation of the case of Figure 4.4, 4.5 and 4.6 are summarized in Table (4.1).



สถาบันวิทยบริการ  
จุฬาลงกรณ์มหาวิทยาลัย

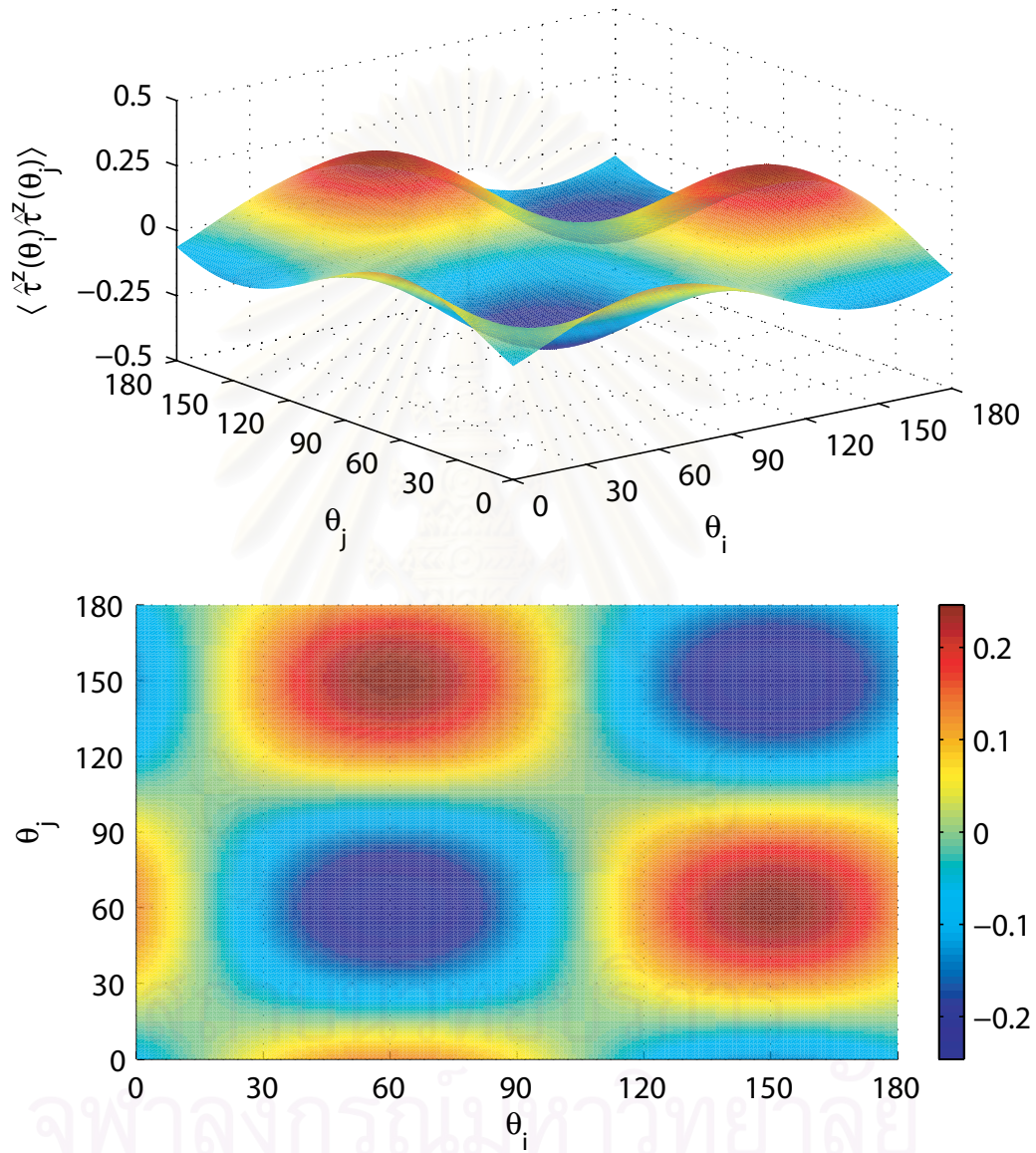


Figure 4.4: A plot of  $\langle \hat{\tau}_i^z(\theta_i) \hat{\tau}_j^z(\theta_j) \rangle$  on x-axis in  $\theta_i$  and  $\theta_j$  space.

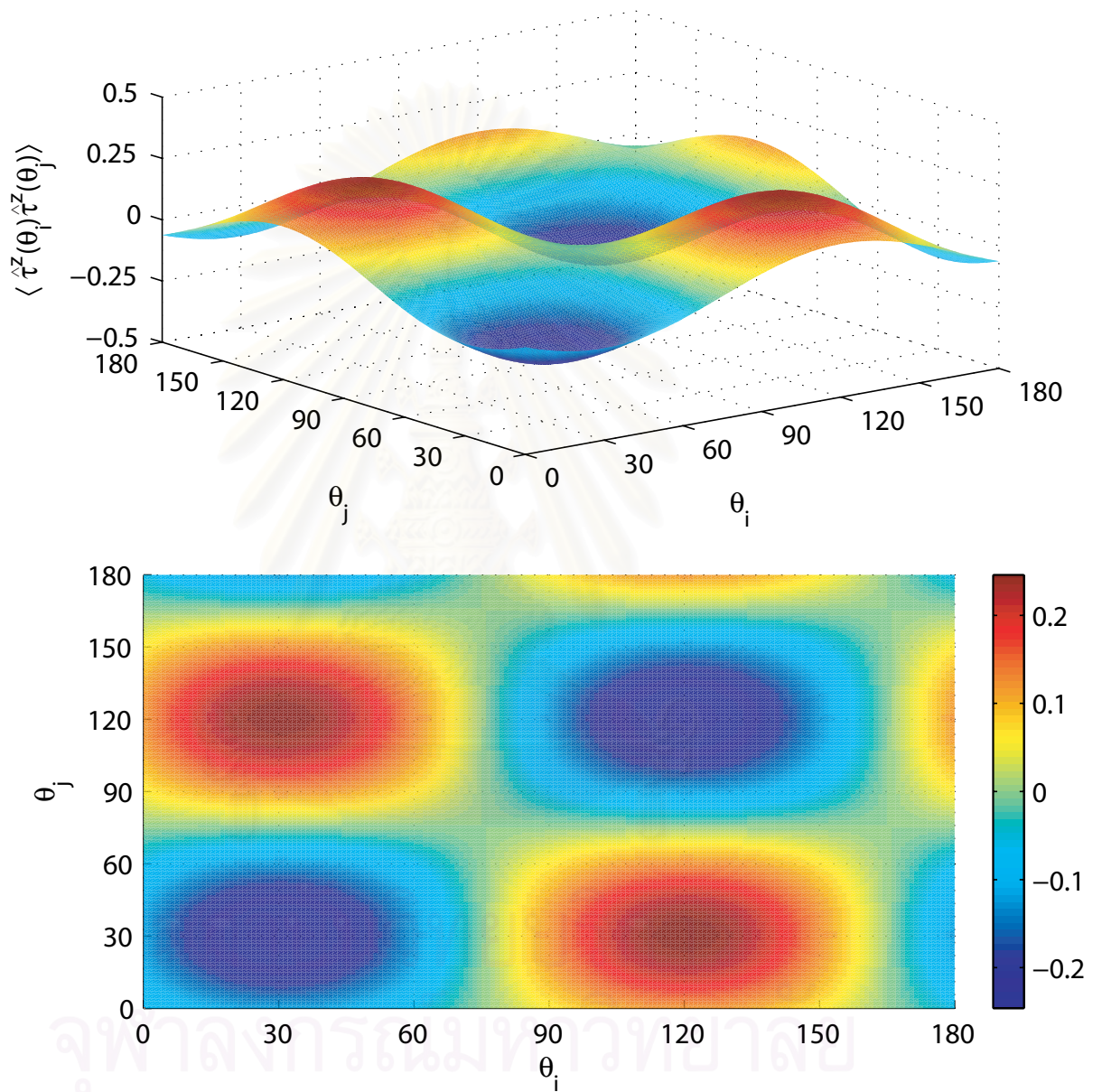


Figure 4.5: A plot of  $\langle \hat{\tau}_i^z(\theta_i) \hat{\tau}_j^z(\theta_j) \rangle$  on y-axis in  $\theta_i$  and  $\theta_j$  space.

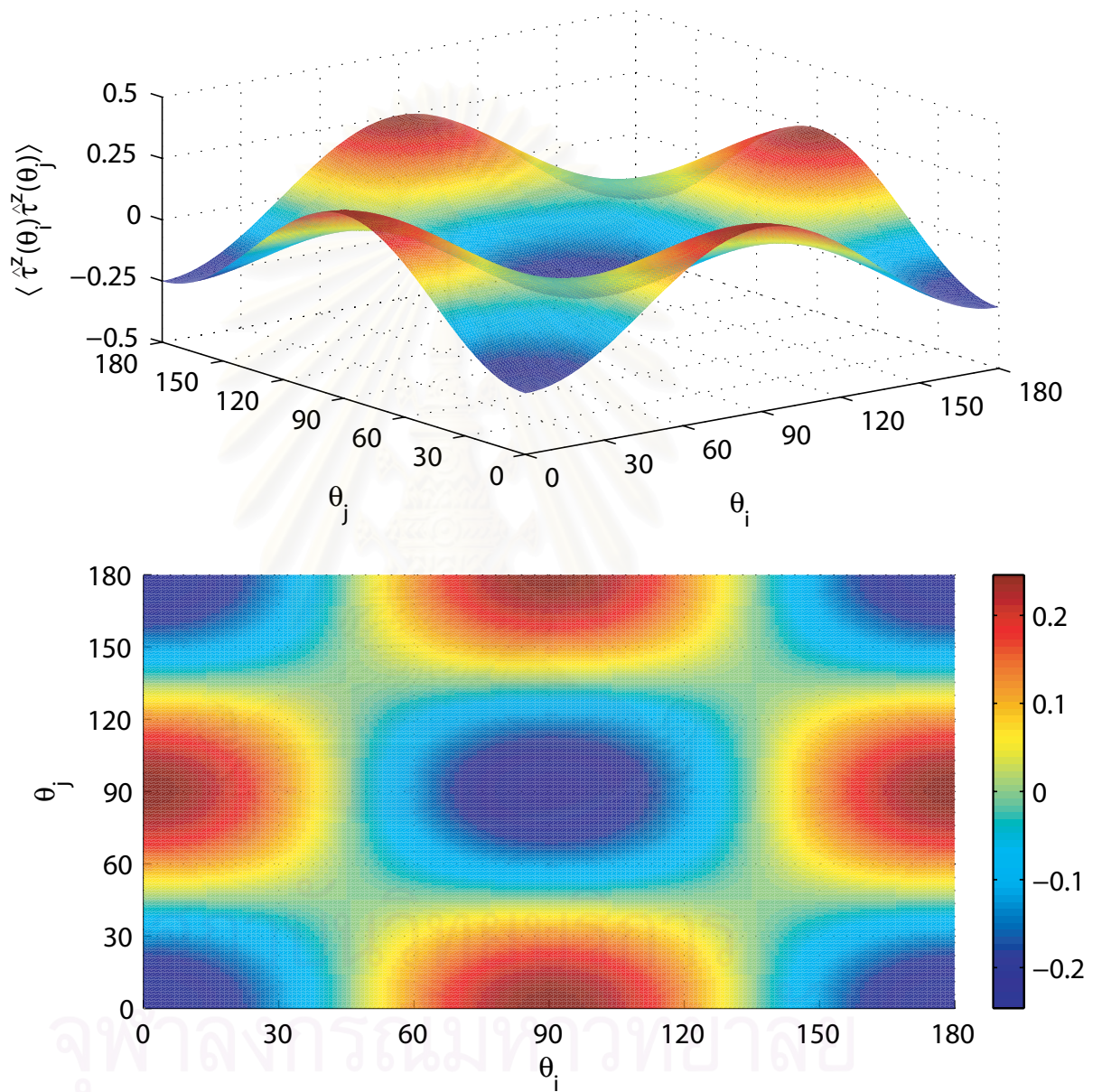


Figure 4.6: A plot of  $\langle \hat{\tau}_i^z(\theta_i) \hat{\tau}_j^z(\theta_j) \rangle$  on z-axis in  $\theta_i$  and  $\theta_j$  space.

Table 4.1: DMRG calculation of the orbital correlation for ground state at one dimension setting the number of sites to be 2002 and considering peaks from Figure 4.4, 4.5 and 4.6,  $\theta_i$  and  $\theta_j$  are chosen from the maximum of the expectation value of the pseudo-spin correlation operator.

Axis	$\theta_i$	$\theta_j$	Occupied orbital (i) at site i	Occupied orbital (j) at site j	Orbital correlation
X	60°	150°	$\frac{1}{2} a\rangle + \frac{\sqrt{3}}{2} b\rangle$	$-\frac{\sqrt{3}}{2} a\rangle + \frac{1}{2} b\rangle$	AF
			$-\frac{\sqrt{3}}{2} a\rangle + \frac{1}{2} b\rangle$	$-\left(\frac{1}{2} a\rangle + \frac{\sqrt{3}}{2} b\rangle\right)$	AF
Y	30°	120°	$\frac{\sqrt{3}}{2} a\rangle + \frac{1}{2} b\rangle$	$-\frac{1}{2} a\rangle + \frac{\sqrt{3}}{2} b\rangle$	AF
			$-\frac{1}{2} a\rangle + \frac{\sqrt{3}}{2} b\rangle$	$-\left(\frac{\sqrt{3}}{2} a\rangle + \frac{1}{2} b\rangle\right)$	AF
Z	0°	90°	$ a\rangle$	$ b\rangle$	AF
			$ b\rangle$	$- a\rangle$	AF

\*AF=Antiferro-orbital

Shape of electron wave functions of the states in Table (4.1) are shown in Figure 4.7, 4.8 and 4.9.

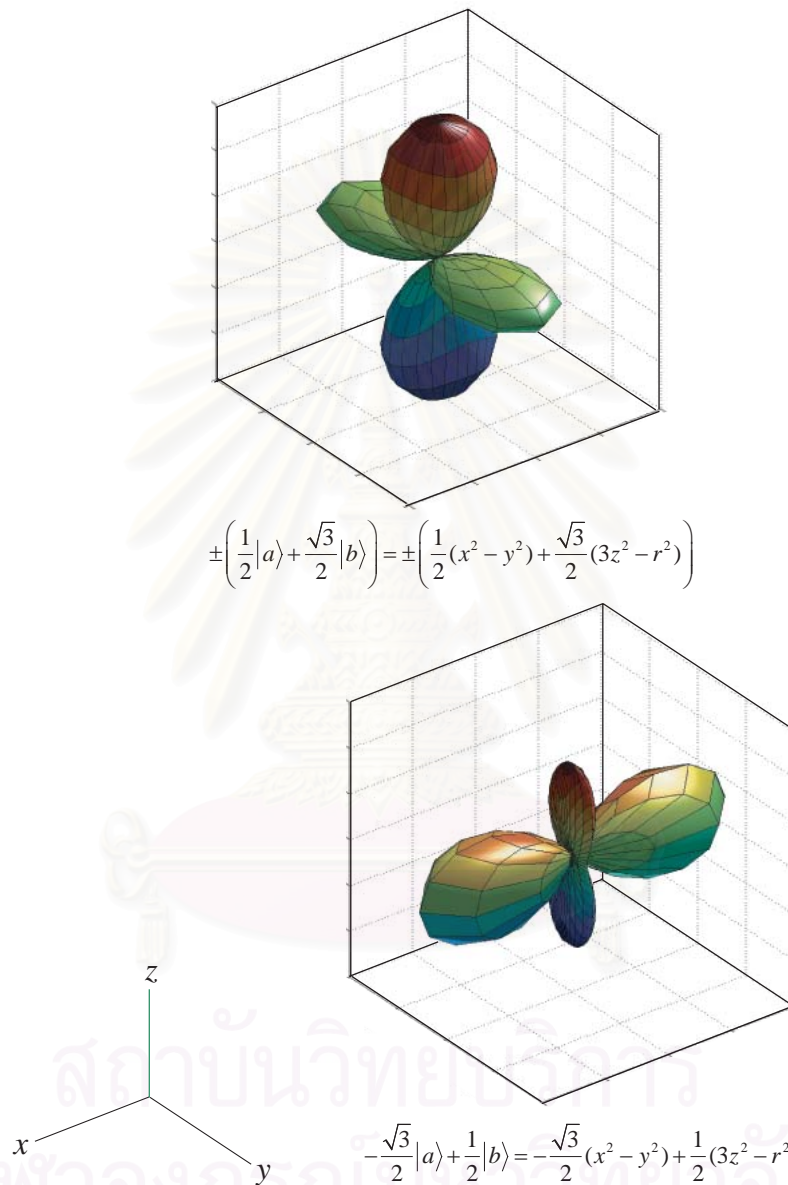


Figure 4.7: Shape of electron density of states  $\pm \left( \frac{1}{2}|a\rangle + \frac{\sqrt{3}}{2}|b\rangle \right) = \pm \left( \frac{1}{2}(x^2 - y^2) + \frac{\sqrt{3}}{2}(3z^2 - r^2) \right)$  and  $-\frac{\sqrt{3}}{2}|a\rangle + \frac{1}{2}|b\rangle = -\frac{\sqrt{3}}{2}(x^2 - y^2) + \frac{1}{2}(3z^2 - r^2)$ .

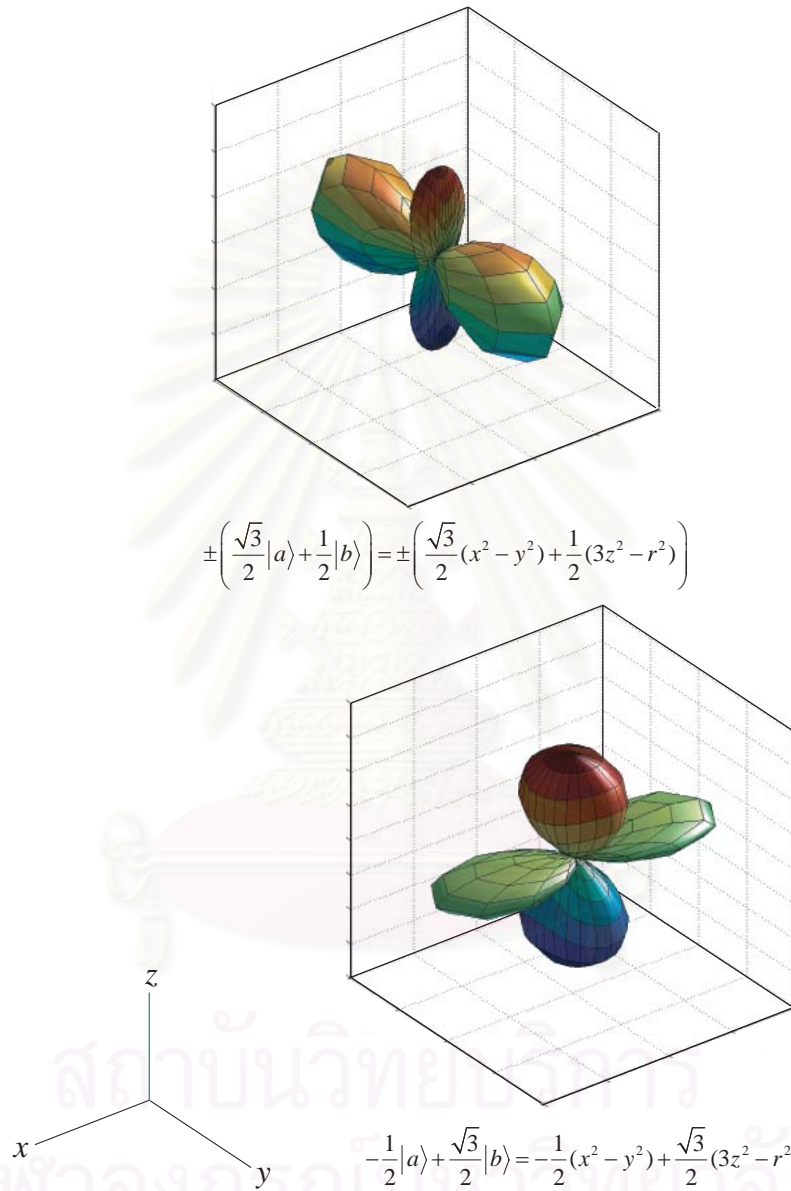


Figure 4.8: Shape of electron density of states  $\pm \left( \frac{\sqrt{3}}{2} |a\rangle + \frac{1}{2} |b\rangle \right) = \pm \left( \frac{\sqrt{3}}{2} (x^2 - y^2) + \frac{1}{2} (3z^2 - r^2) \right)$  and  $-\frac{1}{2} |a\rangle + \frac{\sqrt{3}}{2} |b\rangle = -\frac{1}{2} (x^2 - y^2) + \frac{\sqrt{3}}{2} (3z^2 - r^2)$ .



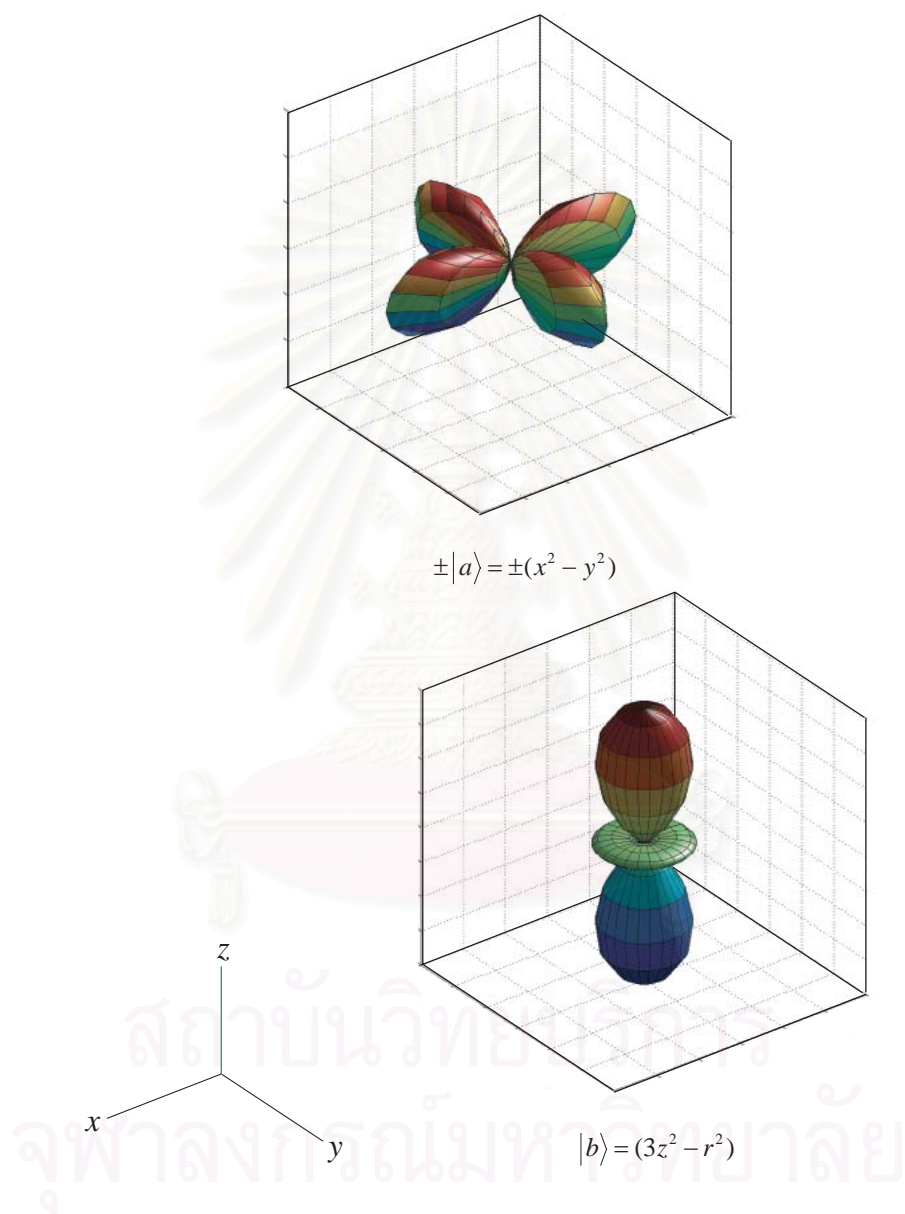


Figure 4.9: Shape of electron density of states  $\pm|a\rangle = \pm(x^2 - y^2)$  and  $|b\rangle = 3z^2 - r^2$ .

# CHAPTER V

## SUMMARY AND CONCLUSION

In this thesis we have been able to derive the effective model for strongly correlated electrons in two-fold degenerate  $e_g$  band. This model consists of the orbital degrees of freedom in the absence of spin degrees of freedom in large- $U$  limit and half-filling, namely the two orbital Hubbard model. This model has been realized in the system with ferromagnetic metallic phase of several metal oxide compounds. Afterward, the ground-state properties of the effective Hamiltonian in one-dimension have been calculated.

We start with the Hubbard Hamiltonian for the electron in transition metal oxides with perovskite structure. Accordingly, the orbital degrees of freedom is added in this effective model. On the other hand, the spin degrees of freedom can be neglected since the spin arrangement of electrons of Mn ions are the ferromagnetic. Moreover, the effective Hamiltonian can be derived in the form of the pseudo-spin operator with the aid of canonical transformation. This transformation has separated the overlapped states occurring from the hopping of electron between nearest neighbor sites. As a result the doubly occupied and singly occupied states can be separated. We choose the effective Hamiltonian that operates on the single occupied states only.

We have used the infinite DMRG algorithm as the numerical method to study the ground-state properties of the interested system. It is constructed and

tested with the spin 1/2 Heisenberg model in which the exact result for one-dimension nearest neighbor sites interacting system has been known. In this work, the number of kept states is 16 states and the number of iterations is 1000, meaning that the number of sites is 2002 which is enough for the ground-state to converge. When we compare the results from our program with the exact result, we get satisfactory results.

In addition, the hopping amplitudes are crucial parameters to find the ground-state properties of the two orbital Hubbard model. These are defined according to the manganite system. However, we have only operated the effective Hamiltonian in one-dimension. Then, the hopping amplitude parameters in each axis (x-, y- and z- axes) are considered. In this work,  $pd\sigma = -1.97$  eV is used. The infinite DMRG method is used with this model to calculate the ground-state energy and the ground-state wave function. We have found that the ground-state energy are equivalent for the electrons moving in x-, y- or z-axis. The ground-state energy has been found to be  $-3.7635$  eV. The ground-state wave function is used to calculate the nearest neighbor orbital correlation. The evidence suggests that these correlations are in antiferro-orbital phase in the orbital pseudo-spin space in all axes.

The complexity of the interested model in the general cases, such as including the spin degree of freedoms as well as the difficulties to understand and program the DMRG algorithm in higher dimensions, lead to the restricted conditions such as the large- $U$  limit and half filling in one dimension. Furthermore, infinite DMRG algorithm has been programmed with MATLAB and has been run in a personal computer then the numbers of kept states are restricted due to the memory and speed of the computer, therefore affecting the accuracy of the ground state. However, the result is satisfied because the ground state of this system is reasonably converged.

Although we have only studied the system in one dimension, it provides

us an opportunity to study the basic many-body quantum systems and to use a numerical method to solve the interesting problem. For the future this work would be implemented in the higher dimensions (2D and 3D) which will provide results resemble to real systems in the thermodynamic limit.



สถาบันวิทยบริการ  
จุฬาลงกรณ์มหาวิทยาลัย

# REFERENCES

1. E. Dagotto. *Nanoscale Phase Separation and Colossal Magnetoresistance*, Series in Solid-State Sciences, Springer, Heidelberg, 2002.
2. P. W. Anderson. *Theory of Superconductivity in the High- $T_c$  Cuprates*, Princeton Series in Physics, Princeton University Press, New Jersey, 1997.
3. Y. Tokura and N. Nagaosa. Orbital Physics in Transition-Metal Oxide *Science* **288** (2000):462-468.
4. Fabian H. L. Essler et al, *The One-Dimension Hubbard Model*, Cambridge University Press, Cambridge, 2005.
5. Q. Yuan, T. Yamamoto, and P. Thalmei. Phase diagram of a generalized Hubbard model applied to orbital order in manganites, *Phys. Rev. B* **62** (2000): 12696-12699.
6. P. Horsch, J. Jaklič and F. Mack. Optical conductivity of colossal-magnetoresistance compounds: Role of orbital degeneracy in the ferromagnetic phase *Phys. Rev. B* **59** (1999): 6217-6228 .
7. C. Srinithiwarawong and G. A. Gehring. Charge and orbital states in spinless Hubbard clusters, *J. Phys.:Condens. Matter* **14** (2002): 1-16.
8. K. A. Chao, J. Spáték and A. M. Oles. Canonical perturbation expansion of the Hubbard model, *Phys. Rev. B* **18** (1978): 3453-3464.
9. S. R. White. Density matrix formulation for quantum renormalization groups, *Phys. Rev. Lett.* **69** (1992): 2863-2866.
10. S. R. White. Density-matrix algorithms for quantum renormalization groups, *Phys. Rev. B* **48** (1993): 10345-10356.

11. E. Dagotto et al. Colossal Magneto-resistance Materials: The Key Role of Phase Separation, *Physics Reports* **344** (2001):1-153.
12. Patrik Fazekas. *Lecture Notes on Electron Correlation and Magnetism*, Series in Modern Condensed Matter Physics-Vol.5, World Scientific, Singapore, 1999.
13. Y. Tokura. Correlated-Electron Physics in Transition-Metal Oxides, *Physics Today* (2003):50-55.
14. C. Srinithirawong. Experimental and Theoretical Studies of Manganite and Magnetic Compounds, Ph.D. thesis, Department of Physics and Astronomy University of Sheffield, 2002.
15. L. Chen and S. Moukouri. Numerical renormalization-group study of the one-dimensional  $t$ - $J$  model, *Phys. Rev. B* **53** (1995): 1866-1870.
16. A. L. Malvezzi. An Introduction to Numerical Methods in Low-Dimensional Quantum Systems, *Brazilian Journal of Physics***33** (2003): 55-72.
17. U. Schollwöck. The density-matrix renormalization group, *Rev. Mod. Phys.* **77** (2005): 259-316.
18. A. Juozapavičius. *Density-Matrix Renormalization-group Analysis of Kondo and XY models*, Ph.D. thesis, Department of Physics, Royal Institute of Technology, Stockholm, 2001.
19. E. J. Bergholtz. *The Density Matrix Renormalization Group Analysis of Spin Chains and Quantum Hall Systems*, Master's thesis, Department of Physics, Stockholm University, 2002.
20. Dan Bohr. *The Density Matrix Renormalization Group Applied to Mesoscopic Structures*, Master's thesis, Department of Micro and Nanotechnology Technical, University of Denmark Lyngby, 2004.

21. S. Blundell. *Magnetism in Condensed Matter*, Oxford Master Series in Condensed Matter Physics, Oxford University Press, 2001.
22. W. Zheng and J. Oitmaa, Local spin correlation in Heisenberg antiferromagnets, *Phys. Rev. B* **63** (2001):0644251–0644259.
23. J. C. Slater and G. F. Koster. Simplified LCAO Method for the Periodic Potential Problem, *Phys. Rev.* **94** (1954): 1498-1524.
24. M. Imada, A. Fujimori and Y. Tokura. Metal-insulator transitions, *Rev. Mod. Phys.* **70** (1998): 1039-1260.
25. A. Mookerjee and D. D. Sarma. Electronic Interaction Strengths, *Electronic Structure of Alloys, Surface and Cluster*, 1<sup>st</sup> ed., Taylor & Francis, London, 2003.



สถาบันวิทยบริการ  
จุฬาลงกรณ์มหาวิทยาลัย



## APPENDICES

สถาบันวิทยบริการ  
จุฬาลงกรณ์มหาวิทยาลัย



# APPENDIX A

## HUBBARD OPERATORS

When we consider the electron states before and after the hopping, the process can be described via Hubbard operator. For example, notation of Hubbard operator show that an  $a$ -state becomes a  $b$ -state at the same site  $j$  after the hopping process

$$X_j^{b \leftarrow a} = |b\rangle_{jj} \langle a| \quad (\text{A.1})$$

which all events will be written

$$\begin{aligned} X_j^{a \leftarrow a} &= |a\rangle_{jj} \langle a|, \\ X_j^{a \leftarrow b} &= |a\rangle_{jj} \langle b|, \\ X_j^{b \leftarrow b} &= |b\rangle_{jj} \langle b|, \\ X_j^{d \leftarrow a} &= |d\rangle_{jj} \langle a|, \\ X_j^{d \leftarrow b} &= |d\rangle_{jj} \langle b|, \\ X_j^{a \leftarrow d} &= |a\rangle_{jj} \langle d|, \\ X_j^{b \leftarrow d} &= |b\rangle_{jj} \langle d|, \\ X_j^{a \leftarrow 0} &= |a\rangle_{jj} \langle 0|, \\ X_j^{b \leftarrow 0} &= |b\rangle_{jj} \langle 0|, \\ X_j^{0 \leftarrow a} &= |0\rangle_{jj} \langle a|, \\ X_j^{0 \leftarrow b} &= |0\rangle_{jj} \langle b|, \end{aligned} \quad (\text{A.2})$$

where  $|a\rangle$  and  $|b\rangle$  denote the basis of occupation of an electron in  $a$  and  $b$  orbital respectively. Products of Hubbard operators behave like

$$X_j^{c \leftarrow f} X_j^{b \leftarrow a} = \delta_{bf} X_j^{c \leftarrow f} X_j^{b \leftarrow a} = X_j^{c \leftarrow a}. \quad (\text{A.3})$$

In this thesis, the orbital Hubbard model in the large- $U$  limit and half-filled are written in creation and annihilation operators, which are substituted with the

Hubbard operators form as

$$c_{ja}^\dagger = X_j^{a\leftarrow 0} + X_j^{d\leftarrow b}, \quad (\text{A.4})$$

$$c_{jb}^\dagger = X_j^{b\leftarrow 0} - X_j^{d\leftarrow a}, \quad (\text{A.5})$$

$$c_{ja} = X_j^{0\leftarrow a} + X_j^{b\leftarrow d}, \quad (\text{A.6})$$

$$c_{jb} = X_j^{0\leftarrow b} - X_j^{a\leftarrow d}. \quad (\text{A.7})$$

These equations series can be expressed as

$$c_{j\sigma}^\dagger = X_j^{\sigma\leftarrow 0} + \eta(\sigma)X^{d\leftarrow\leftarrow\sigma} \quad (\text{A.8})$$

$$c_{j\sigma} = X_j^{0\leftarrow\sigma} + \eta(\sigma)X^{-\sigma\leftarrow d} \quad (\text{A.9})$$

where  $\eta(\sigma)$  is defined depending on  $\sigma$

$$\eta(\sigma) = \begin{cases} +1 & \text{if } \sigma = a \\ -1 & \text{if } \sigma = b. \end{cases} \quad (\text{A.10})$$

Another form that the Hubbard operators link with the creation and annihilation operators are

$$\begin{aligned} X_i^{a\leftarrow a} &= c_{ia}^\dagger c_{ia}, \\ X_i^{a\leftarrow b} &= c_{ia}^\dagger c_{ib}, \\ X_i^{b\leftarrow a} &= c_{ib}^\dagger c_{ia}, \\ X_i^{b\leftarrow b} &= c_{ib}^\dagger c_{ib}. \end{aligned} \quad (\text{A.11})$$

# APPENDIX B

## DERIVATION

In this appendix we show the detail of some parameters used for the Canonical transformation method. Furthermore, some solving processes are elucidated for more understanding.

### B.1 Choosing of $S'$

The term of  $i[S', H_U]$  is important for the reason to choose  $S'$ . The  $S'$  should consists of  $H_t^+$  and  $H_t^-$ . First we consider a set of commuting operators as

$$[\hat{n}_{ib}c_{ia}^\dagger c_{ja}(1 - \hat{n}_{jb}), \hat{n}_{ia}\hat{n}_{ib}] = -\hat{n}_{ib}c_{ia}^\dagger c_{ja}(1 - \hat{n}_{jb}), \quad (\text{B.1})$$

$$[\hat{n}_{ia}c_{ib}^\dagger c_{ja}(1 - \hat{n}_{jb}), \hat{n}_{ia}\hat{n}_{ib}] = -\hat{n}_{ia}c_{ib}^\dagger c_{ja}(1 - \hat{n}_{jb}), \quad (\text{B.2})$$

$$[\hat{n}_{ib}c_{ia}^\dagger c_{jb}(1 - \hat{n}_{ja}), \hat{n}_{ia}\hat{n}_{ib}] = -\hat{n}_{ib}c_{ia}^\dagger c_{jb}(1 - \hat{n}_{ja}), \quad (\text{B.3})$$

$$[\hat{n}_{ia}c_{ib}^\dagger c_{jb}(1 - \hat{n}_{ja}), \hat{n}_{ia}\hat{n}_{ib}] = -\hat{n}_{ia}c_{ib}^\dagger c_{jb}(1 - \hat{n}_{ja}). \quad (\text{B.4})$$

We can rewrite Eqs. (B.1) - (B.4) as

$$[H_{taa}^+, H_U] = -UH_{taa}^+, \quad (\text{B.5})$$

$$[H_{tab}^+, H_U] = -UH_{tab}^+, \quad (\text{B.6})$$

$$[H_{tba}^+, H_U] = -UH_{tba}^+, \quad (\text{B.7})$$

$$[H_{tbb}^+, H_U] = -UH_{tbb}^+. \quad (\text{B.8})$$

Thus, they can be written as

$$[H_t^+, H_U] = -UH_t^+. \quad (\text{B.9})$$

Similarly,

$$[(1 - \hat{n}_{ib})c_{ia}^\dagger c_{ja}\hat{n}_{jb}, \hat{n}_{ia}\hat{n}_{ib}] = (1 - \hat{n}_{ib})c_{ia}^\dagger c_{ja}\hat{n}_{jb}, \quad (\text{B.10})$$

$$[(1 - \hat{n}_{ia})c_{ib}^\dagger c_{ja} \hat{n}_{jb}, \hat{n}_{ia} \hat{n}_{ib}] = (1 - \hat{n}_{ia})c_{ib}^\dagger c_{ja} \hat{n}_{jb}, \quad (\text{B.11})$$

$$[(1 - \hat{n}_{ib})c_{ia}^\dagger c_{jb} \hat{n}_{ja}, \hat{n}_{ia} \hat{n}_{ib}] = (1 - \hat{n}_{ib})c_{ia}^\dagger c_{jb} \hat{n}_{ja}, \quad (\text{B.12})$$

$$[(1 - \hat{n}_{ia})c_{ib}^\dagger c_{jb} \hat{n}_{ja}, \hat{n}_{ia} \hat{n}_{ib}] = (1 - \hat{n}_{ia})c_{ib}^\dagger c_{jb} \hat{n}_{ja}, \quad (\text{B.13})$$

which they can be written as

$$[H_{taa}^-, H_U] = U H_{taa}^-, \quad (\text{B.14})$$

$$[H_{tab}^-, H_U] = U H_{tab}^-, \quad (\text{B.15})$$

$$[H_{tba}^-, H_U] = U H_{tba}^-, \quad (\text{B.16})$$

$$[H_{tbb}^-, H_U] = U H_{tbb}^-. \quad (\text{B.17})$$

Accordingly, they are given by

$$[H_t^-, H_U] = U H_t^-. \quad (\text{B.18})$$

The both  $U H_t^-$  and  $U H_t^+$  have the order of  $t$  (hopping amplitude). Then, we will choose  $S'$  as

$$S' = \frac{-i}{U}(H_t^+ - H_t^-). \quad (\text{B.19})$$

## B.2 Substitute $S'$ in $i[S', H_U]$

Substituting  $S'$  from Eq. (B.19) into the operator  $i[S', H_U]$ , it becomes

$$\begin{aligned} i[S', H_U] &= \frac{1}{U}[H_t^+ - H_t^-, H_U] \\ &= -(H_t^+ + H_t^-). \end{aligned} \quad (\text{B.20})$$

## B.3 Execution with $\frac{i^2}{2}[S, [S, H_U]]$

When  $\frac{i^2}{2}[S, [S, H_U]]$  is substituted with  $S = S' + S''$ , it becomes

$$\frac{i^2}{2}[S' + S'', [S' + S'', H_U]] = \frac{i^2}{2}[S', [S' + S'', H_U]] + \frac{i^2}{2}[S'', [S' + S'', H_U]]$$

$$\begin{aligned}
&= \frac{i^2}{2}[S', [S', H_U]] + \frac{i^2}{2}[S', [S'', H_U]] \\
&\quad + \frac{i^2}{2}[S'', [S', H_U]] + \frac{i^2}{2}[S'', [S'', H_U]] \quad (\text{B.21})
\end{aligned}$$

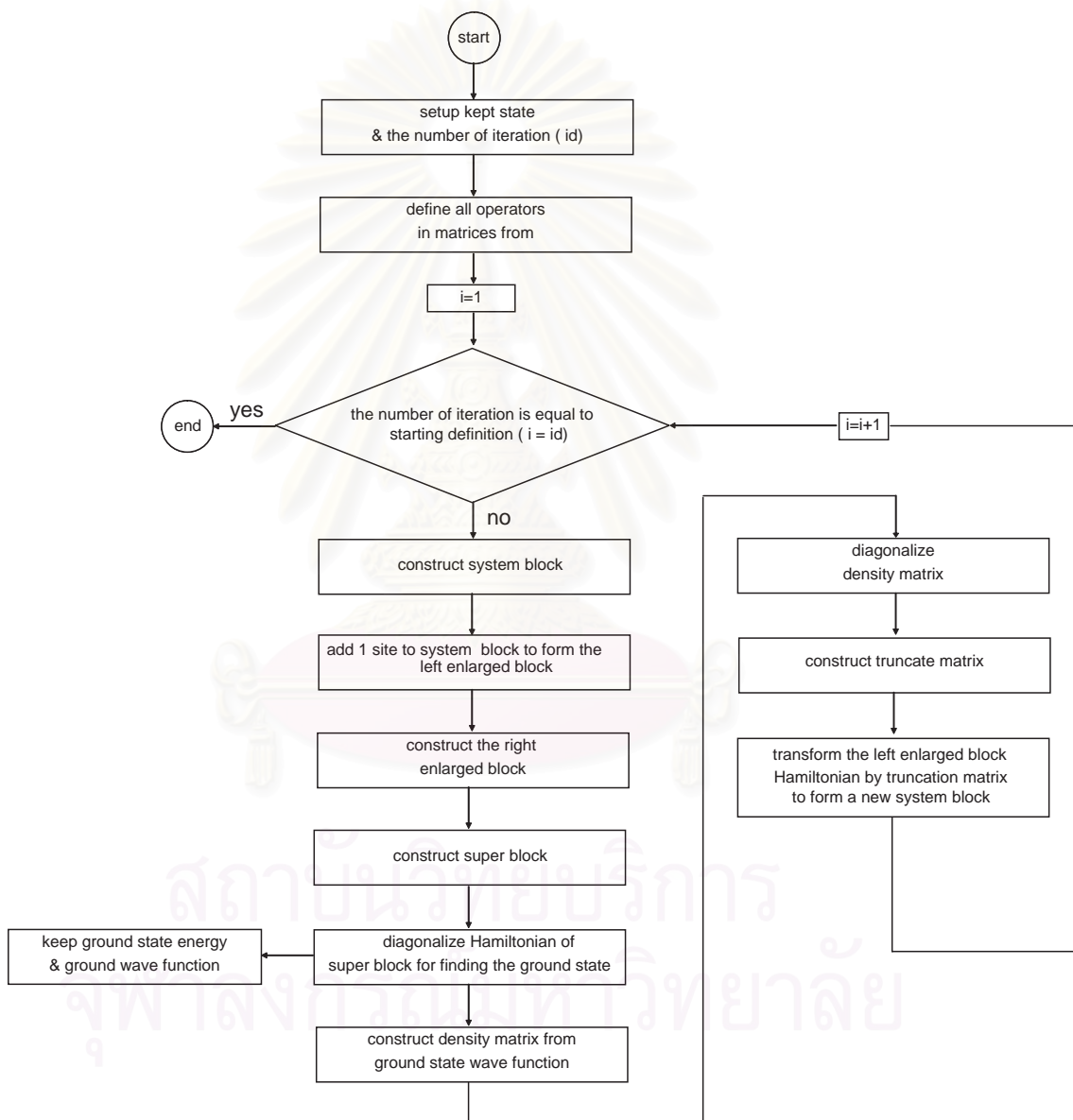
where the underlined terms of the right hand side can be neglected because they are higher order than  $t^2$  when we know that  $S'$  and  $S''$  are in the order of  $t$  and  $t^2$  respectively. The remaining terms become

$$\begin{aligned}
\frac{i^2}{2}[S', [S', H_U]] &= -\frac{1}{U}[H_t^+ - H_t^-, H_t^+ + H_t^-] \\
&= -\frac{1}{U}[H_t^+, H_t^-]. \quad (\text{B.22})
\end{aligned}$$

สถาบันวิทยบริการ  
จุฬาลงกรณ์มหาวิทยาลัย

# APPENDIX C

## FLOW CHART OF DMRG



# APPENDIX D

## HAMILTONIAN IN THE FIRST LOOP

In these results, the spinless two-orbital Hubbard model is calculated in the first loop of MATLAB programming with DMRG algorithm. The calculation are separated in three cases following the direction of an electron hopping as the number of kept states is 16.

### D.1 Left Enlarged Block Hamiltonian

#### D.1.1 The Electron Hopping Along x-axis

$$\begin{pmatrix} -1.412 & -0.81522 & -0.81522 & 1.412 \\ -0.81522 & -2.3533 & 1.412 & 0.81522 \\ -0.81522 & 1.412 & -2.3533 & 0.81522 \\ 1.412 & 0.81522 & 0.81522 & -1.412 \end{pmatrix} \quad (\text{D.1})$$

### D.1.2 The Electron Hopping Along y-axis

$$\begin{pmatrix} -1.412 & 0.81522 & 0.81522 & 1.412 \\ 0.81522 & -2.3533 & 1.412 & -0.81522 \\ 0.81522 & 1.412 & -2.3533 & -0.81522 \\ 1.412 & -0.81522 & -0.81522 & -1.412 \end{pmatrix} \quad (\text{D.2})$$

### D.1.3 The Electron Hopping Along z-axis

$$\begin{pmatrix} 0 & 0 & 0 & 0 \\ 0 & -3.7653 & 0 & 0 \\ 0 & 0 & -3.7653 & 0 \\ 0 & 0 & 0 & 0 \end{pmatrix} \quad (\text{D.3})$$



## D.2 Superblock Hamiltonian

### D.2.1 The Electron Hopping Along x-axis

$$\begin{pmatrix}
 -4\ 236 & -0\ 81522 & -1\ 6304 & 1\ 412 & -1\ 6304 & 0 & 1\ 412 & 0 & -0\ 81522 & 0 & 0 & 0 & 1\ 412 & 0 & 0 & 0 \\
 -0\ 81522 & -5\ 1774 & 1\ 412 & 0 & 0 & -1\ 6304 & 0 & 1\ 412 & 0 & -0\ 81522 & 0 & 0 & 0 & 1\ 412 & 0 & 0 \\
 -1\ 6304 & 1\ 412 & -6\ 1187 & 0\ 81522 & 1\ 412 & 0 & 0 & 0 & 0 & 0 & -0\ 81522 & 0 & 0 & 0 & 1\ 412 & 0 \\
 1\ 412 & 0 & 0\ 81522 & -5\ 1774 & 0 & 1\ 412 & 0 & 0 & 0 & 0 & 0 & -0\ 81522 & 0 & 0 & 0 & 1\ 412 \\
 -1\ 6304 & 0 & 1\ 412 & 0 & -6\ 1187 & -0\ 81522 & 0 & 1\ 412 & 1\ 412 & 0 & 0 & 0 & 0\ 81522 & 0 & 0 & 0 \\
 0 & -1\ 6304 & 0 & 1\ 412 & -0\ 81522 & -7\ 06 & 1\ 412 & 1\ 6304 & 0 & 1\ 412 & 0 & 0 & 0 & 0\ 81522 & 0 & 0 \\
 1\ 412 & 0 & 0 & 0 & 0 & 1\ 412 & -6\ 1187 & 0\ 81522 & 0 & 0 & 1\ 412 & 0 & 0 & 0 & 0\ 81522 & 0 \\
 0 & 1\ 412 & 0 & 0 & 1\ 412 & 1\ 6304 & 0\ 81522 & -5\ 1774 & 0 & 0 & 0 & 1\ 412 & 0 & 0 & 0 & 0\ 81522 \\
 -0\ 81522 & 0 & 0 & 0 & 1\ 412 & 0 & 0 & 0 & -5\ 1774 & -0\ 81522 & -1\ 6304 & 1\ 412 & 0 & 0 & 1\ 412 & 0 \\
 0 & -0\ 81522 & 0 & 0 & 0 & 1\ 412 & 0 & 0 & -0\ 81522 & -6\ 1187 & 1\ 412 & 0 & 0 & 0 & 0 & 1\ 412 \\
 0 & 0 & -0\ 81522 & 0 & 0 & 0 & 1\ 412 & 0 & -1\ 6304 & 1\ 412 & -7\ 06 & 0\ 81522 & 1\ 412 & 0 & 1\ 6304 & 0 \\
 0 & 0 & 0 & -0\ 81522 & 0 & 0 & 0 & 1\ 412 & 1\ 412 & 0 & 0\ 81522 & -6\ 1187 & 0 & 1\ 412 & 0 & 1\ 6304 \\
 1\ 412 & 0 & 0 & 0 & 0\ 81522 & 0 & 0 & 0 & 0 & 0 & 1\ 412 & 0 & -5\ 1774 & -0\ 81522 & 0 & 1\ 412 \\
 0 & 1\ 412 & 0 & 0 & 0 & 0\ 81522 & 0 & 0 & 0 & 0 & 0 & 1\ 412 & -0\ 81522 & -6\ 1187 & 1\ 412 & 1\ 6304 \\
 0 & 0 & 1\ 412 & 0 & 0 & 0 & 0\ 81522 & 0 & 1\ 412 & 0 & 1\ 6304 & 0 & 0 & 1\ 412 & -5\ 1774 & 0\ 81522 \\
 0 & 0 & 0 & 1\ 412 & 0 & 0 & 0 & 0\ 81522 & 0 & 1\ 412 & 0 & 1\ 6304 & 1\ 412 & 1\ 6304 & 0\ 81522 & -4\ 236
 \end{pmatrix}$$

(D.4)

## D.2.2 The Electron Hopping Along y-axis

$$\begin{pmatrix}
 -4\ 236 & 0\ 81522 & 1\ 6304 & 1\ 412 & 1\ 6304 & 0 & 1\ 412 & 0 & 0\ 81522 & 0 & 0 & 0 & 1\ 412 & 0 & 0 & 0 \\
 0\ 81522 & -5\ 1774 & 1\ 412 & 0 & 0 & 1\ 6304 & 0 & 1\ 412 & 0 & 0\ 81522 & 0 & 0 & 0 & 1\ 412 & 0 & 0 \\
 1\ 6304 & 1\ 412 & -6\ 1187 & -0\ 81522 & 1\ 412 & 0 & 0 & 0 & 0 & 0 & 0\ 81522 & 0 & 0 & 0 & 1\ 412 & 0 \\
 1\ 412 & 0 & -0\ 81522 & -5\ 1774 & 0 & 1\ 412 & 0 & 0 & 0 & 0 & 0 & 0\ 81522 & 0 & 0 & 0 & 1\ 412 \\
 1\ 6304 & 0 & 1\ 412 & 0 & -6\ 1187 & 0\ 81522 & 0 & 1\ 412 & 1\ 412 & 0 & 0 & 0 & -0\ 81522 & 0 & 0 & 0 \\
 0 & 1\ 6304 & 0 & 1\ 412 & 0\ 81522 & -7\ 06 & 1\ 412 & -1\ 6304 & 0 & 1\ 412 & 0 & 0 & 0 & -0\ 81522 & 0 & 0 \\
 1\ 412 & 0 & 0 & 0 & 0 & 1\ 412 & -6\ 1187 & -0\ 81522 & 0 & 0 & 1\ 412 & 0 & 0 & 0 & -0\ 81522 & 0 \\
 0 & 1\ 412 & 0 & 0 & 1\ 412 & -1\ 6304 & -0\ 81522 & -5\ 1774 & 0 & 0 & 0 & 1\ 412 & 0 & 0 & 0 & -0\ 81522 \\
 0\ 81522 & 0 & 0 & 0 & 1\ 412 & 0 & 0 & 0 & -5\ 1774 & 0\ 81522 & 1\ 6304 & 1\ 412 & 0 & 0 & 1\ 412 & 0 \\
 0 & 0\ 81522 & 0 & 0 & 0 & 1\ 412 & 0 & 0 & 0\ 81522 & -6\ 1187 & 1\ 412 & 0 & 0 & 0 & 0 & 1\ 412 \\
 0 & 0 & 0\ 81522 & 0 & 0 & 0 & 1\ 412 & 0 & 1\ 6304 & 1\ 412 & -7\ 06 & -0\ 81522 & 1\ 412 & 0 & -1\ 6304 & 0 \\
 0 & 0 & 0 & 0\ 81522 & 0 & 0 & 0 & 1\ 412 & 1\ 412 & 0 & -0\ 81522 & -6\ 1187 & 0 & 1\ 412 & 0 & -1\ 6304 \\
 1\ 412 & 0 & 0 & 0 & -0\ 81522 & 0 & 0 & 0 & 0 & 0 & 1\ 412 & 0 & -5\ 1774 & 0\ 81522 & 0 & 1\ 412 \\
 0 & 1\ 412 & 0 & 0 & 0 & -0\ 81522 & 0 & 0 & 0 & 0 & 0 & 1\ 412 & 0\ 81522 & -6\ 1187 & 1\ 412 & -1\ 6304 \\
 0 & 0 & 1\ 412 & 0 & 0 & 0 & -0\ 81522 & 0 & 1\ 412 & 0 & -1\ 6304 & 0 & 0 & 1\ 412 & -5\ 1774 & -0\ 81522 \\
 0 & 0 & 0 & 1\ 412 & 0 & 0 & 0 & -0\ 81522 & 0 & 1\ 412 & 0 & -1\ 6304 & 1\ 412 & -1\ 6304 & -0\ 81522 & -4\ 236
 \end{pmatrix}$$

(D.5)

### D.2.3 The Electron Hopping Along z-axis

$$\begin{pmatrix}
 0 & 0 & 0 & 0 & 0 & 0 & 0 & 0 & 0 & 0 & 0 & 0 & 0 & 0 & 0 & 0 \\
 0 & -3\,7653 & 0 & 0 & 0 & 0 & 0 & 0 & 0 & 0 & 0 & 0 & 0 & 0 & 0 & 0 \\
 0 & 0 & -7\,5307 & 0 & 0 & 0 & 0 & 0 & 0 & 0 & 0 & 0 & 0 & 0 & 0 & 0 \\
 0 & 0 & 0 & -3\,7653 & 0 & 0 & 0 & 0 & 0 & 0 & 0 & 0 & 0 & 0 & 0 & 0 \\
 0 & 0 & 0 & 0 & -7\,5307 & 0 & 0 & 0 & 0 & 0 & 0 & 0 & 0 & 0 & 0 & 0 \\
 0 & 0 & 0 & 0 & 0 & -11\,296 & 0 & 0 & 0 & 0 & 0 & 0 & 0 & 0 & 0 & 0 \\
 0 & 0 & 0 & 0 & 0 & 0 & -7\,5307 & 0 & 0 & 0 & 0 & 0 & 0 & 0 & 0 & 0 \\
 0 & 0 & 0 & 0 & 0 & 0 & 0 & -3\,7653 & 0 & 0 & 0 & 0 & 0 & 0 & 0 & 0 \\
 0 & 0 & 0 & 0 & 0 & 0 & 0 & 0 & -3\,7653 & 0 & 0 & 0 & 0 & 0 & 0 & 0 \\
 0 & 0 & 0 & 0 & 0 & 0 & 0 & 0 & 0 & -7\,5307 & 0 & 0 & 0 & 0 & 0 & 0 \\
 0 & 0 & 0 & 0 & 0 & 0 & 0 & 0 & 0 & 0 & -11\,296 & 0 & 0 & 0 & 0 & 0 \\
 0 & 0 & 0 & 0 & 0 & 0 & 0 & 0 & 0 & 0 & 0 & -7\,5307 & 0 & 0 & 0 & 0 \\
 0 & 0 & 0 & 0 & 0 & 0 & 0 & 0 & 0 & 0 & 0 & 0 & -3\,7653 & 0 & 0 & 0 \\
 0 & 0 & 0 & 0 & 0 & 0 & 0 & 0 & 0 & 0 & 0 & 0 & 0 & -7\,5307 & 0 & 0 \\
 0 & 0 & 0 & 0 & 0 & 0 & 0 & 0 & 0 & 0 & 0 & 0 & 0 & 0 & -3\,7653 & 0 \\
 0 & 0 & 0 & 0 & 0 & 0 & 0 & 0 & 0 & 0 & 0 & 0 & 0 & 0 & 0 & 0
 \end{pmatrix}
 \tag{D.6}$$

# VITAE

Mr. Pongpun Punpet was born on June 15, 1979 in Phitsanulok. He is the first child of Mr. Surasee Punpet and Mrs. Somphon Punpet. He received his B.Sc. degree in physics from Chulalongkorn University (CU) in 2001.

## Conference Presentations:

- 2005 P. Punpet, Orbital Hubbard Model in Large-U Limit, *5th National Symposium on Graduate Research*, Kasetsart University, Bangkok (10-11 October 2005): O-ST-0127



สถาบันวิทยบริการ  
จุฬาลงกรณ์มหาวิทยาลัย